

**KINEMATIC DESIGN AND ANALYSIS OF MUNITION
EJECTOR RELEASE UNIT**

**MÜHİMMAT BIRAKMA ÜNİTESİNİN KİNEMATİK
TASARIM VE ANALİZİ**

TOLGA ERGEN

PROF. DR. VOLKAN PARLAKTAŞ

Supervisor

Submitted to

Graduate School of Science and Engineering of Hacettepe University

As a Partial Fulfillment to the Requirements for the Award of the Degree of Master of
Science in Mechanical Engineering.

2023

ABSTRACT

KINEMATIC DESIGN AND ANALYSIS OF MUNITION EJECTOR RELEASE UNIT

Tolga ERGEN

Master of Science Degree, Department of Mechanical Engineering

Supervisor: Prof. Dr. Volkan PARLAKTAŞ

January 2023, 141 pages

In this study; design, analysis and optimizations will be done to open the hanger handles at fixed intervals on the ammunition attached to a release mechanism. The hook arms are held by the mechanism and release the hook arms at equal angles and at equal speeds when the last opening command is given. Munitions which have a 30-inch lug distance, can be used in this system.

The boundary conditions of this rigid mechanism are determined. The design and analysis of this mechanism is done analytically and numerically. After various designs and analyzes, dimensions are achieved suitable and optimized for the angle ranges that rigid mechanism works. Through this design, kinematic of the hooks and parts are obtained. The mechanism that performs desired movement are analyzed with the finite element method; the kinematic movement data of the created 3D design is verified to confirm.

Keywords: Rigid Body Dynamics, Release Mechanism, Munition, Mechanism Optimization, Analysis, Kinematic

ÖZET

MÜHİMMAT BIRAKMA ÜNİTESİNİN KİNEMATİK TASARIM VE ANALİZİ

Tolga ERGEN

Yüksek Lisans, Makina Mühendisliği Bölümü

Tez Danışmanı: Prof. Dr. Volkan PARLAKTAŞ

Ocak 2023, 141 sayfa

Bu çalışmada; bir salma mekanizmasına bağlı mühimmat üzerindeki askı kollarının sabit aralıklarla açılması için tasarım, analiz ve optimizasyonlar yapılacaktır. Kanca kolları mekanizma tarafından tutulur ve son açma komutu verildiğinde kanca kollarını eşit açılarda ve eşit hızlarda serbest bırakır. Bu sistemde 30 inçlik kulp mesafesine sahip mühimmat kullanılabilir.

Bu rijit mekanizmanın sınır koşulları belirlidir. Bu mekanizmanın tasarımı ve analizi analitik ve sayısal olarak yapılmıştır. Çeşitli tasarım ve analizlerden sonra rijit mekanizmanın çalıştığı açı aralıklarına uygun ve optimize edilmiş boyutlar elde edilmiştir. Bu tasarım sayesinde kancaların ve parçaların kinematiği elde edilmiştir. Sonlu elemanlar yöntemi ile istenilen hareketi gerçekleştiren mekanizma analiz edilip; oluşturulan 3D tasarımın kinematik hareket verileri doğrulanmıştır.

Anahtar Kelimeler: Rijit Gövde Dinamiği, Bırakma Mekanizması, Mühimmat, Mekanizma Optimizasyonu, Analiz, Kinematik

ACKNOWLEDGEMENTS

First and foremost, I would like to thank Prof. Dr. Volkan PARLAKTAŞ for his profound, patient guidance through all the process and it was an honor for me to be my supervisor.

I would like to express my gratitude to my family for always telling me what I can do in this difficult time.

Finally, getting through the long and difficult process of writing and completing my thesis would not have been possible without my wife Nazlı, she was the most supportive person behind me. I would like to give thanks to my wife for her moral support, patience, and endless love.

Tolga ERGEN

January 2023, Eindhoven

TABLE OF CONTENTS

ABSTRACT	i
ÖZET.....	ii
ACKNOWLEDGEMENTS	iii
TABLE OF CONTENTS	iv
LIST OF FIGURES.....	vi
LIST OF TABLES	ix
LIST OF SYMBOLS & ABBREVIATIONS	x
1. INTRODUCTION AND BACKGROUND.....	1
1.1. Introduction to Mechanisms.....	1
1.2. Aim and Scope of the Study.....	1
1.3. Literature Survey of Ejector Release Units.....	2
2. DESIGN MODEL DEVELOPMENT	7
2.1. Mechanism Design Principles.....	7
2.2. Position, Velocity and Acceleration Analysis of Four-Bar Mechanism	10
2.3. Degree of Freedom.....	12
2.4. Gruebler's Equation	13
2.5. Degree of Freedom/Mobility of Ejector Release Unit	14
3. DESIGN OF THE EJECTOR RELEASE UNIT	16
3.1. Standard Parts.....	16
3.2. Length Optimization for Mechanism Linkages	18
3.3. Components of ERU	27
3.4. Working Principle of Mechanism	28
3.5. Detail System Knowledge of Input Data and Parts.....	31
4. KINEMATIC ANALYSIS OF EJECTOR RELEASE UNIT	38
4.1. Angle, Velocity and Acceleration (Kinematic) Analyzes Outputs	38

4.1.1. Numerical Analysis in MATLAB.....	38
4.1.1.1. Angle Analyzes.....	38
4.1.1.2. Angular Velocity Analyzes.....	44
4.1.1.3. Angular Acceleration Analysis.....	50
4.1.1.4. Linear Acceleration Analysis.....	56
4.1.2. Analytical Analysis in ANSYS.....	63
4.1.2.1. ANSYS Settings.....	63
4.1.2.2. Angular Velocity Outputs.....	71
4.1.2.3. Angular Acceleration Outputs.....	73
4.1.2.4. Linear Acceleration Outputs.....	76
4.2. ANSYS Rigid Body Dynamic Interface Output.....	79
5. CONCLUSION.....	80
REFERENCES.....	81
APPENDICES.....	83
APPENDIX A.....	83

LIST OF FIGURES

Figure 1 - (a) Pitch/Lift Module (b) Pliers	1
Figure 2 - Complex Ejector Release Unit [3].....	3
Figure 3 - (a) Same Direction (b) Opposite Direction [9] / [10]	4
Figure 4 - (a)Pyrotechnic/Cartridge Actuation (b)Gas Tank/Storage Container Actuation [13] / [14].....	5
Figure 5 - (a)Closed(Lock) Position (b)Open(Release) Position [16]	6
Figure 6 - Initial Sketch.....	7
Figure 7 – Final 3D Mechanism Design	8
Figure 8 - Four Bar Mechanism [18]	8
Figure 9 – General Four-Bar Representative for Kinematic Analysis [19]	10
Figure 14 – Stewart Platform [25].....	13
Figure 15 - Mobility of Mechanisms.....	14
Figure 16 - Number of Links and Joints Representative.....	15
Figure 17 - 30-inch Spaced Lugs for Stores up to 2,000-lb Weight Class [22]	16
Figure 18 - Dimensions of the Mark-84 Warhead [23].....	16
Figure 19 - Location of Store Case Components, 30-inch Lug Stores [22].....	17
Figure 20 - 3D Model of MK-84 Ammunition [22].....	17
Figure 21 - First Position of Left-Hand Side of Four-Bar.....	18
Figure 22 – Last Position of Left-Hand Side of Four-Bar	19
Figure 23 - First Position of Left-Hand Side of Mechanism.....	20
Figure 24 - Last Position of Left-Hand Side of Mechanism	20
Figure 25 - First Position of Right-Hand Side of Four-Bar	21
Figure 26 - Last Position of Right-Hand Side of Four-Bar.....	21
Figure 27 - First Position of Right-Hand Side of Mechanism	23
Figure 28 - Last Position of Right-Hand Side of Mechanism.....	23
Figure 29 - First Position of Compiled Mechanism.....	24
Figure 30 – Last Position of Compiled Mechanism.....	24
Figure 31 - Exploded View of System	27
Figure 32 - General View of System.....	28
Figure 33 – Installed Position of the ERU	29
Figure 34 - Pneumatic Actuation	29

Figure 35 - Impulse from Lock Mechanism to Hinge	30
Figure 36 - Release Mechanism Movement	30
Figure 37 - Release of Ammunition	31
Figure 38 - 3D Model of Tension Spring (6).....	31
Figure 39 - 3D Model of Compression Spring	32
Figure 40 - 3D Model of Pneumatic Supply.....	32
Figure 41 - Pressure Level in Gas Storage [24].....	33
Figure 42 – 3D Model of Lock Part 2.....	34
Figure 43 - (a)3D Model of Lock Part2 (b)Sketches of Lock Part2	35
Figure 44- Representative Force on Lock Part 2	36
Figure 45 – Angles of Mechanism.....	38
Figure 46 - Angle Range of “a ₃ ”	39
Figure 47 - Angle Range of “a ₇ ”	40
Figure 48 - Transmission Angles.....	41
Figure 49 – Angle Range of “a ₄ ”	42
Figure 50 – Angle Range of “a ₈ ”	43
Figure 51 - Angle Difference Between Two Hook.....	44
Figure 52 - Angular Velocity of “a ₂ ” and “a ₆ ”	45
Figure 53 - Angular Velocity of “a ₃ ”	46
Figure 54 - Angular Velocity of “a ₄ ”.....	47
Figure 55 - Angular Velocity of “a ₇ ” and “a ₈ ”	49
Figure 56 - Angular Velocity Difference Between Two Hook	50
Figure 57 - Angular Acceleration of “a ₂ ” and “a ₆ ”	51
Figure 58 - Angular Acceleration of “a ₃ ”	52
Figure 59 - Angular Acceleration of “a ₇ ”	53
Figure 60 - Angular Acceleration of “a ₄ ”	54
Figure 61 - Angular Acceleration of “a ₈ ”	55
Figure 62 - Angular Acceleration Difference between Two Hook	56
Figure 63 – Linear Acceleration Representative Points	57
Figure 64 – Linear Acceleration Point on Left Mechanism	57
Figure 65 - Linear Acceleration Point on Right Mechanism.....	58
Figure 66 - Linear Acceleration of “a ₂ ” and “a ₆ ”	59
Figure 67 – Linear Acceleration of “a ₃ ”	60
Figure 68 – Linear Acceleration of “a ₇ ”	61

Figure 69 - Linear Acceleration of “a ₄ ”	62
Figure 70 – Linear Acceleration of “a ₈ ”	63
Figure 71 – ANSYS Workbench Window	64
Figure 72 – 3D Model in ANSYS Mechanical	64
Figure 73 – Contacts and Joint in ANSYS	66
Figure 74 – Tension Spring Model in ANSYS	67
Figure 75 – Tension Spring Properties in ANSYS	67
Figure 76 – Compression Spring Model in ANSYS	68
Figure 77 – Compression Spring Properties in ANSYS	68
Figure 78 – Pneumatic Actuation Assignment	69
Figure 79 – Mesh Analysis of Mechanism	69
Figure 80 – Solutions Tab in ANSYS	70
Figure 81 - Angular Velocity of “a ₂ ” and “a ₆ ”	71
Figure 82 - Angular Velocity of “a ₃ ”	71
Figure 83 - Angular Velocity of “a ₇ ”	72
Figure 84 - Angular Velocity of “a ₄ ”	72
Figure 85 - Angular Velocity of “a ₈ ”	73
Figure 86 - Angular Acceleration of “a ₂ ” and “a ₆ ”	73
Figure 87 - Angular Acceleration of “a ₃ ”	74
Figure 88 - Angular Acceleration of “a ₇ ”	74
Figure 89 - Angular Acceleration of “a ₄ ”	75
Figure 90 - Angular Acceleration of “a ₈ ”	75
Figure 91 - Linear Acceleration of “a ₂ ” and “a ₆ ”	76
Figure 92 - Linear Acceleration of “a ₃ ”	76
Figure 93 - Linear Acceleration of “a ₇ ”	77
Figure 94 - Linear Acceleration of “a ₄ ”	77
Figure 95 - Linear Acceleration of “a ₈ ”	78
Figure 96 - Representation of the Mechanism Running	79

LIST OF TABLES

Table 1 - Part Names	28
----------------------------	----

LIST OF SYMBOLS & ABBREVIATIONS

List of Symbols:

a_1 : Ground Member of Left Four Bar Mechanism

a_2 : Hinge Member of Left Four Bar Mechanism

a_3 : Arm 1 Member of Left Four Bar Mechanism

a_4 : Hook Member of Left Four Bar Mechanism

a_5 : Ground Member of Right Four Bar Mechanism

a_6 : Hinge Member of Right Four Bar Mechanism

a_7 : Arm 2 Member of Right Four Bar Mechanism

a_8 : Hook Member of Right Four Bar Mechanism

a_{G2} : Linear Acceleration of CoG of “ a_2 ”

a_{G2x} : X-Direction Linear Acceleration of CoG of “ a_2 ”

a_{G2y} : Y-Direction Linear Acceleration of CoG of “ a_2 ”

a_{G3} : Linear Acceleration of CoG of “ a_3 ”

a_{G3x} : X-Direction Linear Acceleration of CoG of “ a_3 ”

a_{G3y} : Y-Direction Linear Acceleration of CoG of “ a_3 ”

a_{G4} : Linear Acceleration of CoG of “ a_4 ”

a_{G4x} : X-Direction Linear Acceleration of CoG of “ a_4 ”

a_{G4y} : Y-Direction Linear Acceleration of CoG of “ a_4 ”

a_{G6} : Linear Acceleration of CoG of “ a_6 ”

a_{G7} : Linear Acceleration of CoG of “ a_7 ”

a_{G8} : Linear Acceleration of CoG of “ a_8 ”

A_0A : Represent a_2 Rigid Member

AB : Represent a_3 Rigid Member

$A_0 B_0$: Represent a_1 Fixed(Ground) Member

$B_0 B$: Represent a_4 Rigid Member

f_1 : Total Number of Primary Joint

f_2 : Total Number of Higher Order Joint

f_3 : Distance between “ B_0 ” Pivot Point and External “ F_{13} ” Force Member

f_4 : Distance between “ A ” Pivot Point and External “ F_{14} ” Force Member

F_{12} : External Force to “ a_2 ” Member

F_{13} : External Force to “ a_3 ” Member

F_{14} : External Force to “ a_4 ” Member

F_{23x} : X-Direction of Reaction Force Between a_2 and a_3 Rigid Member

F_{23y} : Y-Direction of Reaction Force Between a_2 and a_3 Rigid Member

F_{34x} : X-Direction of Reaction Force Between a_3 and a_4 Rigid Member

F_{34y} : Y-Direction of Reaction Force Between a_3 and a_4 Rigid Member

F_{a_2,a_3} : Reaction Force Between a_2 and a_3 Rigid Member

F_{a_3,a_4} : Reaction Force Between a_3 and a_4 Rigid Member

F_{a_6,a_7} : Reaction Force Between a_6 and a_7 Rigid Member

F_{a_7,a_8} : Reaction Force Between a_7 and a_8 Rigid Member

F_H : Ground Joint of Hinge Reaction Force (a_2 and a_5 Rigid Member)

F_{LH} : Ground Joint of Left Hook Reaction Force (a_4 Rigid Member)

F_{RH} : Ground Joint of Right Hook Reaction Force (a_8 Rigid Member)

F_{SC} : Compression Spring Reaction Force

F_{ST} : Tension Spring Reaction Force

g_2 : Length to “ a_2 ”s Center of Gravity

g_3 : Length to “ a_3 ”s Center of Gravity

g_4 : Length to “ a_4 ”s Center of Gravity

g_6 : Length to “ a_6 ”s Center of Gravity

g_7 : Length to “ a_7 ”s Center of Gravity

g_8 : Length to “ a_8 ”s Center of Gravity

G_{12x} : X-Direction Reaction Force from Ground “ A_0 ” Pivot Point of “ a_2 ”

G_{12y} : Y-Direction Reaction Force from Ground “ A_0 ” Pivot Point of “ a_2 ”

G_{14x} : X-Direction Reaction Force from Ground “ B_0 ” Pivot Point of “ a_4 ”

G_{14y} : Y-Direction Reaction Force from Ground “ B_0 ” Pivot Point of “ a_4 ”

i : Number of Step Size

I_2 : Moment of Inertia of “ a_2 ”

I_3 : Moment of Inertia of “ a_3 ”

I_4 : Moment of Inertia of “ a_4 ”

K_x : Length Ratio of the Left-Side Rigid Members

K'_x : Length Ratio of the Right-Side Rigid Members

m_2 : Mass of “ a_2 ”

m_3 : Mass of “ a_3 ”

m_4 : Mass of “ a_4 ”

n : Total Number of Links

r : Distance between “ A ” and “ B ” Points in Four-Bar (Virtual Line)

T_{12} : External Moment to “ a_2 ”

T_{13} : External Moment to “ a_3 ”

T_{14} : External Moment to “ a_4 ”

u : Step Size

θ : Angle of Position of the a_2 Rigid Member relative to Horizontal Axis

θ' : Angle of Position of the a_6 Rigid Member relative to Horizontal Axis

θ_1 : Angle of First Position of the a_2 Rigid Member relative to a_1 Ground Member
 θ_2 : Angle of Last Position of the a_2 Rigid Member relative to a_1 Ground Member
 θ_{12} : Angle of the a_2 Rigid Member (Hinge) relative to a_1 Ground Member
 θ_{13} : Angle of the a_3 Rigid Member (Arm1) relative to a_1 Ground Member
 θ_{14} : Angle of the a_4 Rigid Member (Left Hook) relative to a_1 Ground Member ($\phi_{1,2}$)
 θ_{16} : Angle of the a_6 Rigid Member (Hinge) relative to a_1 Ground Member
 θ_{17} : Angle of the a_7 Rigid Member (Arm2) relative to a_1 Ground Member
 θ_{18} : Angle of the a_8 Rigid Member (Left Hook) relative to a_5 Ground Member ($\phi'_{1,2}$)
 $\theta_{1,2}$: Angle Range Between Last and First Position of the a_2 with respect to a_1
 $\theta'_{1,2}$: Angle Range Between Last and First Position of the a_6 with respect to a_5
 ϕ : Angle of Position of the a_4 Rigid Member relative to Horizontal Axis
 ϕ' : Angle of Position of the a_8 Rigid Member relative to Horizontal Axis
 ϕ_1 : Angle of First Position of the a_4 Rigid Member relative to a_1 Ground Member
 ϕ_2 : Angle of Last Position of the a_4 Rigid Member relative to a_1 Ground Member
 ϕ'_1 : : Angle of First Position of the a_8 Rigid Member relative to a_5 Ground Member
 ϕ'_2 : : Angle of Last Position of the a_8 Rigid Member relative to a_5 Ground Member
 ω_{12} : Angular Velocity of the a_2 Rigid Member
 ω_{13} : Angular Velocity of the a_3 Rigid Member
 ω_{14} : Angular Velocity of the a_4 Rigid Member
 ω_{16} : Angular Velocity of the a_6 Rigid Member
 ω_{17} : Angular Velocity of the a_7 Rigid Member
 ω_{18} : Angular Velocity of the a_8 Rigid Member
 r : Representative Angle of “ r ” relative to “ a_1 ” Ground Member
 ϑ : Angle of “ r ” relative to “ a_1 ” Ground Member
 ϑ_2 : Representative Angle of External Force to 2nd Link relative to “ a_1 ” Ground Member

ϑ_3 : Representative Angle of External Force to 3rd Link relative to “ a_1 ” Ground Member

ϑ_4 : Representative Angle of External Force to 4th Link relative to “ a_1 ” Ground Member

α_{12} : Angular Acceleration of the a_2 Rigid Member

α_{13} : Angular Acceleration of the a_3 Rigid Member

α_{14} : Angular Acceleration of the a_4 Rigid Member

α_{16} : Angular Acceleration of the a_6 Rigid Member

α_{17} : Angular Acceleration of the a_7 Rigid Member

α_{18} : Angular Acceleration of the a_8 Rigid Member

β_2 : Angle between “ a_2 ” and CoG of “ a_2 ” (g_2)

β_3 : Angle between “ a_3 ” and CoG of “ a_3 ” (g_3)

β_4 : Angle between “ a_4 ” and CoG of “ a_4 ” (g_4)

μ_1 : Transmission Angle of the Left Four Bar Mechanism

μ_2 : Transmission Angle of the Right Four Bar Mechanism

φ : Angle Between a_2 Rigid Member and a_6 Rigid Member

λ : Angle Between “ r ” and “ a_4 ”

List of Abbreviations:

CAD: Computer Aided Design

CoG: Center of Gravity

CW: Clock Wise

CCW: Counter Clock Wise

DOF: Degree of Freedom

FBD: Free Body Diagram

M: Mobility

MIL-STD: Military Standard

1. INTRODUCTION AND BACKGROUND

1.1. Introduction to Mechanisms

Solid mechanics is a branch of physics that includes three major subbranches: kinematics, which is dealing with the study of forces and moments other than motion; statics, which is concerned with the study of forces and moments other than motion; and kinetics, which is concerned with the action of forces on bodies. The term "dynamics" refers to the combination of kinematics and kinetics. These all three are required to accomplish a mechanism. A mechanism is a mechanical device that transfers motion or force from one location to another [1].

The mechanisms brought together by these three factors are used in every part of our lives. In some areas, different kind of mechanisms are using for simple usage or even critical aims. We can see the mechanisms that we use in our daily life in Figure 1. Although such tools in our lives which have a simple mechanism, they are tools and mechanisms that make our lives easier. Also, these kind of rigid linkage bodies are more reliable and long lasting. The same reasons why mechanical mechanisms are used in many of critical mechanisms.

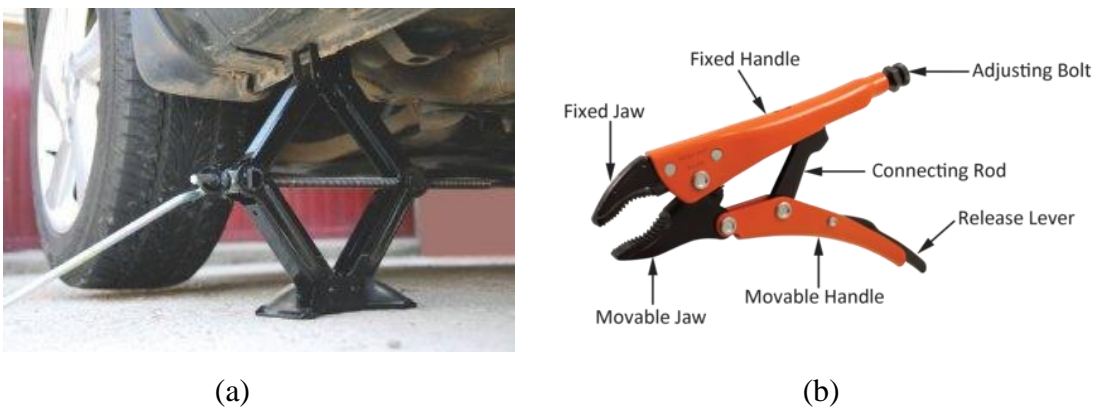


Figure 1 - (a) Pitch/Lift Module (b) Pliers

1.2. Aim and Scope of the Study

With this system, which includes a rigid mechanism, it is desired to introduce a new ammunition release system mechanism to the literature. Such mechanisms can be used

for multiple purposes in aircraft. Although the suspension hook mechanism is designed specifically for such systems, it can also be used in other holding and releasing systems. The dimensions and positions of the arms of the mechanism are very important. In such systems, a locking lever is usually placed. The position of the handles of the suspension hook mechanism, even if the hanger handles are installed in the system and the locking lever required for precaution is inactive; the system must be positioned to stay closed or be a spring preloaded design. Otherwise, after deactivating the locking lever, undesirable results may occur as a result of an incorrect mechanism positioning and design of loads up to 1000lb falling from the aircraft with its own weight and loads from flight maneuvers without receiving the release command. Again, if there is a problem with the load or mechanism attached to the hook, it may be necessary to perform a Jettison, in such cases, even if the safety lever is open, it is not desired to be released and it is requested to release the load without activating the ammunition with the load dump command. Systems driven by pneumatic tubes or pyro-technical cartridges must be reliable and safe for these reasons. At the same time, the reason why these opening and closing drives consist of a mechanical mechanism is that they are considered more reliable when faced with the problems just mentioned. It is inevitable that a system that will meet the stress values that will be created by the flight maneuver loads of the loads up to 1000lb. will be a mechanical mechanism consisting of rigid arms. Another plus of mechanical mechanisms is, it has a simpler structure than systems that operate by taking more than one engine or more than one complex input [2]. In this context, a reliable ammunition holding/release mechanism that opens at equal angles and speeds will be designed.

1.3. Literature Survey of Ejector Release Units

In the aerospace industry so many mechanisms and units are being used. One of the very common and important unit to use in aerospace industry is Ejector Release Unit. Release mechanisms are utilized especially in combat aircrafts, in maritime and surveillance aircrafts, unmanned aerial combat vehicles, light warplanes and helicopters. Not only munitions but also fuel tanks, machine guns, rocket launchers and multiple bomb ejector can be hanged depending on suitable interface to this system. Since the multiple conditions are required for this release mechanisms. In line with the usage of this kind of release units, sometimes its design might be very complex, as you can see in Figure 2.

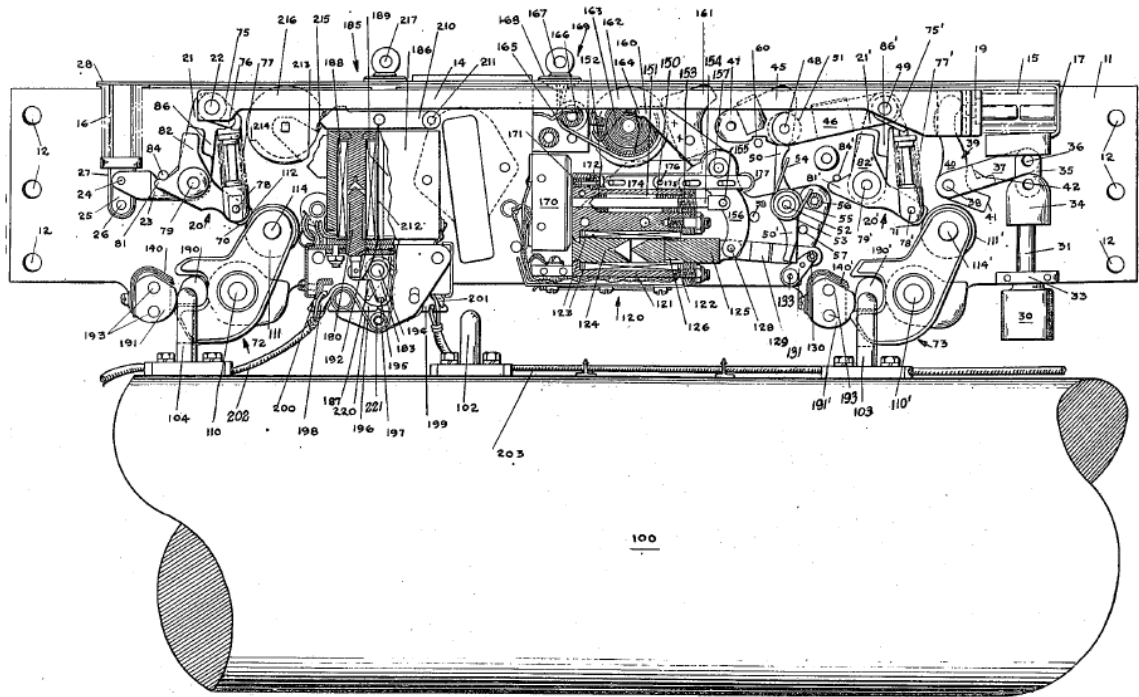
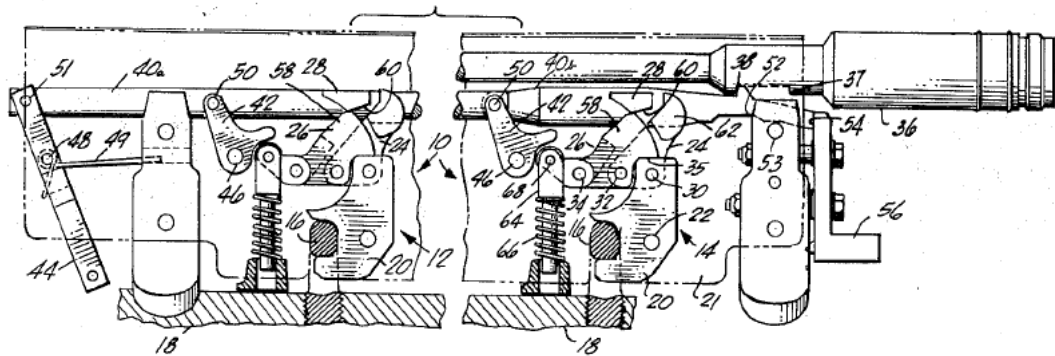
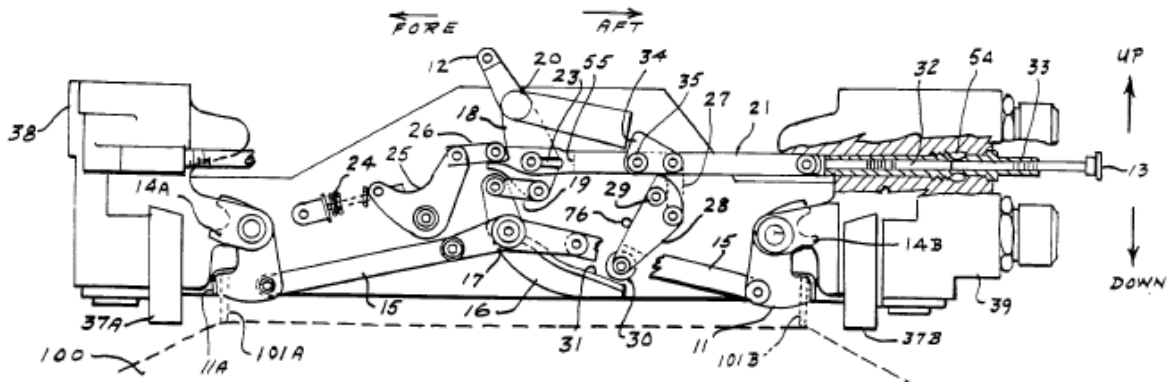


Figure 2 - Complex Ejector Release Unit [3]

There are many patents regarding the ejector release unit mechanism[4]/[5]/[6]/[7]. In the studies mostly rotating movement are used for the release mechanism and hooks can be varied as different shapes and facing direction[8]. We can see in Figure 3; hooks can be located opposite or same direction for given determined or fixed distance.



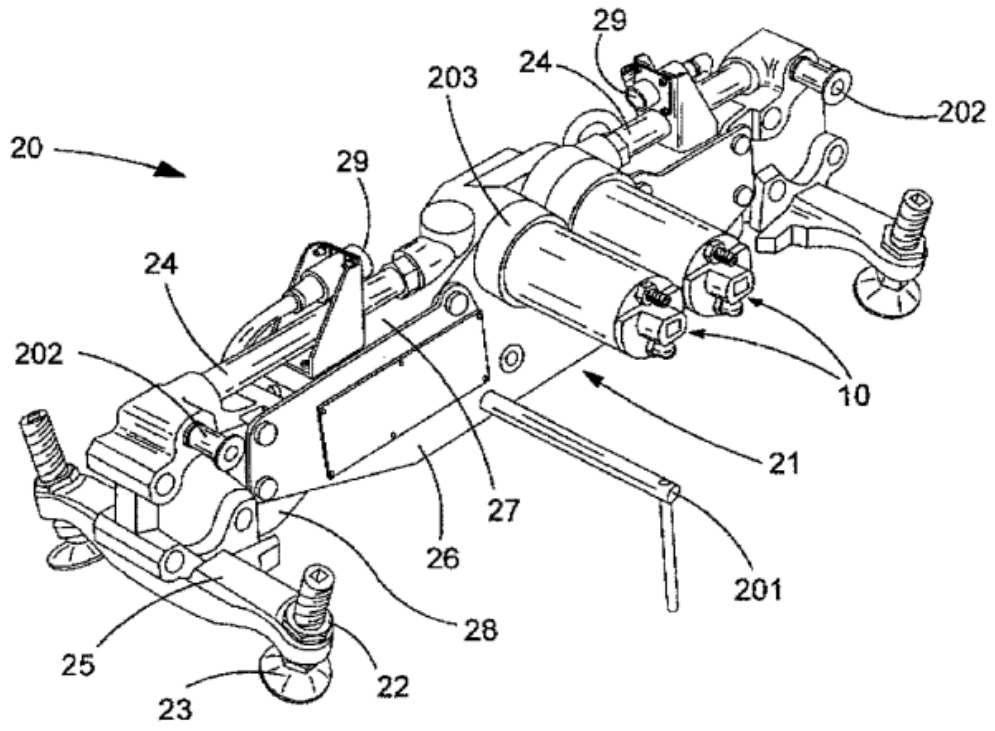
(a)



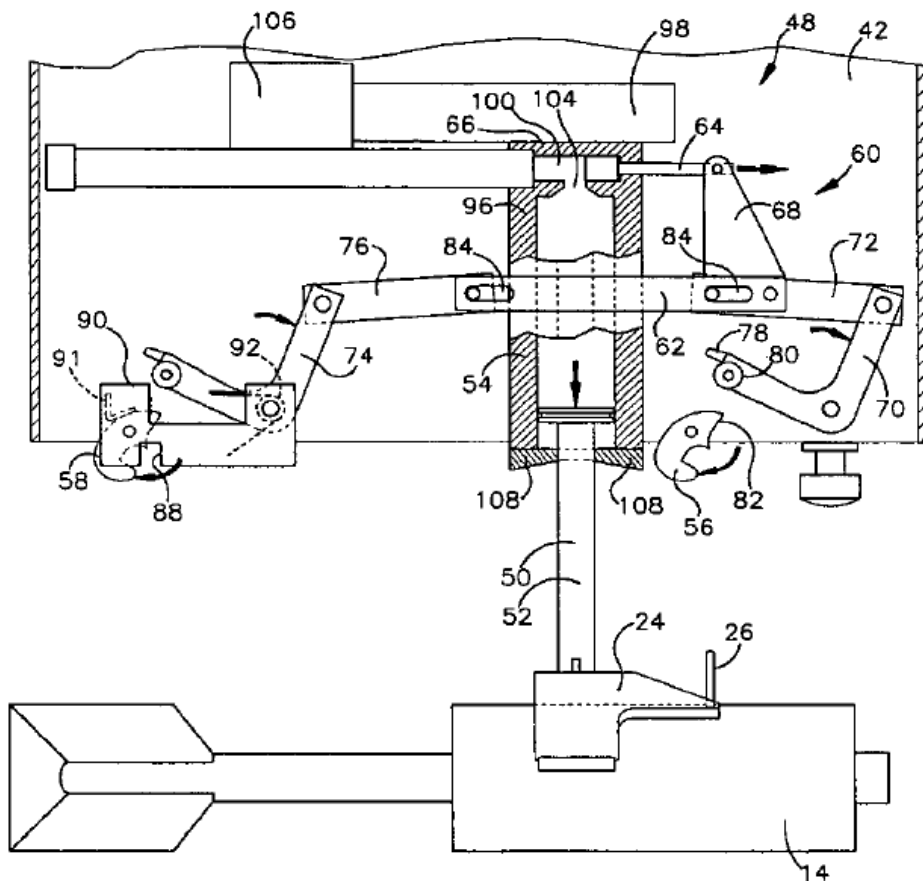
(b)

Figure 3 - (a) Same Direction (b) Opposite Direction [9] / [10]

As seen in patents, this kind of release mechanisms have actuations. Due to triggering the mechanism some input is needed. Actuation require only instant force/moment to give a movement to linkages. So, this actuation must be rapid and has big impact. In line with these reason, pneumatic actuation is the most utilizable solution for this release mechanism. This pneumatic can be used not only actuate the mechanism but also for impulse to munition by pistons[11]. Pneumatic should be stored beforehand since the aircraft cannot be loaded anymore while in the operation or air. Therefore, gas can be stored by pyrotechnic solution with one time use changeable cartridge or pneumatic gas tank with cold gas energy unit [12]. Negative things on pyrotechnic ejection we can see that every time before operation cartridges must be renewed and maintained. So, we can evaluate that a gas storage container more reliable and easier to use than pyrotechnic cartridges. We can see in Figure 4; actuation storage can be distinguished with their volume needed.



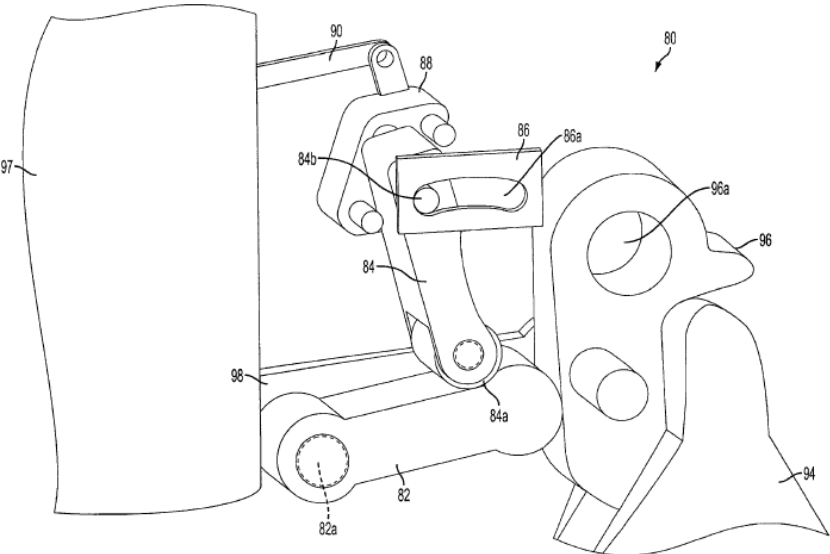
(a)



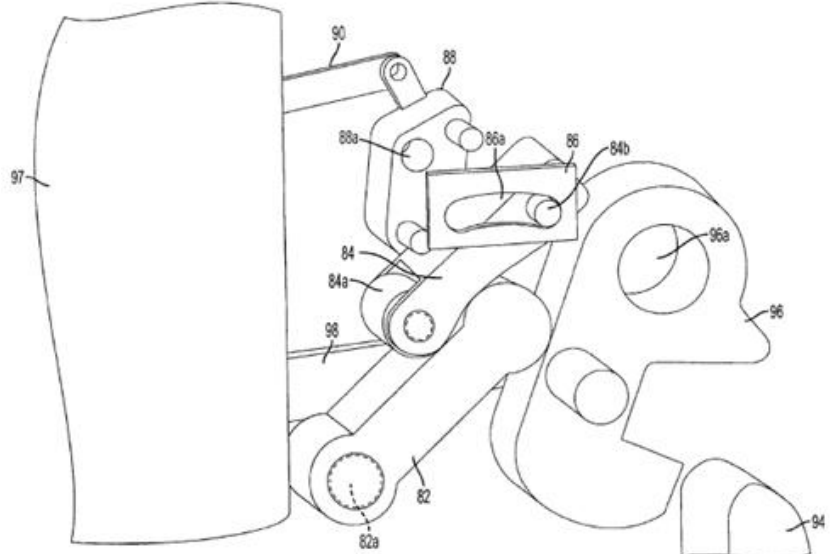
(b)

Figure 4 - (a)Pyrotechnic/Cartridge Actuation (b)Gas Tank/Storage Container Actuation

The working logic of the ejector release unit, while the aircraft on the air before the release of the munition, the hooks are wanted to be locked. So precautional design should be done to not open by itself while flying. Must ensure that mostly mechanical stops or mechanical lock mechanisms are design and located to contrary of the opening side which sometimes can be clockwise or counterclockwise[15]. One of the examples that we can see in Figure 5; Lock part is holding hook's opening side and not allow it to turn clockwise. But after actuating the mechanism, one rigid linkage pulls back the additional lock part and the part that is preventing the hooks turn, it lifts and allow to turn the hook and release occurs.



(a)



(b)

Figure 5 - (a)Closed(Lock) Position (b)Open(Release) Position [16]

2. DESIGN MODEL DEVELOPMENT

2.1. Mechanism Design Principles

A four-bar mechanism can be designed by selecting three arm lengths and a fixed length of ground in a design program. If there are no specific angle and length constraints, it is easy to design a four-bar rigid mechanism. However, there are some rules for designing a specific four-bar mechanism. Unless it is followed, it is difficult to get the desired output angle from the mechanism designed with the estimated dimensions given the entry angle. Before starting the calculation, boundary conditions with some angles and pivot points should be determined. Some specific equations should be followed when designing the mechanism. These equations are derived from each other, starting with the loop closure equation, and ending with some derivative equation of Freudenstein. Optimized dimensions can be obtained analytically with Freudenstein's four-bar mechanism equation[17].

In this thesis it is aimed to obtain the output angles of the mechanism designed for a specific purpose in certain dimensions and depending on certain entry angles. If a mechanism connected to two separate mechanisms is required, as will be done in this thesis, additional studies should be carried out to repeat these steps twice. Since there are two circuits for one mechanism, compiling should be performed. In the preliminary design phase, the sketch can be seen as Figure 6. Two circuit four bar mechanism will merge to obtain one integrated mechanism.

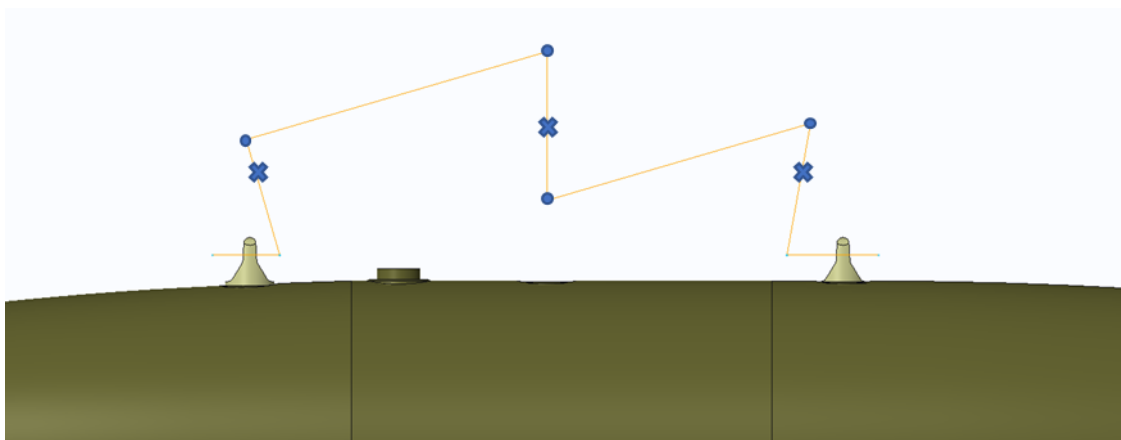


Figure 6 - Initial Sketch

The design that will be obtained at the end of the design process as a result of 3D modeling of the design process that starts with the first drawings is shown below.

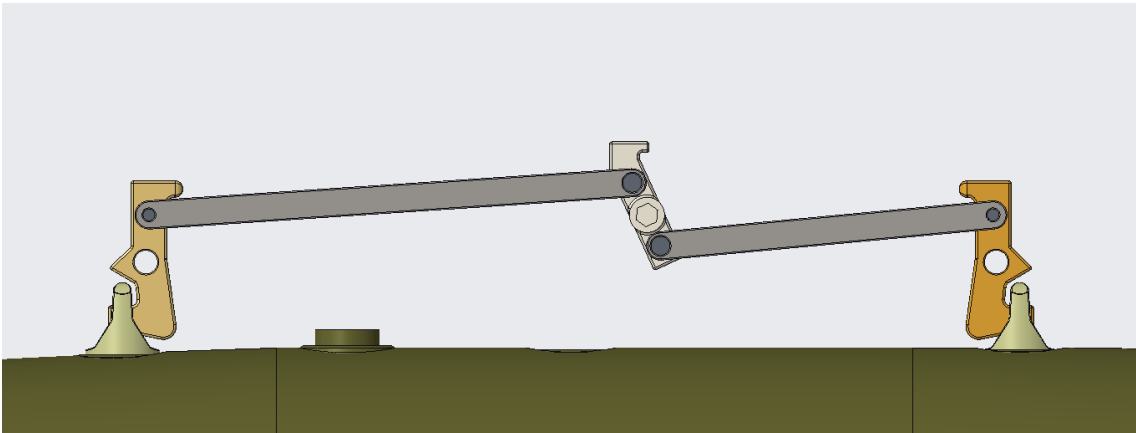


Figure 7 – Final 3D Mechanism Design

Representative links and degrees are shown below and if you go through this example;

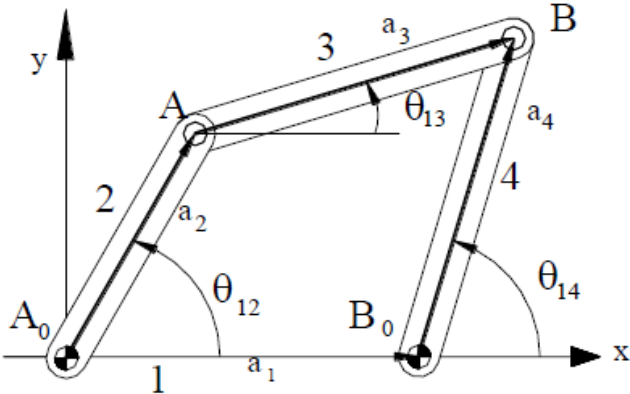


Figure 8 - Four Bar Mechanism [18]

The four-bar mechanism is shown as Figure 8, the loop closure equation for this four-bar mechanism in vectorial form is shown below:

$$A_0A + AB = A_0B_0 + B_0B \tag{1}$$

→ Loop Closure Equation in Vectorial Form

Same equation is in a form of complex numbers:

$$a_2 e^{i\theta_{12}} + a_3 e^{i\theta_{13}} = a_1 + a_4 e^{i\theta_{14}} \quad (2)$$

→ Loop Closure Equation in Complex Numbers (Original Equation)

In complex plane, when we have an equation in complex numbers, the complex conjugate of the equation is also true. The complex conjugate yields vectors which are the mirror image of the original vectors with respect to the real axis (x-axis); e.g., in case of a mechanism, if we place a mirror about the real axis, as we move the original mechanism its image will also move and corresponding to the original closed loop, the loop formed on the mirror image will also be closed at every position. Hence, we obtain another loop closure equation in terms of complex numbers as:

$$a_2 e^{-i\theta_{12}} + a_3 e^{-i\theta_{13}} = a_1 + a_4 e^{-i\theta_{14}} \quad (3)$$

→ Loop Closure Equation in Complex Numbers (Complex Conjugate)

The length ratio is created from multiplying the loop closure equations which are original and complex conjugate. After some steps equation is obtained as below:

$$\frac{a_1}{a_2} \cos \theta_{14} - \frac{a_1}{a_4} \cos \theta_{12} + \frac{(a_1^2 + a_2^2 - a_3^2 + a_4^2)}{2a_4 a_2} = \cos(\theta_{14} - \theta_{12}) \quad (4)$$

If the constant values are assigned as a length ratio of the link, “K” values are obtained as:

$$K_1 = \frac{a_1}{a_2} \quad K_2 = \frac{a_1}{a_4} \quad K_3 = \frac{(a_1^2 + a_2^2 - a_3^2 + a_4^2)}{2a_4 a_2} \quad (5)$$

→ Length Ratios of Links

Finally, the Freudenstein equation[17] is obtained after a couple of steps."Freudenstein's Equation" which can be used for the synthesis of four-bar mechanisms. It gives an implicit relation between the position variables θ_{14} and θ_{12} .

$$K_1 \cos \theta_{14} - K_2 \cos \theta_{12} + K_3 = \cos(\theta_{14} - \theta_{12}) \quad (6)$$

→ Freudenstein's Equation

The generalized shape of the equation with naming the angles by common symbols as it is shown:

$$K_1 \cos \phi - K_2 \cos \theta + K_3 = \cos(\phi - \theta) \quad (7)$$

→ Freudenstein's Equation (Generalized)

2.2. Position, Velocity and Acceleration Analysis of Four-Bar Mechanism

To distinguish among rotation and translation, is an important step. In a terminology it says, if all points on the object follow a circular path throughout the motion, the object is rotating. If all points on the object draw straight lines throughout the motion, the object is in translational motion. In our case links have both movements. According to Dynamic Force Analysis which will be shown as Chapter 2.3, every part has own inertia, mass, and center of gravity of link. Depending on its properties and rotational inputs, linear movements outputs can be obtained.

As it is explained in Chapter 2.1, depend on the step size of the input angles all the angles can be obtained. Also, it is easy to get “ μ_1 ” or “ μ_2 ” and “ θ_{13} ” or “ θ_{17} ” according as position analysis of the four-bar. These angles are also necessary to know, since with “ θ_{13} ” or “ θ_{17} ” will be obtained “ a_3 ” or “ a_7 ”s kinematic and dynamic properties.

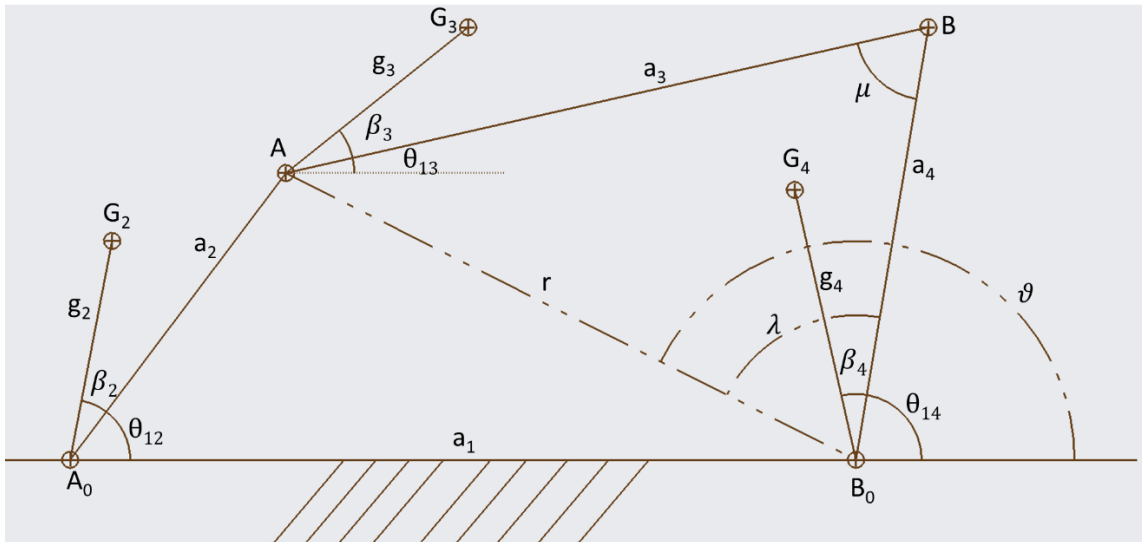


Figure 9 – General Four-Bar Representative for Kinematic Analysis [19]

Position point of view, these equations should be proceeded;

$$r \cos \vartheta = a_2 \cos \theta_{12} - a_1 \quad (8)$$

$$r \sin \vartheta = a_2 \sin \theta_{12} \quad (9)$$

$$\lambda = \cos^{-1} \left(\frac{a_4^2 + r^2 - a_3^2}{2a_4 r} \right) \quad (10)$$

$$\mu = \cos^{-1} \left(\frac{a_4^2 + a_3^2 - r^2}{2a_4 a_3} \right) \quad (11)$$

$$\theta_{14} = \vartheta - \lambda \quad (12)$$

$$\theta_{13} = \theta_{14} - \mu \quad (13)$$

As it is known, one input should be existing to calculate and obtain other unknown angular velocity components. In this case, “ ω_{12} ” will be known as an input for the mechanism this value will be output of FEM analysis.

Angular velocity point of view, these equations should be proceeded;

$$\omega_{13} = \omega_{12} \frac{a_2 \sin(\theta_{12} - \theta_{14})}{a_3 \sin(\theta_{14} - \theta_{13})} \quad (14)$$

$$\omega_{14} = \omega_{12} \frac{a_2 \sin(\theta_{12} - \theta_{13})}{a_4 \sin(\theta_{14} - \theta_{13})} \quad (15)$$

After obtaining angular velocities of the four-bar members, all we need are angular acceleration and linear acceleration of CoG of members. In order to perform Dynamic Force Analysis as an analytical (FEM) solution, these have to be known to use in equations.

Angular acceleration point of view, these equations should be proceeded;

$$\alpha_{12} = \frac{[-a_2 \omega_{12}^2 \cos(\theta_{12} - \theta_{13}) + a_4 \alpha_{14} \sin(\theta_{14} - \theta_{13}) + a_4 \omega_{14}^2 \cos(\theta_{14} - \theta_{13}) - a_3 \omega_{13}^2]}{(a_2 \sin(\theta_{12} - \theta_{14}))} \quad (16)$$

$$\alpha_{13} = \frac{[a_2 \omega_{12}^2 \cos(\theta_{12} - \theta_{14}) + a_2 \alpha_{12} \sin(\theta_{12} - \theta_{14}) + a_3 \omega_{13}^2 \cos(\theta_{14} - \theta_{13}) - a_4 \omega_{14}^2]}{(a_3 \sin(\theta_{12} - \theta_{14}))} \quad (17)$$

$$\alpha_{14} = \frac{[a_2 \omega_{12}^2 \cos(\theta_{12} - \theta_{13}) + a_2 \alpha_{12} \sin(\theta_{12} - \theta_{14}) - a_4 \omega_{14}^2 \cos(\theta_{14} - \theta_{13}) + a_3 \omega_{13}^2]}{(a_4 \sin(\theta_{14} - \theta_{13}))} \quad (18)$$

Or there are other equations that it can obtained with;

$$\alpha_{13} = \omega_{12} \frac{(\omega_{13i+1} - \omega_{13i-1})}{2u} \quad (19)$$

$$\alpha_{14} = \omega_{12} \frac{(\omega_{14i+1} - \omega_{14i-1})}{2u} \quad (20)$$

Depend on unknowns, angular acceleration equations can be written differently as shown above.

Linear acceleration for CoG of members point of view, these equations should be proceeded;

$$a_{G2x} = -g_2 \omega_{12}^2 \cos(\theta_{12} + \beta_2) - g_2 \alpha_{12} \sin(\theta_{12} + \beta_2) \quad (21)$$

$$a_{G2y} = -g_2 \omega_{12}^2 \sin(\theta_{12} + \beta_2) + g_2 \alpha_{12} \cos(\theta_{12} + \beta_2) \quad (22)$$

$$a_{G3x} = -a_2 \omega_{12}^2 \cos(\theta_{12}) - a_2 \alpha_{12} \sin(\theta_{12}) - g_3 \omega_{13}^2 \cos(\theta_{13} + \beta_3) - g_3 \alpha_{13} \sin(\theta_{13} + \beta_3) \quad (23)$$

$$a_{G3y} = -a_2 \omega_{12}^2 \sin(\theta_{12}) + a_2 \alpha_{12} \cos(\theta_{12}) - g_3 \omega_{13}^2 \sin(\theta_{13} + \beta_3) + g_3 \alpha_{13} \cos(\theta_{13} + \beta_3) \quad (24)$$

$$a_{G4x} = -g_4 \omega_{14}^2 \cos(\theta_{14} + \beta_4) - g_4 \alpha_{14} \sin(\theta_{14} + \beta_4) \quad (25)$$

$$a_{G4y} = -g_4 \omega_{14}^2 \sin(\theta_{14} + \beta_4) + g_4 \alpha_{14} \cos(\theta_{14} + \beta_4) \quad (26)$$

Finally, all the necessary properties of the members will be obtained after the calculations performed. With these angle, velocity, and acceleration values, dynamic force analysis can be proceeded.

2.3. Degree of Freedom

An important property in mechanism analysis is the number of degrees of freedom of the linkage. The degree of freedom is the number of independent inputs required to precisely position all links of the mechanism with respect to the ground. It can also be defined as

the number of actuators needed to operate the mechanism. A mechanism actuator could be manually moving one link to another position, connecting a motor to the shaft of one link, or pushing a piston of a hydraulic cylinder.

The number of degrees of freedom of a mechanism is also called the mobility, and it is given the symbol M . When the configuration of a mechanism is completely defined by positioning one link, that system has one degree of freedom. Most commercially produced mechanisms have one degree of freedom. In contrast, robotic arms can have three, or more, degrees of freedom. [20]

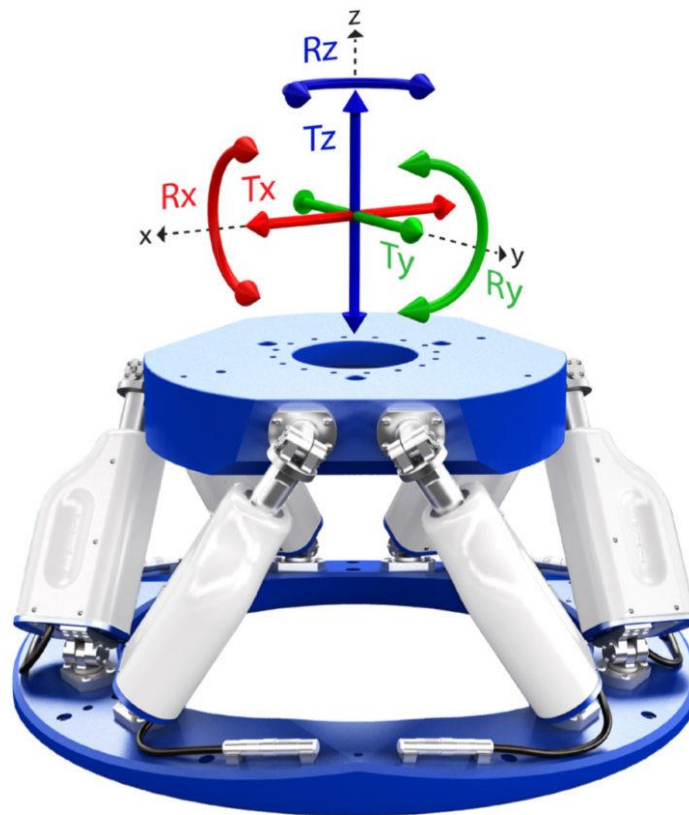


Figure 10 – Stewart Platform [25]

2.4. Gruebler's Equation

Kutzbach-Gruebler's equation is used to calculate the degrees of freedom of linkages. The number of degrees of freedom of a linkage is also called its mobility. A simplified version of the Kutzbach-Gruebler's equation for planar linkages [21]:

$$\text{Degrees of Freedom} = M = 3 * (n - 1) - 2 * j_p - 2 * j_h \quad (36)$$

Where:

n = Total number of links in the mechanism

j_p = Total number of primary joints (pins or sliding joints)

j_h = Total number of higher order joints (cam or gear joints)

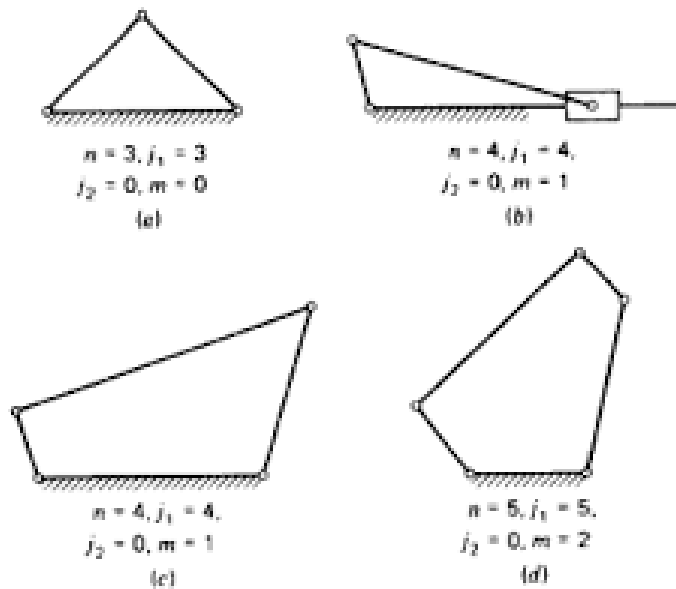


Figure 11 - Mobility of Mechanisms

2.5. Degree of Freedom/Mobility of Ejector Release Unit

The designed mechanism must be actuated by an input while in the aircraft. Ejector release units not only manually but also have to work automatically while aircraft in the air. This creates the need for an actuator. So according to degree of freedom of the system, will change how many actuators will be placed. If calculation of DOF will be more than one, then the system must have more than one actuator which make the system more complex, occupy more space and not only actuators but also its cables or hoses.

In general, this kind of ammunition release mechanism has one or two actuator which makes the mechanism much simpler.

In according to preliminary sketch (Figure 6) if we calculate the DOF of our mechanism the result would be:

$$DOF = 3(6 - 1) - 2 * 7 - 0$$

$$= 1$$

In the mechanism in total “7” joints and/or hinges are existing which is counting for “ j_p ”, indicated as red numbers. Also, there are “6” links existing, indicated as yellow numbers, this refers for “n” number link. This result shows that in the design, one actuator will be enough to give movement to mechanism.

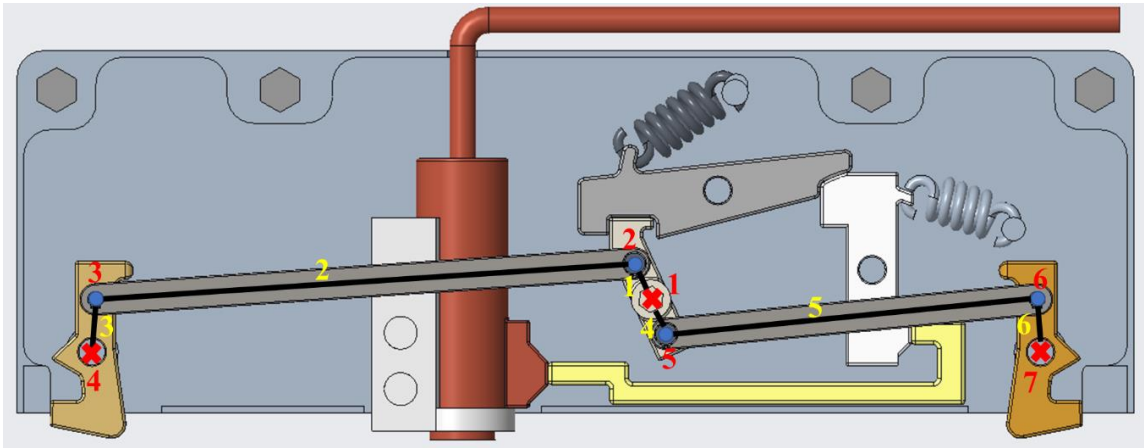


Figure 12 - Number of Links and Joints Representative

3. DESIGN OF THE EJECTOR RELEASE UNIT

3.1. Standard Parts

In the military some parts have to be fixed geometry, so it makes these part universal and even if somebody use these products has to be reliable. For the purpose of using some parts have some limitation and fixed geometry like lug, ammunition etc. As shown below there are some parts which are fixed geometry depending on the MIL-STD drawings.

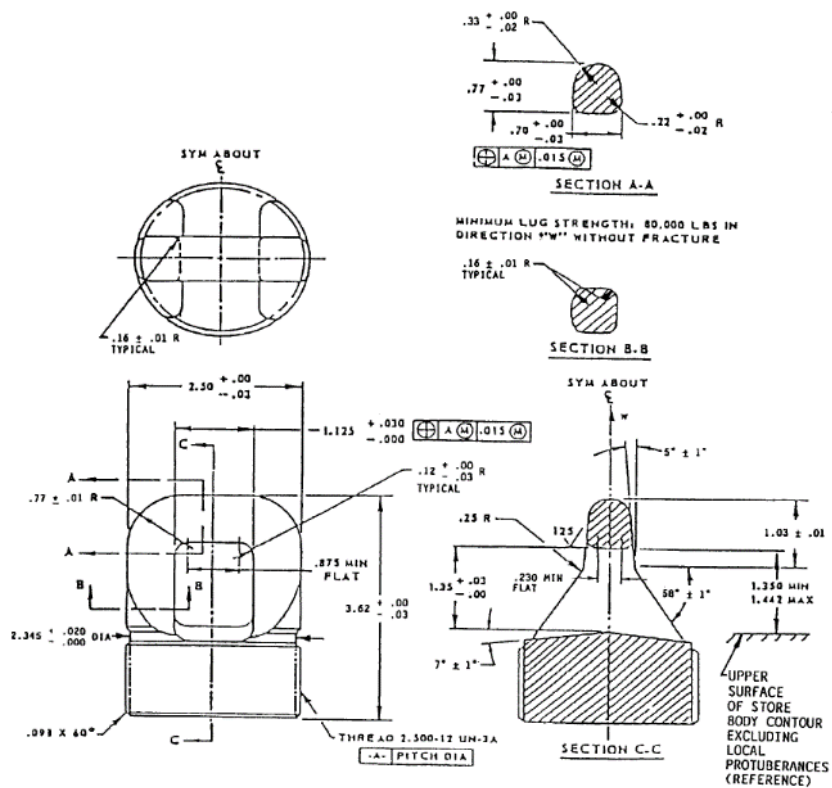


Figure 13 - 30-inch Spaced Lugs for Stores up to 2,000-lb Weight Class [22]

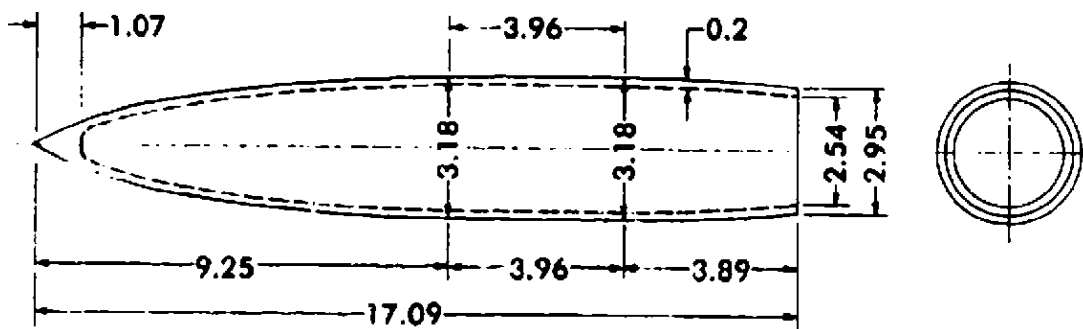


Figure 14 - Dimensions of the Mark-84 Warhead [23]

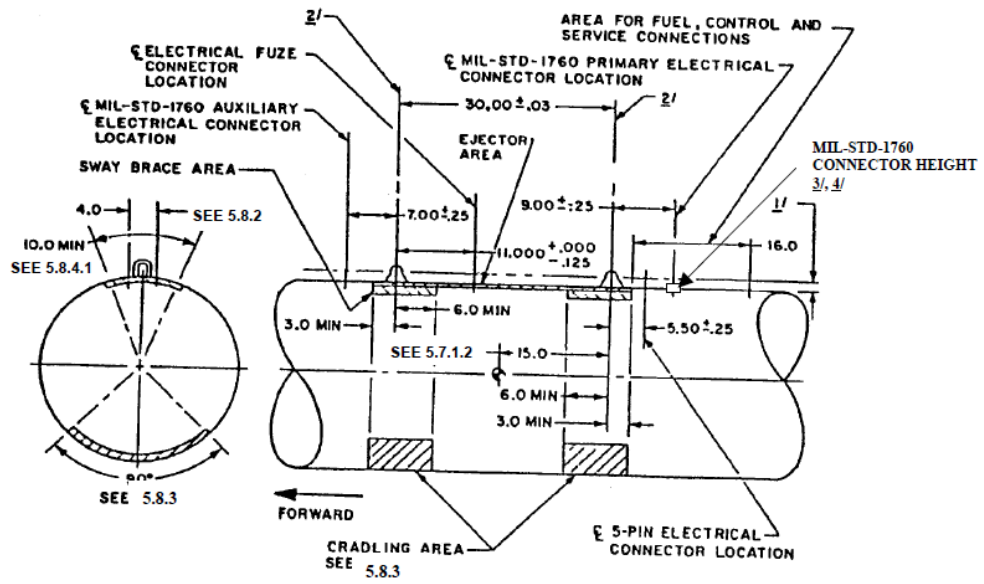


Figure 15 - Location of Store Case Components, 30-inch Lug Stores [22]

In line with the standard dimensions of the warhead, lug and lug's location, general model of the ammunition can be obtained by CAD program.

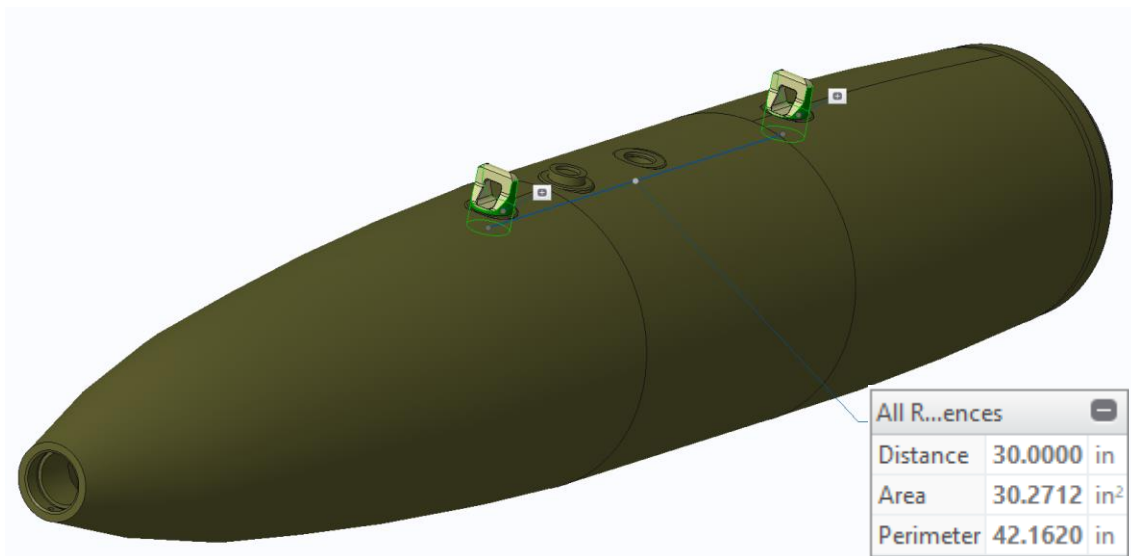


Figure 16 - 3D Model of MK-84 Ammunition [22]

3.2. Length Optimization for Mechanism Linkages

In this study designing mechanism is leading point. The design was made with gains from Chapter 1 and 2. From Chapter 1 the advantages of the literature survey is taken accounted into, and Chapter 2 guided to follow the equation and design the release mechanism.

The first step to get started is to set some values to a constant and start from the simplest to begin with. Thing that is known, it will be two connected circuit four bar mechanism, this is the starting point.

Some values must be determined before starting to calculate. The minimum input that we have to know beforehand are these below;

- Pivot Points Locations
- First and Last Position of the Hooks and Hinge

In addition, since the distance between the hooks, which is 30 inches, is taken into account and it is desired to make room for other parts in the ERU unit, a design that will occupy horizontal space rather than vertical was desired. Therefore, it is desired that the “ a_2 ” and “ a_4 ” link lengths be relatively short and the “ a_3 ” connection long. While designing, it was preferred to design the joint of the hook and the pivot points of hinge to be the same on the horizontal axis. This is because the mechanism is desired to draw relatively symmetrical loads.

The formulas are provided with the design to go step by step. It is shown in Figure 21 and Figure 22, pivot points and the angles of the first and last position is decided. Freudenstein Equation is ready to use it.

$$K_1 \cos \phi_1 - K_2 \cos \theta_1 + K_3 = \cos(\phi_1 - \theta_1) \tag{37}$$

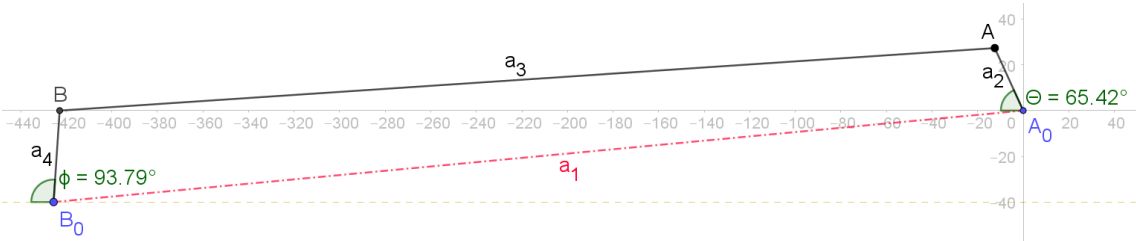


Figure 17 - First Position of Left-Hand Side of Four-Bar

$$K_1 \cos \phi_2 - K_2 \cos \theta_2 + K_3 = \cos(\phi_2 - \theta_2) \quad (38)$$

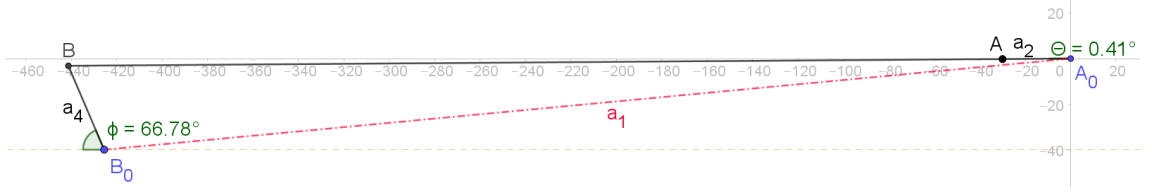


Figure 18 – Last Position of Left-Hand Side of Four-Bar

As we know in the dead center position angle of the lug does not change with respect to hinge, which means derivative of the “ ϕ ” with respect to “ θ ” should be zero. So, in order to solve three unknown equations, derivative can be used for the last Freudenstein equation which is in the dead center position of the mechanism. Last position of the mechanism will be also in dead center position. Therefore, calculation for second position can be done through dead center position.

$$\frac{d\phi}{d\theta} = 0 \quad (39)$$

$$\frac{d}{d\theta} [K_1 \cos \phi_2 - K_2 \cos \theta_2 + K_3] = \frac{d}{d\theta} [\cos(\phi_2 - \theta_2)] \quad (40)$$

$$0 - K_2 \sin \theta_2 + 0 = \sin(\phi_2 - \theta_2) \quad (41)$$

$$K_2 \sin \theta_2 = -\sin(\phi_2 - \theta_2) \quad (42)$$

To obtain “ K ” values which is length ratio of the “ a_1 ”, “ a_2 ”, “ a_3 ” and “ a_4 ”, three unknowns with three equations must be solved.

Formulas are converted to matrix format as shown below;

$$\begin{bmatrix} \cos(\phi_1) & -\cos(\theta_1) & 1 \\ 0 & -\sin(\theta_2) & 0 \\ \cos(\phi_2) & -\cos(\theta_2) & 1 \end{bmatrix} \begin{bmatrix} K_1 \\ K_2 \\ K_3 \end{bmatrix} = \begin{bmatrix} \cos(\phi_1 - \theta_1) \\ \sin(\phi_2 - \theta_2) \\ \cos(\phi_2 - \theta_2) \end{bmatrix} \quad (43)$$

$$\begin{bmatrix} K_1 \cos(\phi_1) + K_3 \\ K_1 \cos(\phi_2) + K_3 \end{bmatrix} = \begin{bmatrix} \cos(\phi_1 - \theta_1) + K_2 \cos(\theta_1) \\ \cos(\phi_2 - \theta_2) + K_2 \cos(\theta_2) \end{bmatrix} \quad (44)$$

$$K_1 [\cos(\phi_1) - \cos(\phi_2)] = \cos(\phi_1 - \theta_1) + K_2 \cos(\theta_1) - \cos(\phi_2 - \theta_2) + K_2 \cos(\theta_2) \quad (45)$$

$$K_1 = \frac{\cos(\phi_1 - \theta_1) + K_2 \cos(\theta_1) - \cos(\phi_2 - \theta_2) + K_2 \cos(\theta_2)}{\cos(\phi_1) - \cos(\phi_2)} \quad (46)$$

In line with the last step calculation, we can obtain “ K_1 ” value. Since the fixed points are predefined, “ a_1 ” can be obtained by geometrical sizing. Thus, other “ K ” values also easily obtained as well.

“ K ” values are unitless values that show the ratio of link lengths to each other. In the Chapter 2.1 detail of how these equation and representative “ K ” values are explained.

$$K_1 = \frac{a_1}{a_2} \quad K_2 = \frac{a_1}{a_4} \quad K_3 = \frac{(a_1^2 + a_2^2 - a_3^2 + a_4^2)}{2a_4a_2} \quad (47)$$

After the proportions are known, length of the links in the left-hand side of the mechanism is achieved. Since the link lengths are known, the design is done according to these values. Left-hand side of the mechanism’s first position and last position are shown in Figure 23 and Figure 24;

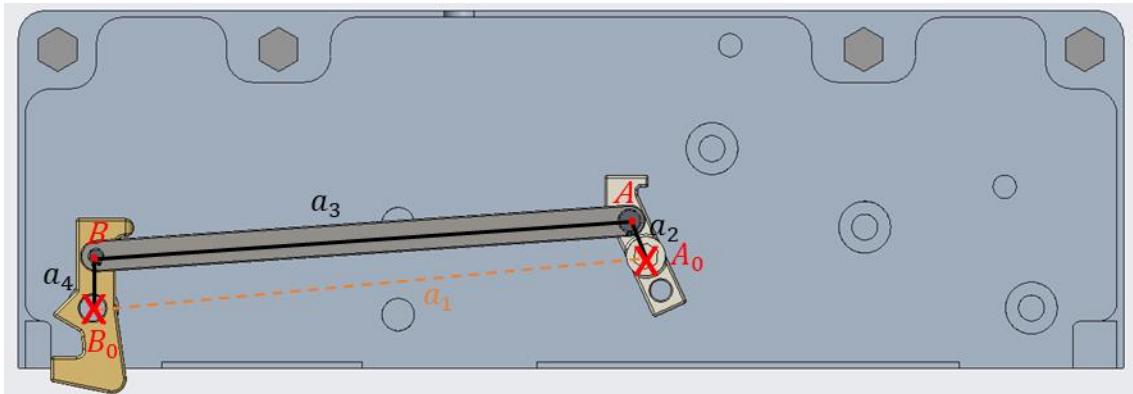


Figure 19 - First Position of Left-Hand Side of Mechanism

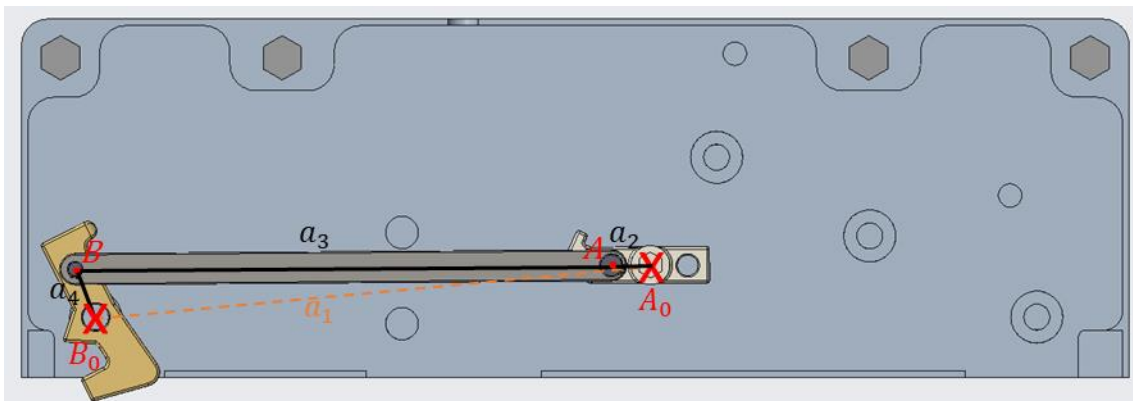


Figure 20 - Last Position of Left-Hand Side of Mechanism

After obtaining the length of the four-bar members with Freudenstein Equation and its derivatives, we can use those equations as well for the right-hand side of the mechanism. The things that must be changed are name of the K values, angles, and members. The minimum requirement is still valid, so we know first and last position of the hooks, hinges, and pivot point.

$$K'_1 \cos \phi'_1 - K'_2 \cos \theta'_1 + K'_3 = \cos(\phi'_1 - \theta'_1) \quad (48)$$

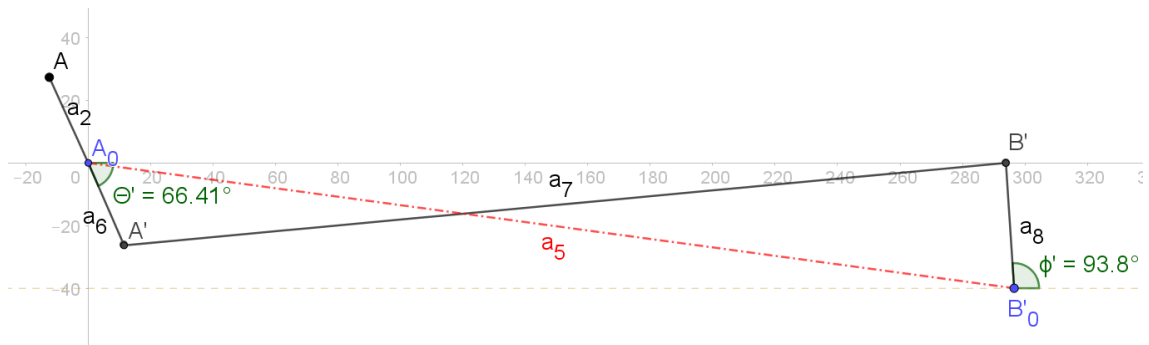


Figure 21 - First Position of Right-Hand Side of Four-Bar

$$K'_1 \cos \phi'_2 - K'_2 \cos \theta'_2 + K'_3 = \cos(\phi'_2 - \theta'_2) \quad (49)$$

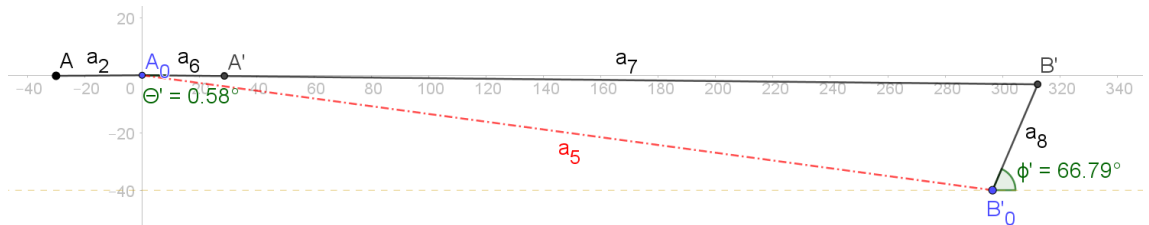


Figure 22 - Last Position of Right-Hand Side of Four-Bar

As design for the left-hand side of the mechanism, right-hand side of the mechanism will be processed the same way and dead center position rule applied for the last position of the right-hand side of the mechanism. This designing way gives a benefit that the hooks will be the same angle for the last position for the both-side of the mechanism. Since the angle interval is known, first positions of the hooks will be same as well. In order to obtain links length, the equations must be used for the right-hand side.

$$\frac{d\phi'}{d\theta'} = 0 \quad (50)$$

$$\frac{d}{d\theta} [K'_1 \cos \phi'_2 - K'_2 \cos \theta'_2 + K'_3] = \frac{d}{d\theta} [\cos(\phi'_2 - \theta'_2)] \quad (51)$$

$$0 - K'_2 \sin \theta'_2 + 0 = \sin(\phi'_2 - \theta'_2) \quad (52)$$

$$K'_2 \sin \theta'_2 = -\sin(\phi'_2 - \theta'_2) \quad (53)$$

To obtain “ K' ” values which is length ratio of the “ a_5 ”, “ a_6 ”, “ a_7 ” and “ a_8 ”, three unknowns with three equations must be solved.

Formulas are converted to matrix format as shown below;

$$\begin{bmatrix} \cos(\phi'_1) & -\cos(\theta'_1) & 1 \\ 0 & -\sin(\theta'_2) & 0 \\ \cos(\phi'_2) & -\cos(\theta'_2) & 1 \end{bmatrix} \begin{bmatrix} K'_1 \\ K'_2 \\ K'_3 \end{bmatrix} = \begin{bmatrix} \cos(\phi'_1 - \theta'_1) \\ \cos(\phi'_2 - \theta'_2) \\ \cos(\phi'_2 - \theta'_2) \end{bmatrix} \quad (54)$$

$$\begin{bmatrix} K'_1 \cos(\phi'_1) + K'_3 \\ K'_1 \cos(\phi'_2) + K'_3 \end{bmatrix} = \begin{bmatrix} \cos(\phi'_1 - \theta'_1) + K'_2 \cos(\theta'_1) \\ \cos(\phi'_2 - \theta'_2) + K'_2 \cos(\theta'_2) \end{bmatrix} \quad (55)$$

$$K'_1 [\cos(\phi'_1) - \cos(\phi'_2)] = \cos(\phi'_1 - \theta'_1) + K'_2 \cos(\theta'_1) - \cos(\phi'_2 - \theta'_2) + K'_2 \cos(\theta'_2) \quad (56)$$

$$K'_1 = \frac{\cos(\phi'_1 - \theta'_1) + K'_2 \cos(\theta'_1) - \cos(\phi'_2 - \theta'_2) + K'_2 \cos(\theta'_2)}{\cos(\phi'_1) - \cos(\phi'_2)} \quad (57)$$

In line with the last step calculation, we can obtain “ K'_1 ” value. Since the fixed points are predefined, “ a_5 ” can be obtained by geometrical sizing. Thus, other “ K' ” values also easily obtained as well.

“ K' ” values are unitless values that show the ratio of link lengths to each other. In the Chapter 2.1 detail of how these equation and representative “ K' ” values are explained.

$$K'_1 = \frac{a_5}{a_6} \quad K'_2 = \frac{a_5}{a_8} \quad K'_3 = \frac{(a_5^2 + a_6^2 - a_7^2 + a_8^2)}{2a_8 a_6} \quad (58)$$

After the proportions are known, length of the links in the left-hand side of the mechanism is achieved. Since the link lengths are known, the design is done according to these values. Right-hand side of the mechanism’s first position and last position are shown in Figure 27 and Figure 28;

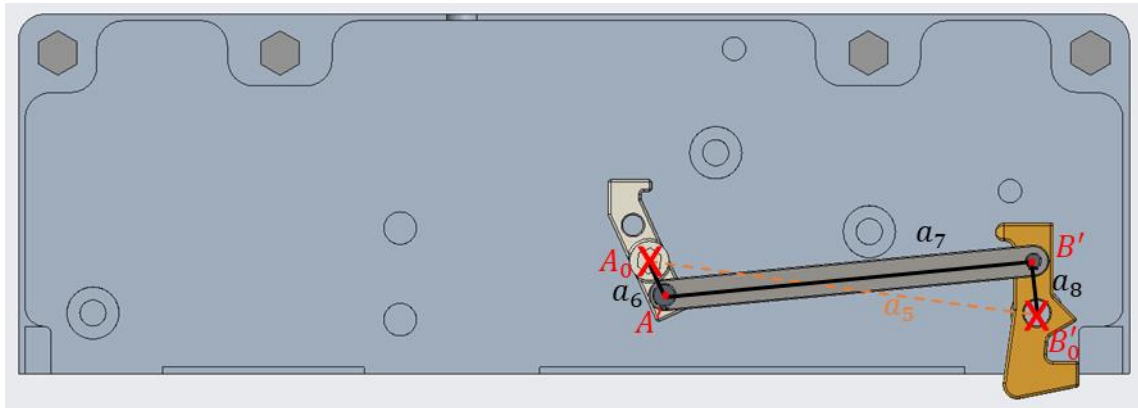


Figure 23 - First Position of Right-Hand Side of Mechanism

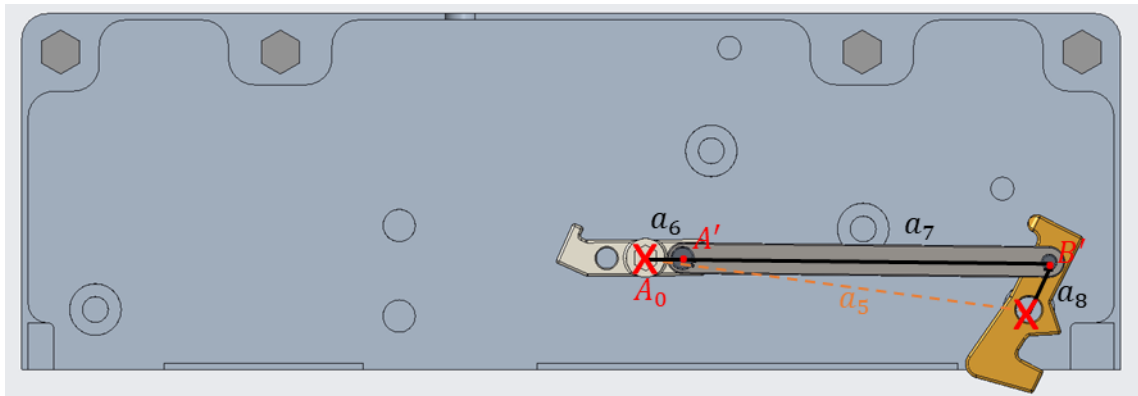


Figure 24 - Last Position of Right-Hand Side of Mechanism

Both side of the mechanism's rigid member lengths are known. So, the optimized two mechanisms are ready to compile. But the thing that should be aware of the design of hinge before the compiling. Since the last position of " a_2 " which is the final angle of the " θ " and the last position of " a_6 " which is the final angle of the " θ " are slightly different than each other, the hinge cannot be 90° . This means that between " a_2 " and " a_6 ", it should be a constant angle which is " φ ".

According to the angles and dimensions of the rigid body members, 3D mechanism is created. Compiled version of the right-hand side and the left-hand side are shown in Figure 29 and Figure 30;

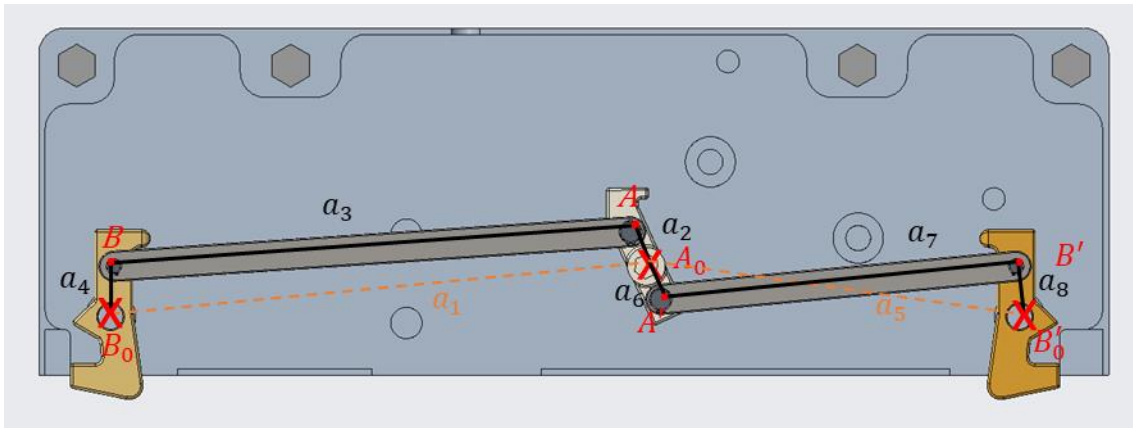


Figure 25 - First Position of Compiled Mechanism

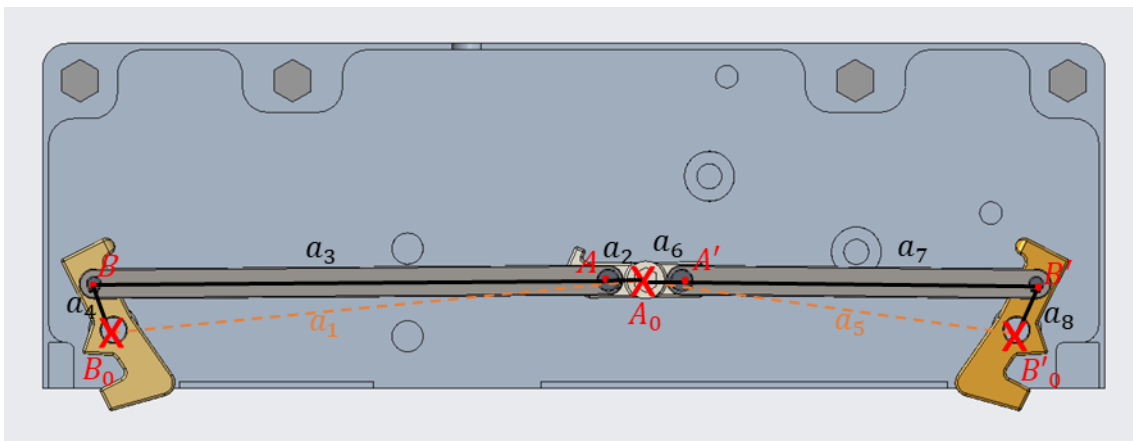


Figure 26 – Last Position of Compiled Mechanism

Compiled mechanism is created in 3D CAD program. The links are converted from 2D to 3D. Depending on the actuation method and the counterpart like a lug which is shown in Figure 12, the hinge part has a head protrusion for impact and hook shape is designed has taken account into with lug dimensions.

If we evaluate the left side of the mechanism;

- First of all, “ A_0 ” and “ B_0 ” points were determined in terms of being suitable for the handles of the ammunition and relatively symmetrical mechanism. And from these coordinates, the length of “ a_1 ” can be obtained from the beginning.

- While determining first and last angles of “ a_2 ” and “ a_4 ”, we have some fixed boundaries. One of them, the design of the hook that will enter to lug part is fixed, approximately due to the shape of the lug. The working range of “ a_4 ” was also found to be sufficient for the hook to open in the range of approximately “25-30” degrees in general ERU designs, and therefore the working range in the design was determined as “27” degrees.
- It was thought that the first angle of “ a_4 ” would be more than “90” degrees, since the opening direction of the hook, and “93.8” degree was chosen to start a little further back. Based on this, it was determined that the hook, which has an operating range of “27” degrees, will be the final position of “66.8” degrees.
- In order for the hook to not wait in the direction that will help opening while carrying the ammunition, it is thought that there should be an angle of over “90” degrees. Therefore, “93.8” degrees was chosen to start which is a little further back. Based on this, it was determined that the hook, which has an operating range of “27” degrees, will be the final position of “66.8” degrees as seen in Figure 22.
- It was determined that the middle hinge should be less than “90” degrees in its initial state. The value is arbitrarily chosen to be about “65.4” degrees so that this part is the part to hit on the head and makes it easier to rotate under the influence of force. As the final angle, the estimated length of “ a_4 ” is chosen as a length equal to the bottom of the hook part, and it is known that the correct value will be found with the length optimization made in MATLAB. Here, a straight line is drawn from the pivot point of hinge to the end of the link “ a_4 ” while the link “ a_4 ” is at its final position. Angle at the final position of “ a_2 ” is approximately is obtained as “-0.4” degrees. The reason we want to leave our mechanism like this in the last position is because we want the mechanism to be in the dead center position, and in this way “ a_3 ” and “ a_2 ” stay on the same straight line and cannot go further. This is a factor that makes it easy for us to find the link lengths through the coefficients K, as can be seen in the matrix calculations in Equation 43.

The a values found by the K values obtained from the matrix calculations written in MATLAB are as follows;

$$K_1 = 14.24$$

$$K_2 = 10.68$$

$$K_3 = 6.66$$

$$a_1 = 427.41 \text{ [mm]}$$

$$a_2 = 29.99 \text{ [mm]}$$

$$a_3 = 411.32 \text{ [mm]}$$

$$a_4 = 40.00 \text{ [mm]}$$

It should be known that most of the calculations made in the left four-arm mechanism are also used in the right mechanism, and therefore the extra ones will be evaluated.

If we evaluate the left side of the mechanism;

- Here, it should be known that " a_2 " and " a_6 " remain constant on the same arm, therefore the two mechanisms must be combined. Even if the angle of entry of the mechanism on the right is different, " θ' " remains a " θ " dependent angle since they are on the same hinge.
- The exit angle and working range of the hook should also be the same as the left mechanism.
- There is a angle gap between " a_2 " and " a_6 " in the last angle, which is the result of the straight line extended from " a_6 " to " a_8 " in the final position of the mechanism. The fact that if " a_2 " and " a_6 " are in the same horizontal plane causes the mechanism on the right to not be able to stay in the dead center position. This shows that there is a total angle difference of "1" degree from the horizontal between " a_2 " and " a_6 " when the middle hinge is in its final position. In the design, when both links are in the final position, an angle of "1" degree is given and both mechanisms are in the dead center position at the same time.

The a values found by the K' values obtained from the matrix calculations written in MATLAB are as follows;

$$K'_1 = 10.43$$

$$K'_2 = 7.47$$

$$K'_3 = 5.01$$

$$a_5 = 299.22 \text{ [mm]}$$

$$a_6 = 28.68 \text{ [mm]}$$

$$a_7 = 283.63 \text{ [mm]}$$

$$a_8 = 40.00 \text{ [mm]}$$

3.3. Components of ERU

In this study, the munition release unit is design with optimized two closed circuit four-bar mechanisms and one actuation mechanism. The system includes some parts which are shown and written in Figure 31 and Table 1;

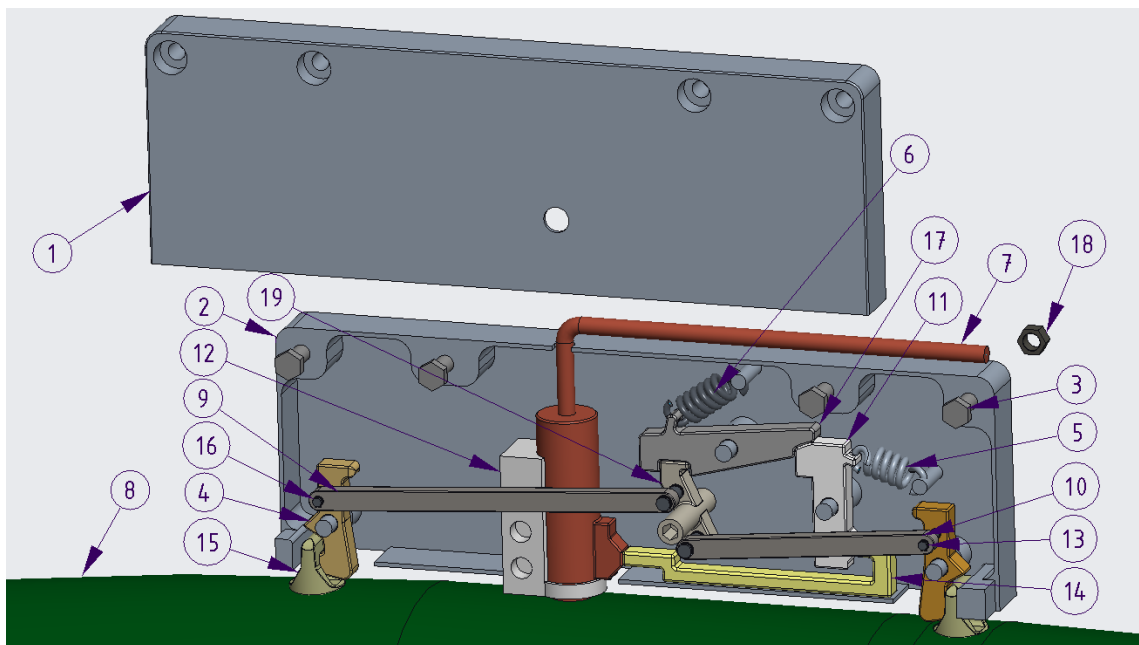


Figure 27 - Exploded View of System

1	2	3	4	5
Front Plate	Back Plate	Screws/Bolts	Hooks	Spring (Compression)
6	7	8	9	10
Spring (Tension)	Pneumatic	Ammunition/Bomb	Arm 1	Arm 2
11	12	13	14	15
Lock Part 2	Pneumatic Holder	Circlips	Tube	Lugs
16	17	18	19	
Pins	Lock Part 1	Nuts	Hinge	

Table 1 - Part Names

3.4. Working Principle of Mechanism

The system has a mechanism which allow to release munition when the actuation occurred. The “Front Plate” is transparency view to see clearly all the mechanism in the ERU, the general view of the system is shown in Figure 32;

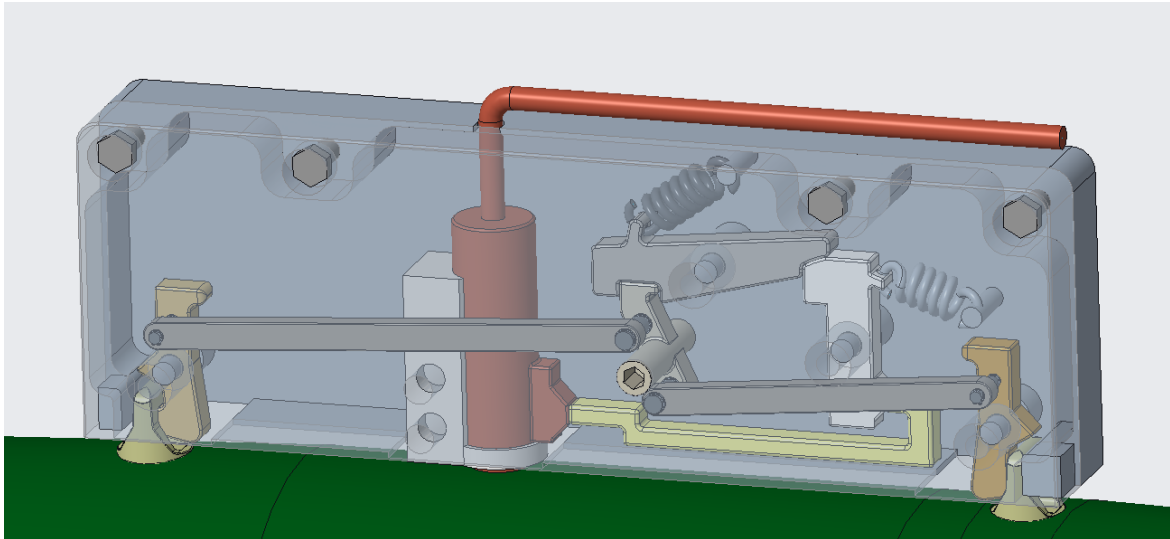


Figure 28 - General View of System

1. All set up position of the mechanism and munition, as it is shown in Figure 33;

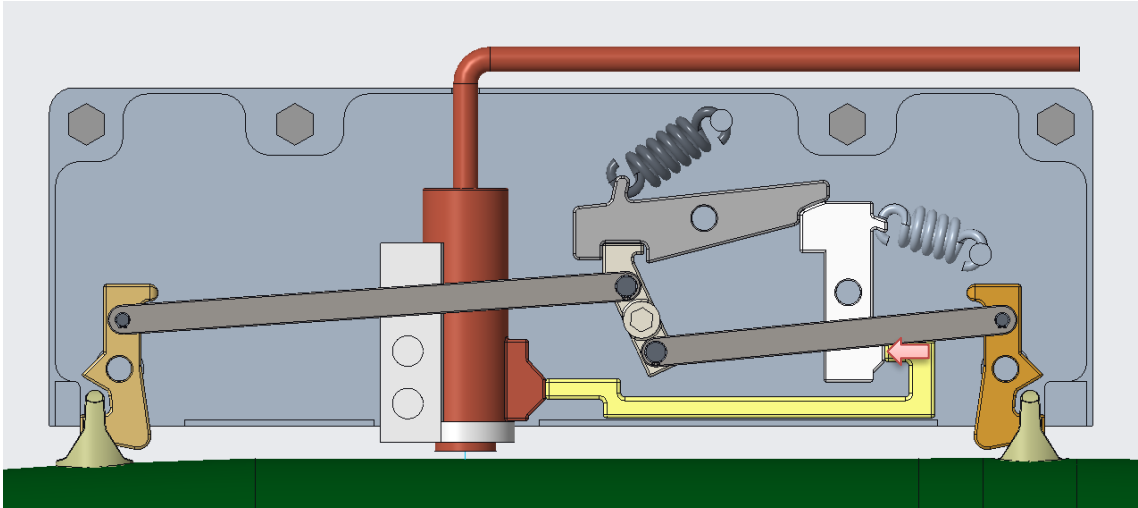


Figure 29 – Installed Position of the ERU

2. Actuation occurred by “Pneumatic” and goes through “Tube”. Impact occurs in the face of the “Lock Part 2” as a force to turn it clockwise, as it is shown in Figure 34;

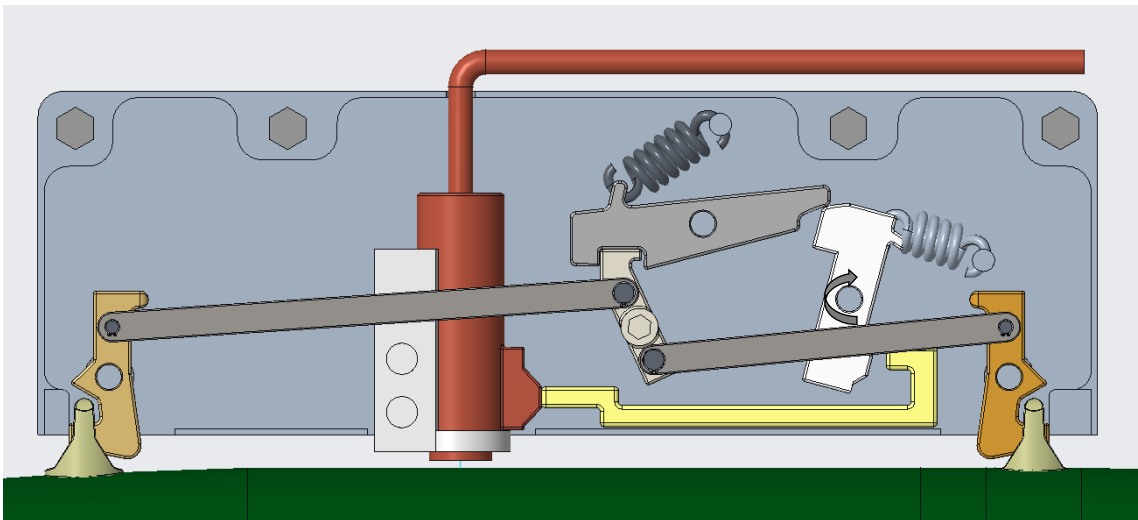


Figure 30 - Pneumatic Actuation

3. After enough rotational movement happened, “Lock Part 1” will gain a freedom to rotate to clockwise direction since the tension spring is preloaded. Also, the design of “Part Lock 1” has two important feature which are let the release mechanism start to rotate with pushing the head of “Hinge” and lock the release mechanism as holding the head of “Hinge”, as it is shown in Figure 35;

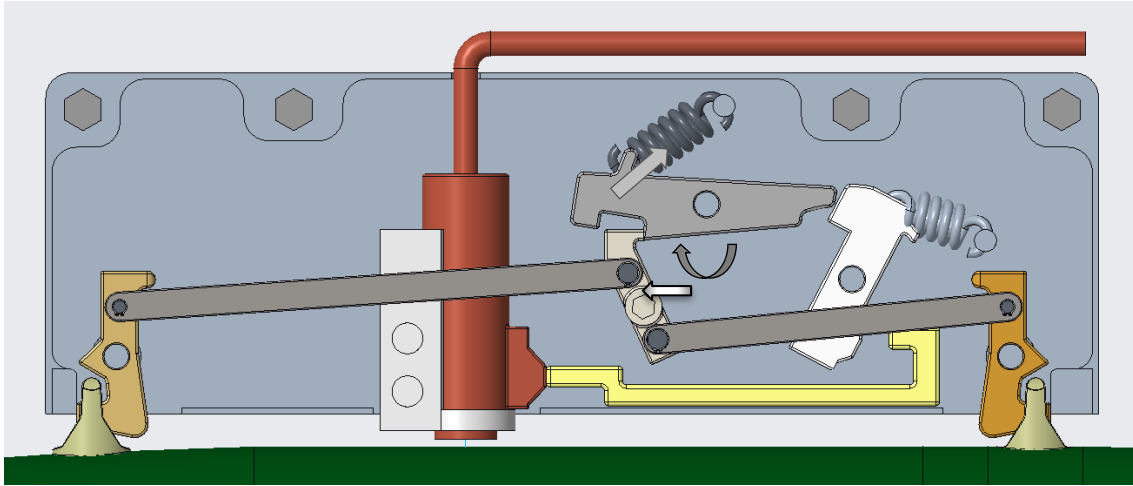


Figure 31 - Impulse from Lock Mechanism to Hinge

4. "Hinge" is activation point of the release mechanism. When the locked "Hinge" got first touch, it will start to rotate with getting impact from "Lock Part 1" and mechanism starts to rotate all linkages and hooks to release munition, as it is shown in Figure 36;

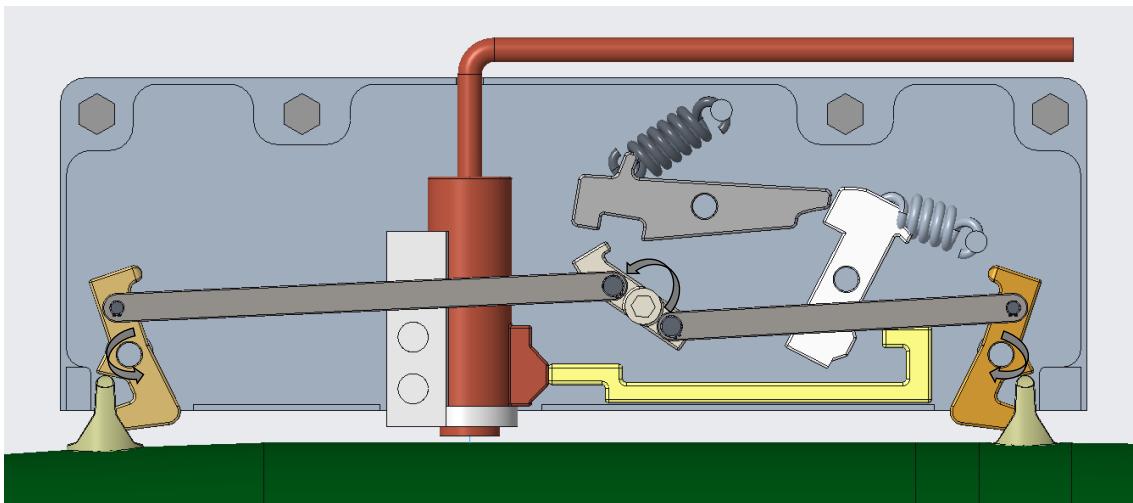


Figure 32 - Release Mechanism Movement

5. Release of the munition occurs, as it is shown in Figure 36;

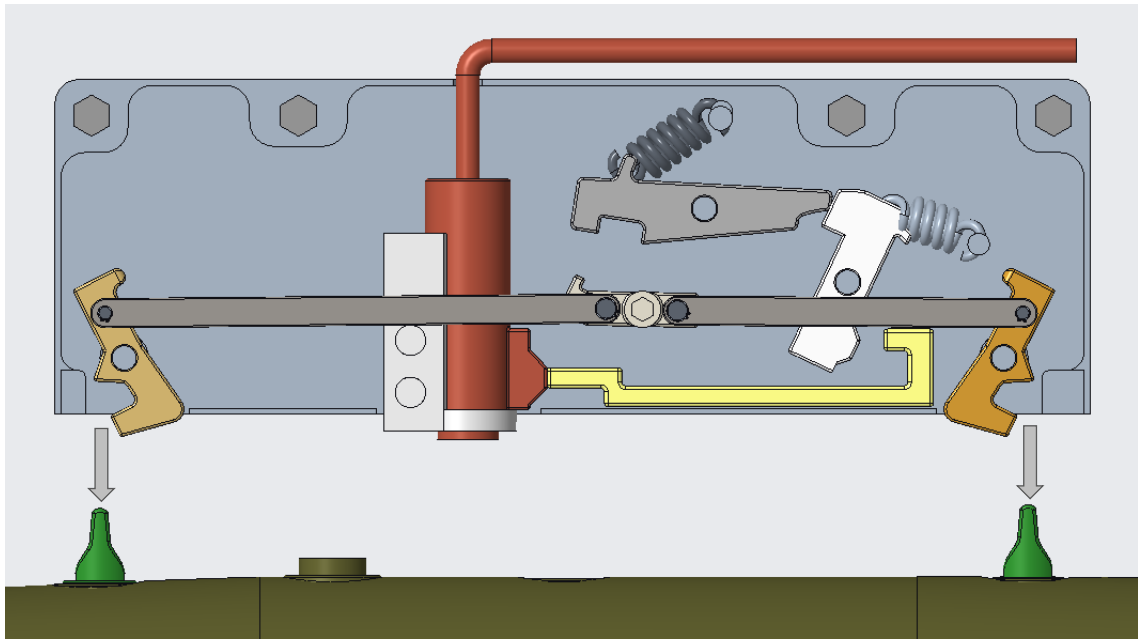


Figure 33 - Release of Ammunition

3.5. Detail System Knowledge of Input Data and Parts

Fighter aircraft are equipped ammunition release units Due to motion is needed for the mechanism triggered, actuation should be required.

The “Spring (Tension)” is preloaded as stretched while it is set up. It is ready to give a movement to “Lock Part 1” when “Lock Part 2” actuated and move depending to pneumatic actuation. In the Figure 38, there is a 3D model of the “Spring (Tension)”.



Figure 34 - 3D Model of Tension Spring (6)

Tension Spring (6):

$$k_{\text{TensionSpring}} = 20 \text{ [N/mm]}$$

Preloaded Length of the Tension Spring ≈ 96 [mm]

Unloaded Length of the Tension Spring = 80 [mm]

The “Spring (Compression)” is preload as itself while it is in free length since it is compression spring. Immediately after the pneumatic implement a force to “Lock Part 2” to turn it clockwise, “Spring (Compression)” tries to stay in its free length since it will squeeze. So, compression spring pushes the “Lock Part 2” back in position until it remains same length. In the Figure 39, there is a 3D model of the “Spring (Compression)”.

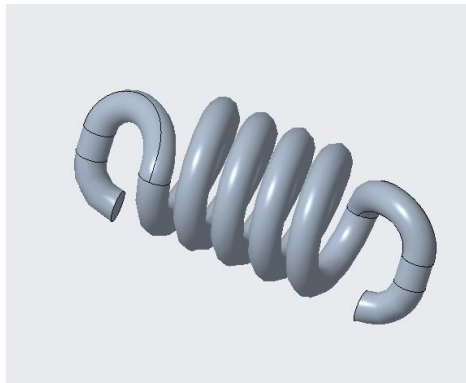


Figure 35 - 3D Model of Compression Spring

Compression Spring (5):

$k_{\text{CompressionSpring}} = 20$ [N/mm]

Unloaded Length of the Tension Spring = 82 [mm]

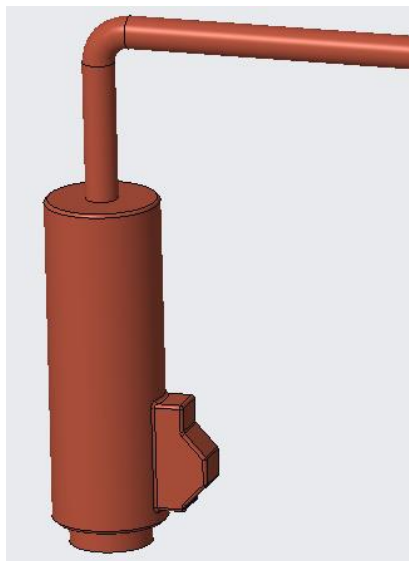


Figure 36 - 3D Model of Pneumatic Supply

Pneumatic Supply Pressure Level = 1 [bar] = 10^5 [Pa]

This type of cold gas sources in the aircraft is stored pressurized gas up to 350[bar] in ambient room temperature as we can see in Figure 41.

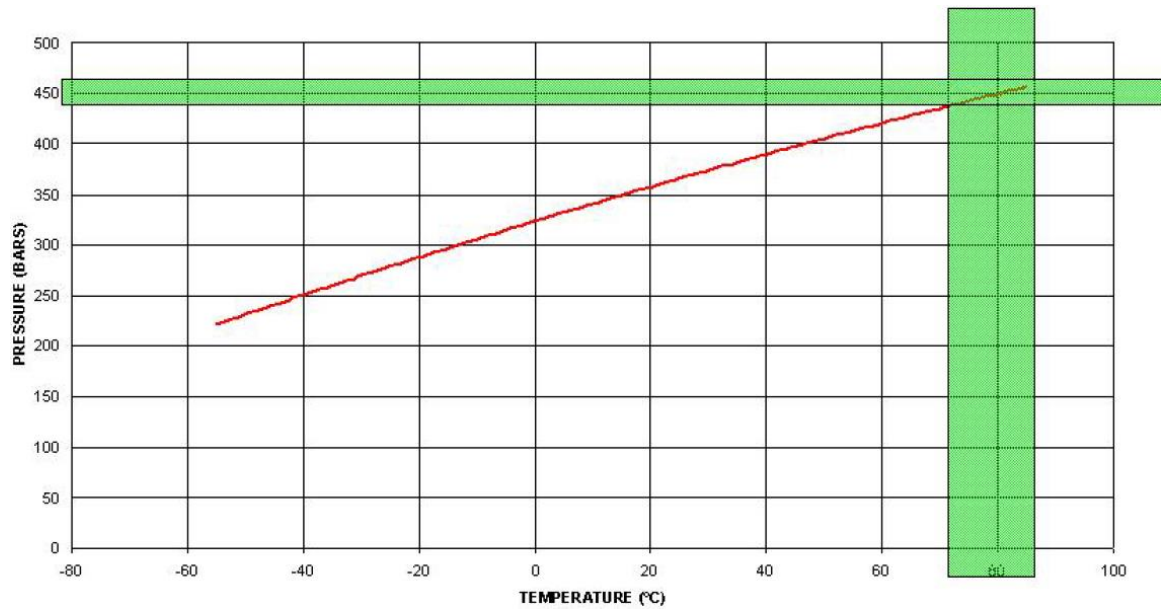


Figure 37 - Pressure Level in Gas Storage [24]

There is important part which is “Lock Part 2”. This part more than one property which are;

- One face of the part is facing the pneumatic force.
- One hanger hole feature which the “Spring (Compression)” located.
- The upper circular face blocks the “Lock Part 1”.

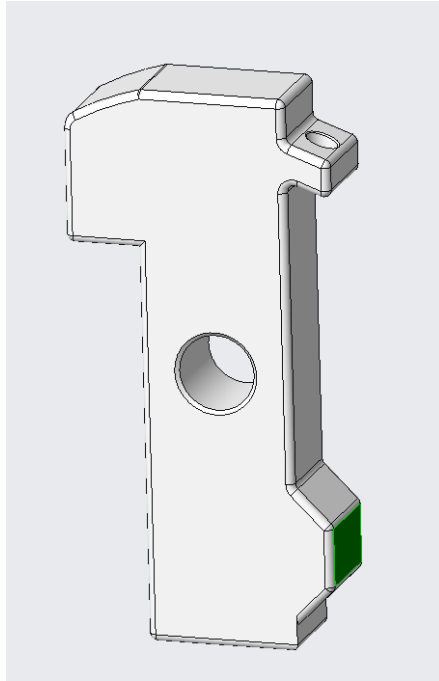


Figure 38 – 3D Model of Lock Part 2

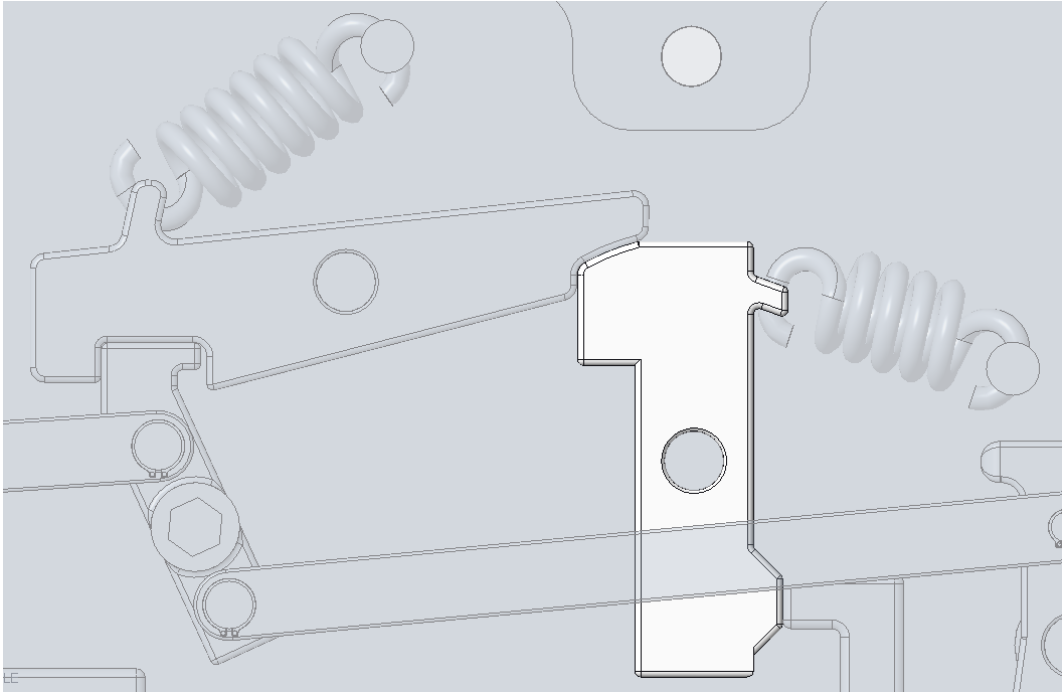
The area of the face that is facing to pneumatic is important. According to the area of the face, we can calculate that how much force it will apply to this face when 10[bar] implement by pneumatic gas tank.

Area of the Part (Green Face) $\approx 338.5 \text{ [mm}^2\text{]}$

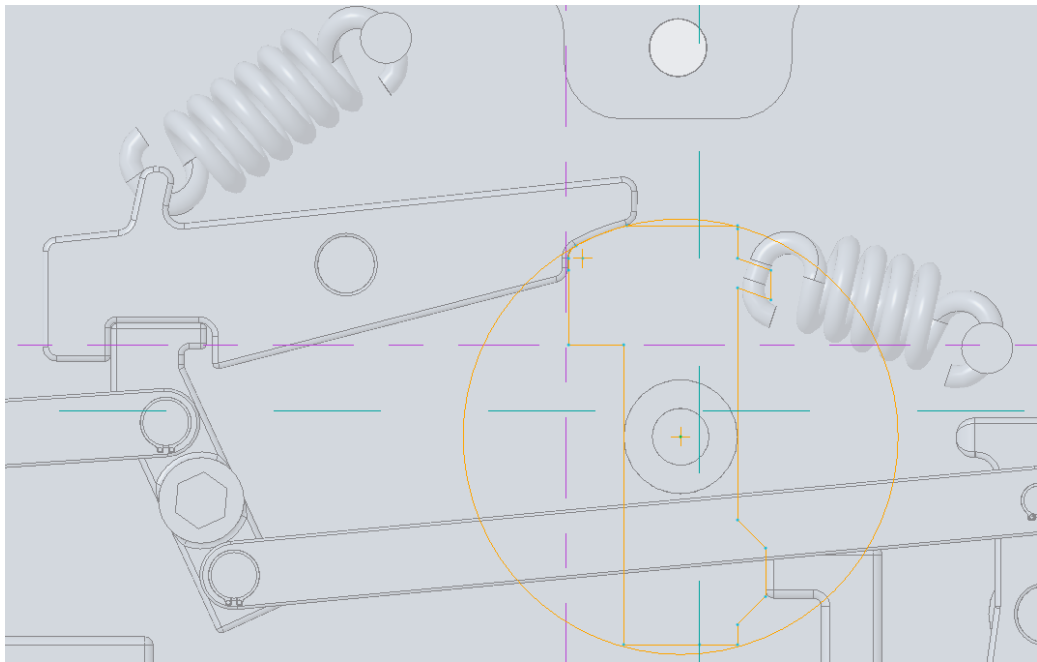
Pneumatic Supply Pressure Level = 10 [bar] = 10^6 [Pa]

$$\text{Force [N]} = \text{Pressure [Pa]} * \text{Area [m}^2\text{]} \rightarrow 10^6 * 338,5 \times 10^{-6} = 338,5 \text{ [N]} \quad (59)$$

Also, for the design of this part has one special thing that we can mention, the curvature face under the “Lock Part1” has same circular origin with its fixed pivot point. So, when the actuation starts, “Lock Part2” smoothly turning over clockwise and does not ever push the “Lock Part1” to counterclockwise. Therefore, while the “Lock Part2” is set up, the beginning of the mechanism already set up too. In the Figure 43 the 3D model of “Lock Part2” and the sketches of it shown.



(a)



(b)

Figure 39 - (a)3D Model of Lock Part2 (b)Sketches of Lock Part2

There are friction forces on Lock Part2 of Compression Spring and Lock Part1 that prevent the necessary pressure force to start the reaction from turning Lock Part 2.

Here, apart from the Force analysis to be made in ANSYS, a hand calculation is made, and it is calculated whether the pneumatic force can defeat the opposing forces or not. A calculation will be made on the moments to be formed in the direction of rotation of the forces shown below.

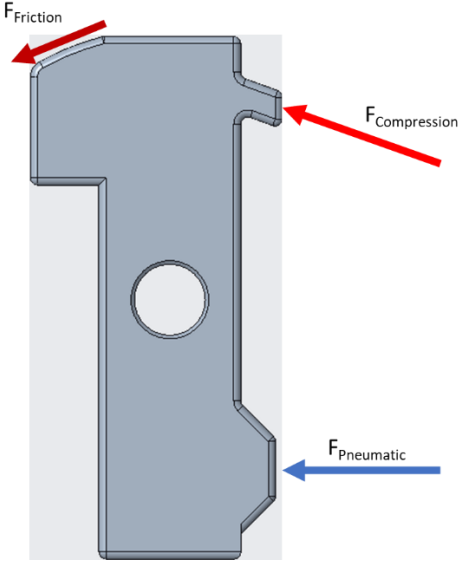


Figure 40- Representative Force on Lock Part 2

The frictional force from the tension spring comes from the vertical force, which is on Lock Part 2;

$$F_{TensionSpring, y} = F_{TensionSpring} * \cos (57) = 325 * 0.544 = 176.58$$

$$F_{Friction} = k * N * \cos(68.76) = 0.6 * 176.58 = 38.40 \text{ [N]}$$

Horizontal force from the pressure spring on Lock Part 2;

$$F_{CompressionSpring} = k * x = 20 * 17 = 340 \text{ [N]}$$

$$F_{CompressionSpring, x} = F_{CompressionSpring} * \cos (15) = 340 * 0.544 = 328 \text{ [N]}$$

This value is calculated over the displacement amount of the compression spring, which is enough to open geometrically.

$$\begin{aligned} \text{Moment} &= -38.40\text{[N]} * 20\text{[mm]} - 328\text{[N]} * 50\text{[mm]} + 338\text{[N]} * 53 \text{ [mm]} \\ &= - 768 - 16400 + 17914 \\ &= 746 \text{ [N*mm] CW} \end{aligned}$$

As seen in this simple hand calculation, it is seen that the pneumatic pressure overcomes the counter forces for the clockwise movement. At the same time, in this force analysis made in ANSYS, it is seen that the pneumatic pressure is sufficient to open the system.

4. KINEMATIC ANALYSIS OF EJECTOR RELEASE UNIT

4.1. Angle, Velocity and Acceleration (Kinematic) Analyzes Outputs

4.1.1. Numerical Analysis in MATLAB

Under this title numerical analyzes outputs are shown and explained. Numerical analyzes performed in MATLAB software.

As a reminder of mechanism while examining the graph, GeoGebra output is located;

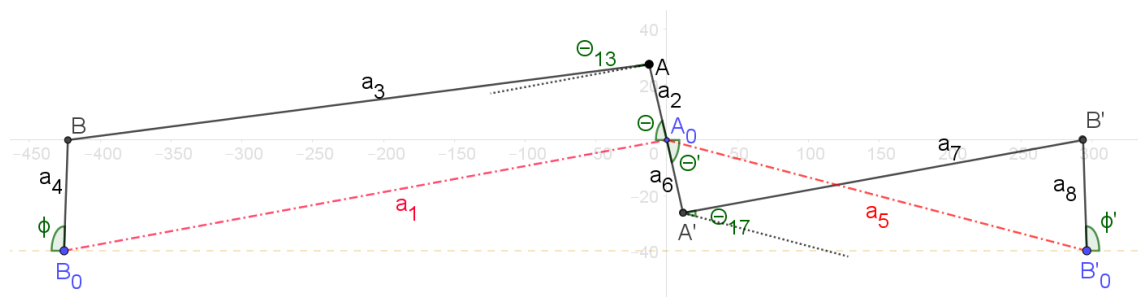


Figure 41 – Angles of Mechanism

4.1.1.1. Angle Analyzes

- In Figure 46, depending on input angles which is “ θ ”, through equations in Chapter 2.2, “ θ_{13} ” can be obtained.

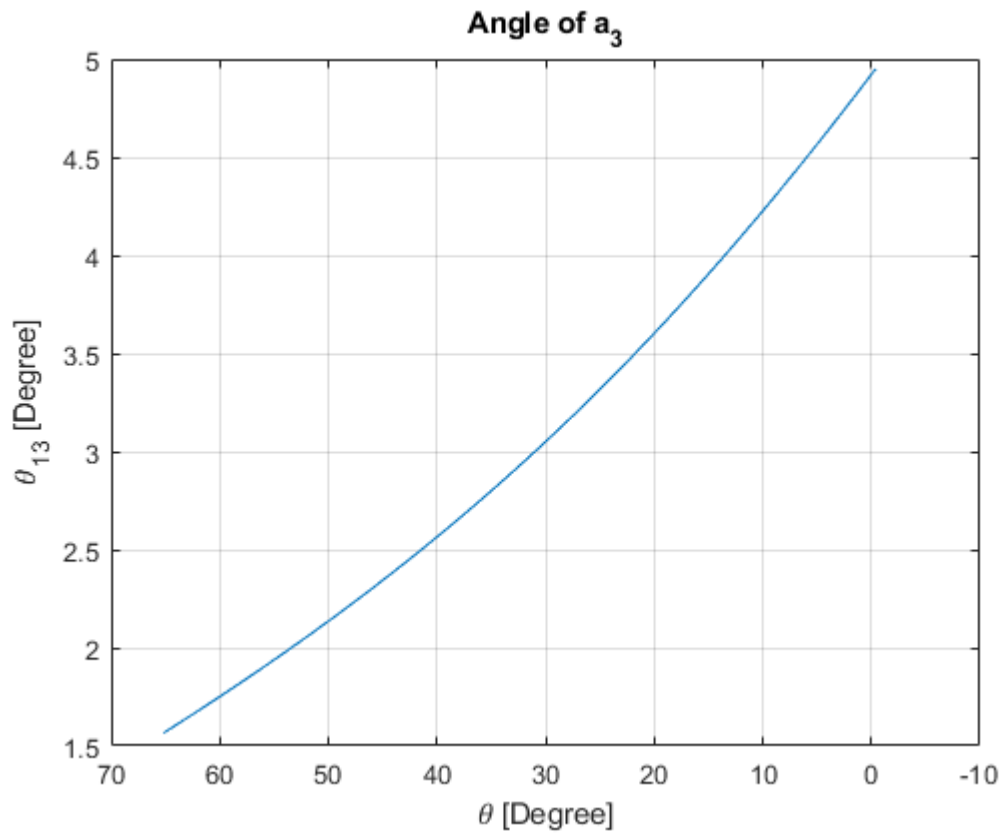


Figure 42 - Angle Range of “a₃”

- In Figure 47, depending on input angles which is “ θ ”, through equations in Chapter 2.2, “ θ_{17} ” can be obtained.

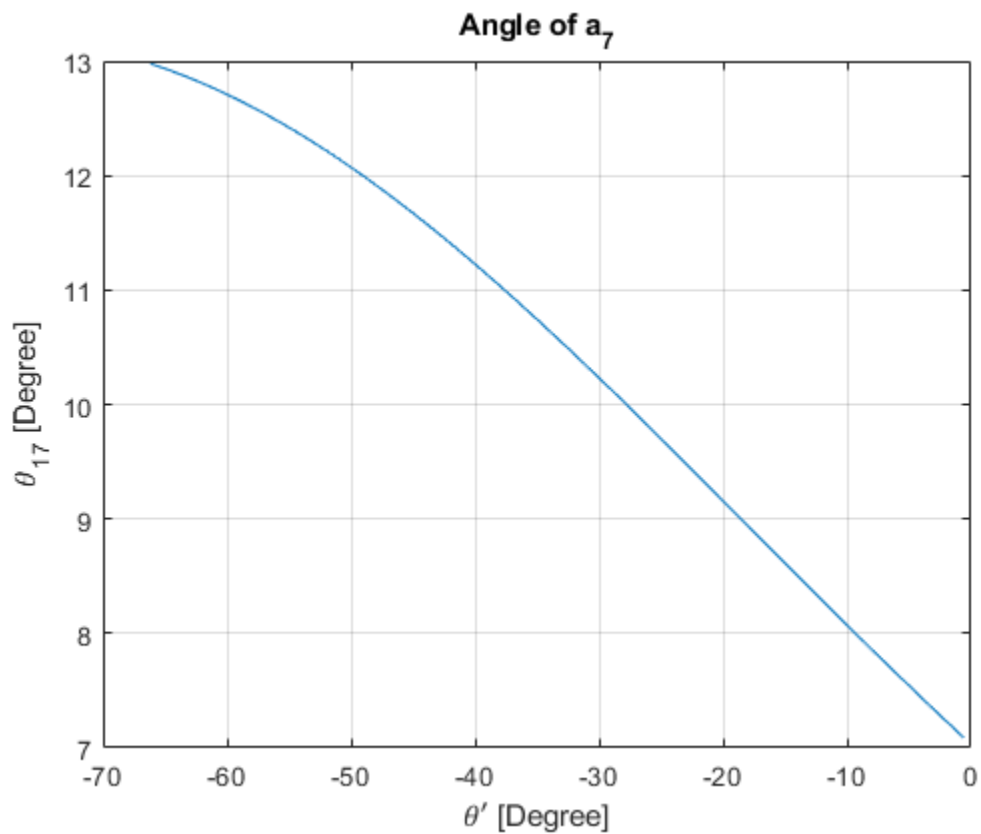


Figure 43 - Angle Range of “a₇”

- From transmission angle point of view, this is kind of scale about how good the mechanism is. The transmission angle mostly deviate from 90°. General knowledge about transmission angles, it should not be more than 40° or 50° deviation, otherwise mechanism can be locked. It is preferred that it is exceed not to much, as it shown in Figure 48, deviation is not quite much and will not be locked in any case. In upper graph shows transmission angle for left four-bar mechanism and bottom graph shows transmission angle for right four-bar mechanism.

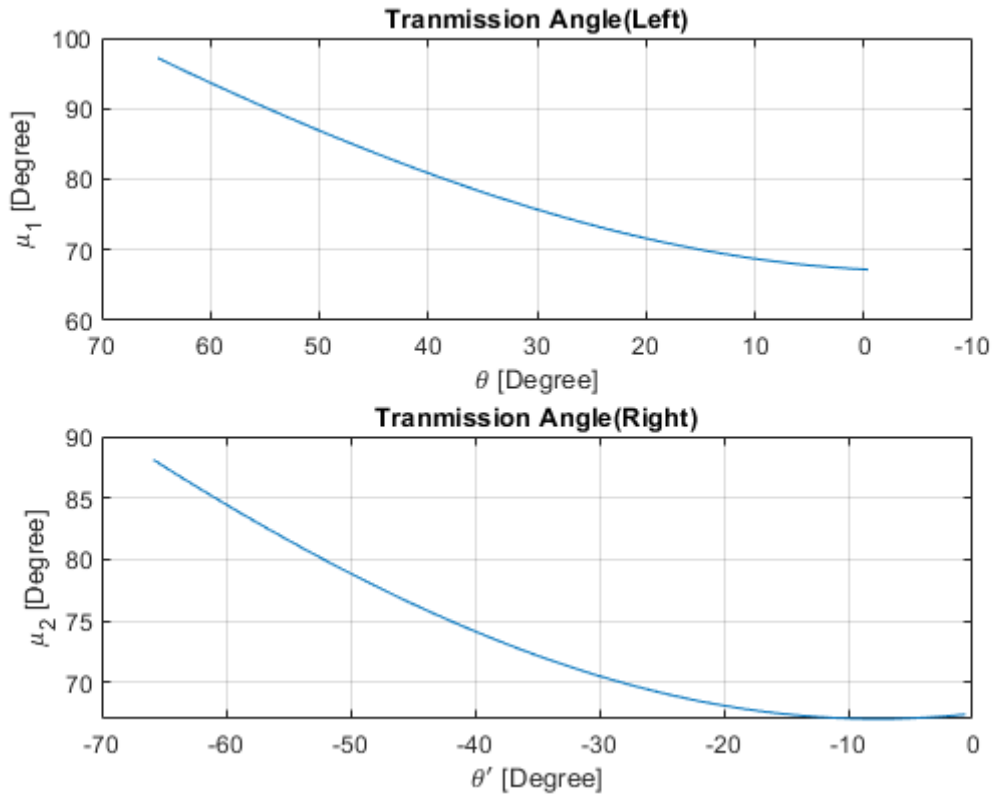


Figure 44 - Transmission Angles

- In Figure 49; after obtaining four-bar rod lengths for left-hand side , every angle should be examined. Both hook angle should be very close since it should be opened at the same time. Therefore every angle in the working range is taken into attention. Depending on the input angles which is “ θ ”, output angles which is “ θ_{14} ” obtained with numerical calculations. Step size is considered before all the calculations explained in Chapter 2.1.

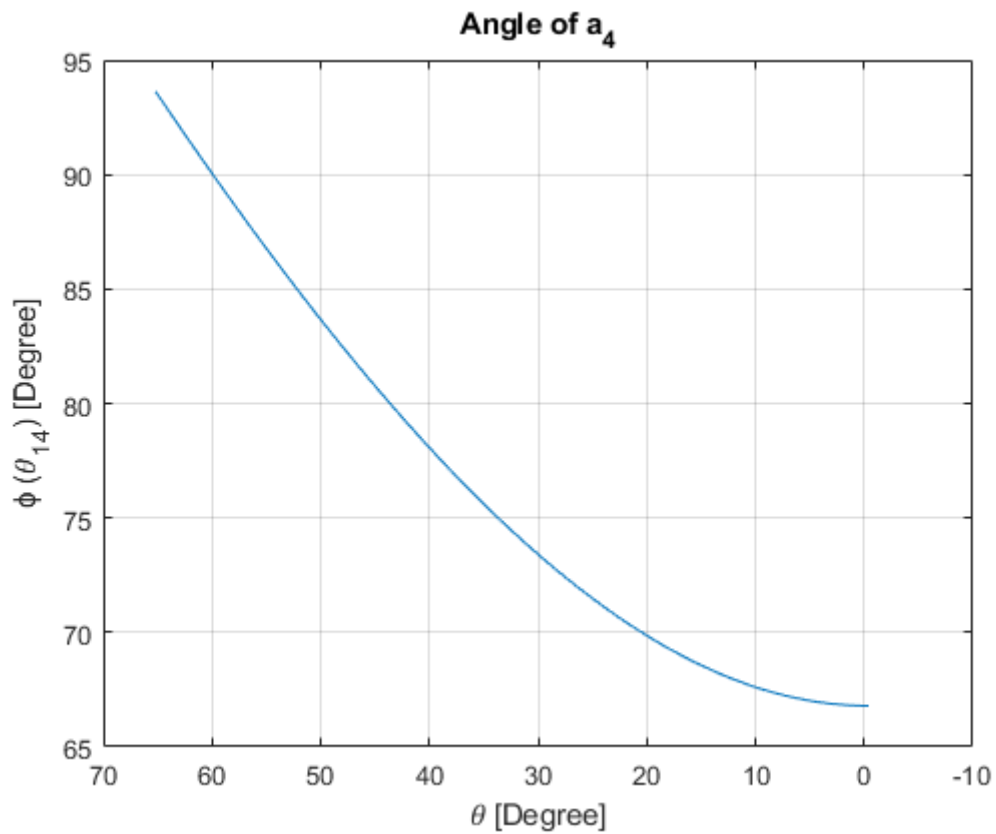


Figure 45 – Angle Range of “a₄”

- In Figure 50; after obtaining four-bar rod lengths for right-hand side, every angle should be examined. Both hook angle should be very close since it should be opened at the same time. Therefore every angle in the working range is taken into attention. Depending on the input angles which is “ θ ”, output angles which is “ θ_{18} ” obtained with numerical calculations. Step size is considered before all the calculations explained in Chapter 2.1.

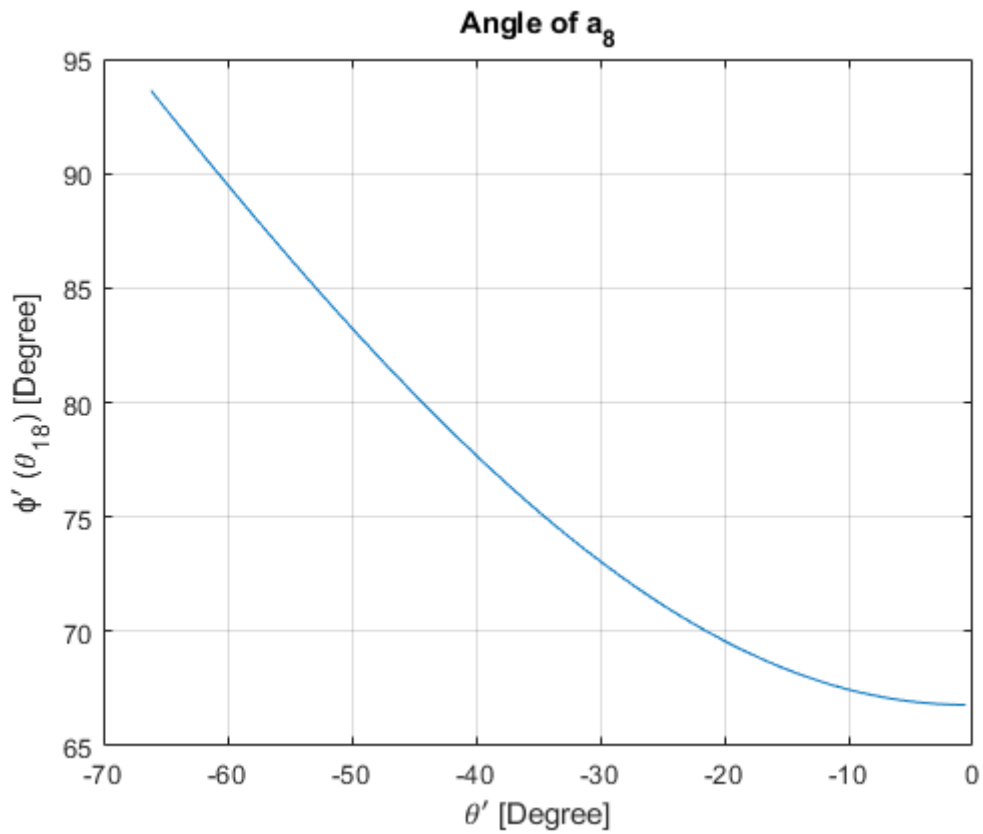


Figure 46 – Angle Range of “a8”

- One of the aim of this thesis is to ensure that both of the hooks should be rotate approximately same since release of the lugs should be released at the same level. So it is obvious from the graph after subtraction of the angles from each other, it can be interpreted as both of the hooks are opening almost at the same level. Since achievement of all length is performed on death position while it is open. Both angles are hundred percent same when both hooks are fully opened and difference exactly “0” degree, which as we can see in Figure 49.

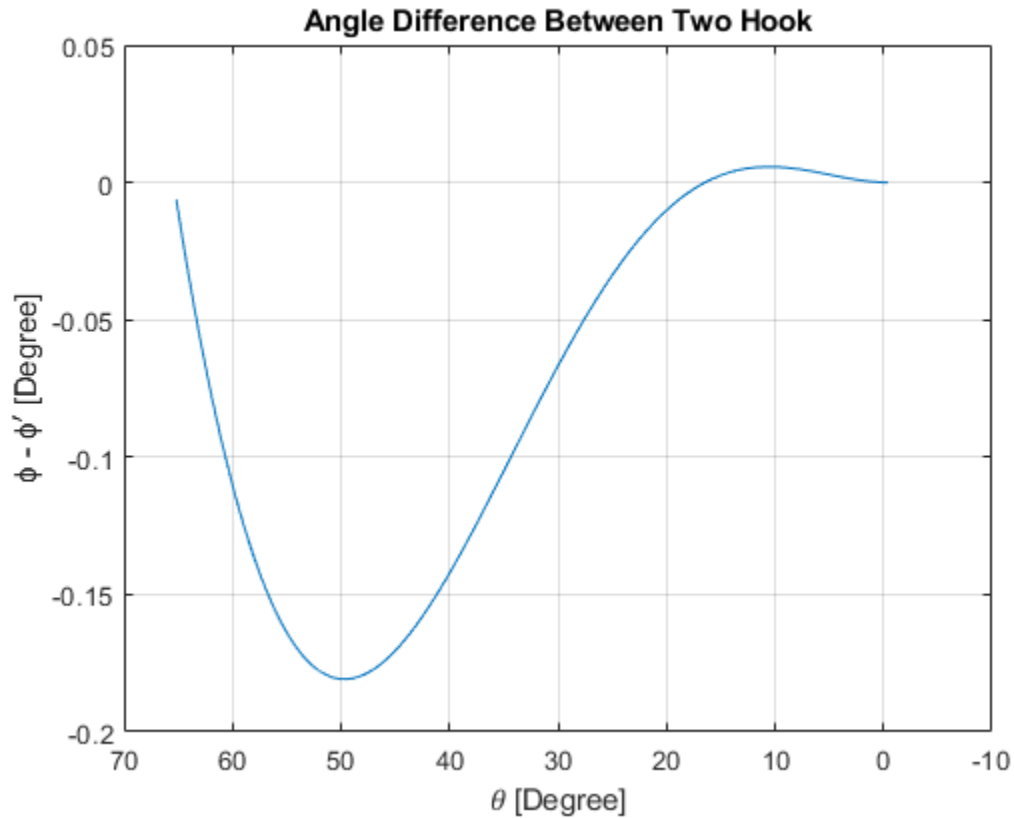


Figure 47 - Angle Difference Between Two Hook

4.1.1.2. Angular Velocity Analyzes

- As it is explained in Chapter 3.4, whole system has one input from pneumatic action. Actuation will be performed by implementing pressurized gas to “Lock Part 2”’s flat face. After this gas release happens, “Lock Part 2” starts to turn and “Lock Part 1” rotates by pulling with “Spring 1”. With its turn, “Lock Part 1” hits head of the ”Hinge” and kinematic action is occurred which leads to velocity. In Figure 52, angular velocity of “ a_2 ” which is “ ω_{12} ” as it is seen.

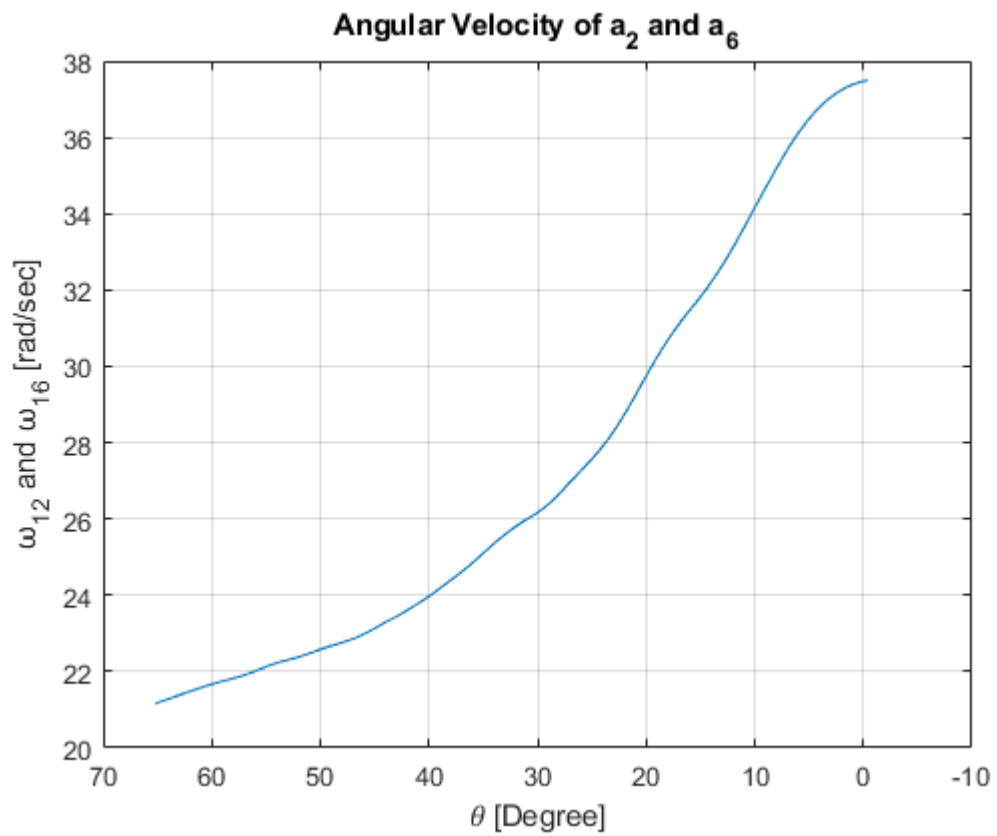


Figure 48 - Angular Velocity of “a₂” and “a₆”

- Numerical equations, which is explain under Chapter 2.2, are used to obtain “ω₁₃” depending on angles and input angular velocity of “a₂”.

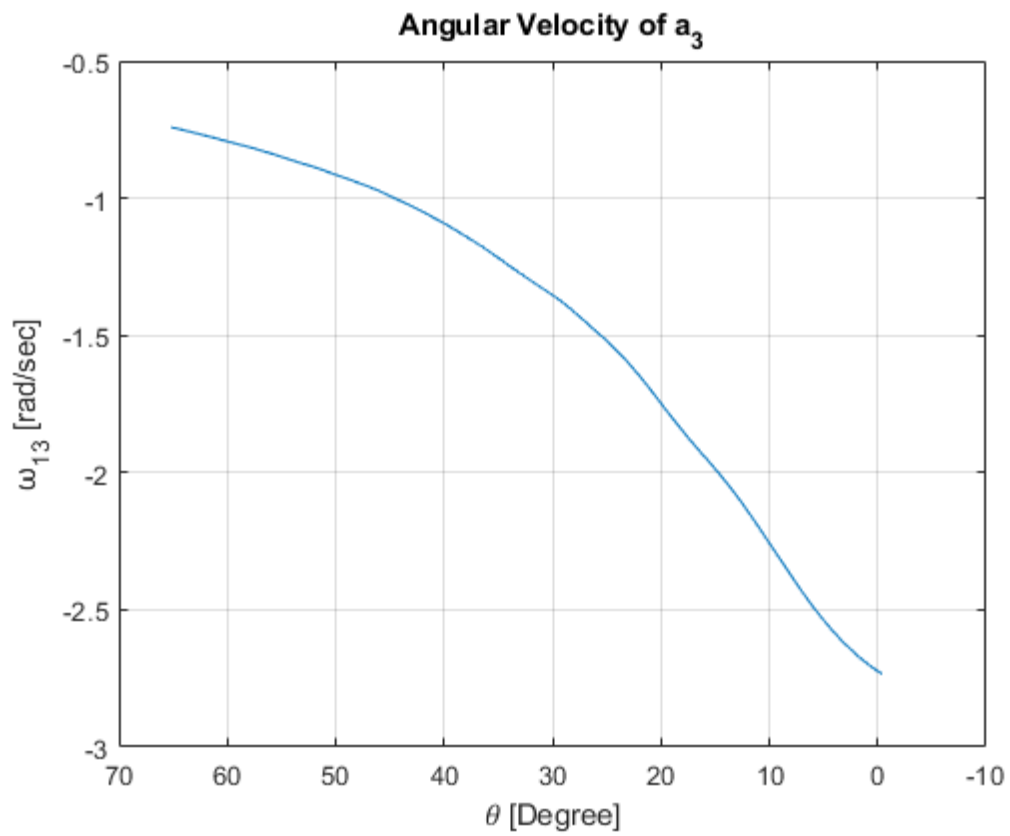


Figure 49 - Angular Velocity of “ a_3 ”

- Numerical equations, which is explain under Chapter 2.2, are used to obtain “ ω_{14} ” depending on angles and input angular velocity of “ a_2 ”.

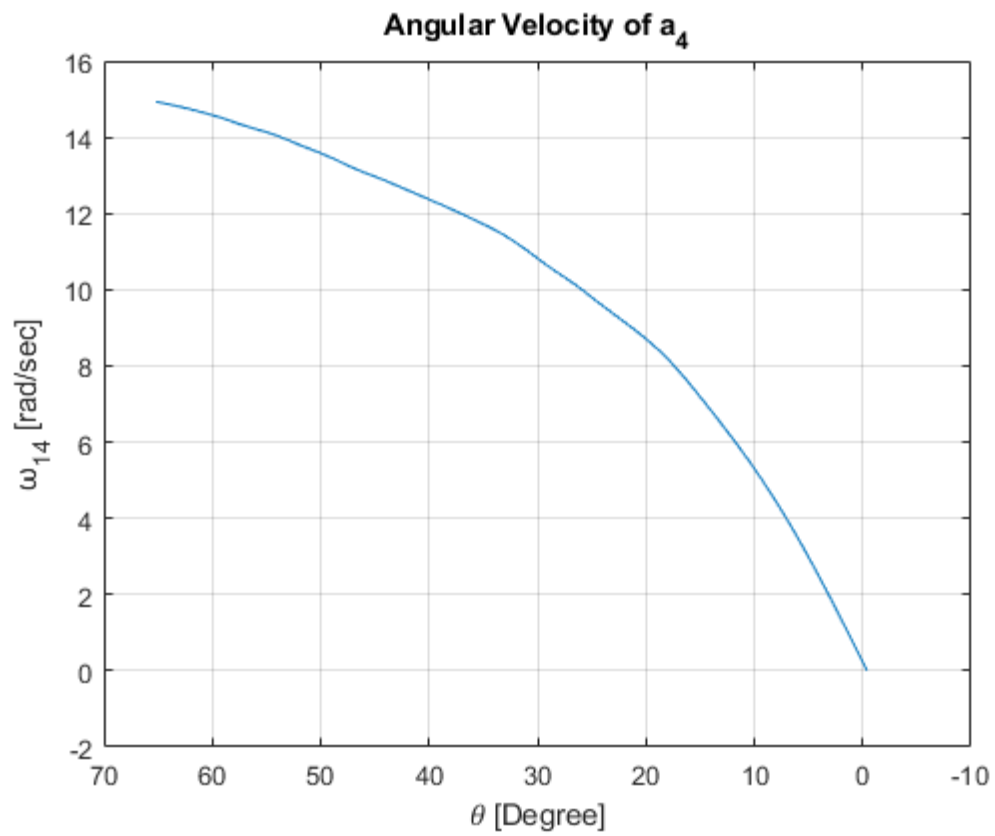
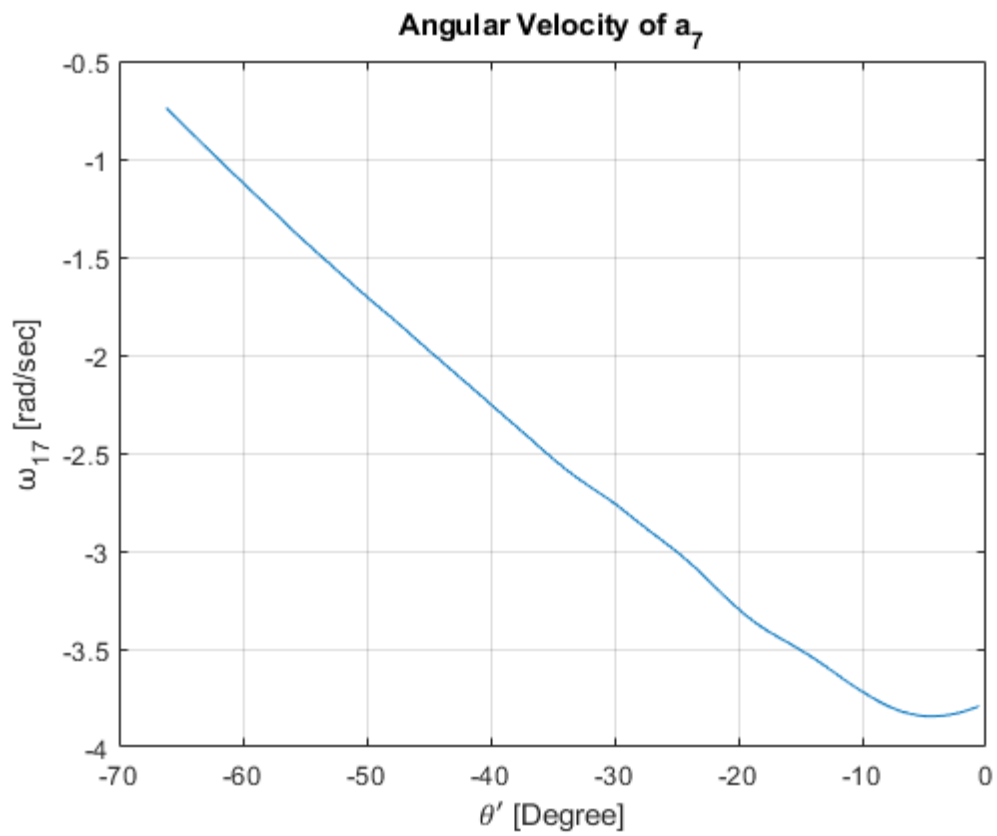


Figure 50 - Angular Velocity of “a4”

- Same numerical equations, which is explain under Chapter 2.2, are used to obtain “ ω_{17} ” and depending on angles and input angular velocity of “ a_6 ”.



- Same numerical equations, which is explain under Chapter 2.2, are used to obtain “ ω_{18} ” depending on angles and input angular velocity of “ a_6 ”.

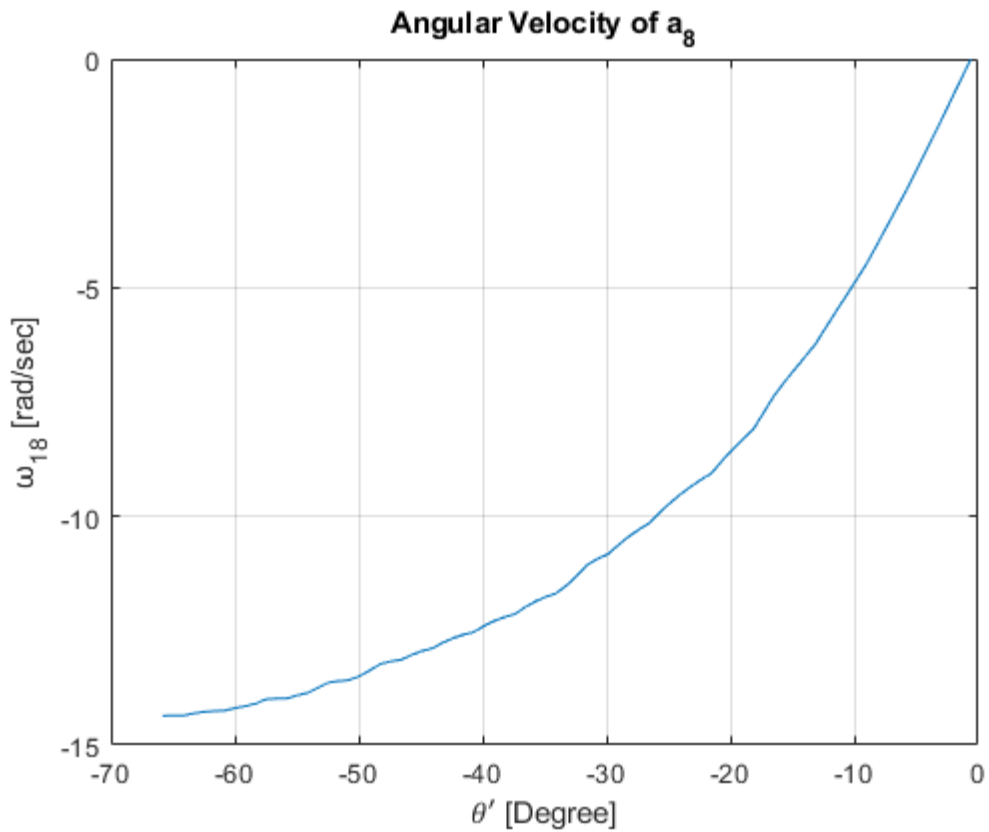


Figure 51 - Angular Velocity of “a₇” and “a₈”

- In Figure 56; after obtaining angular velocity of hooks which are “ω₁₄” and “ω₁₈” depending on the angles, angular velocities are subtracted each other. Hooks’ angular velocity difference are very small relatively its angular velocities. Also angular velocity is converging exactly same value while it is fully opening and difference ends with “0” [rad/sec] as it is shown.

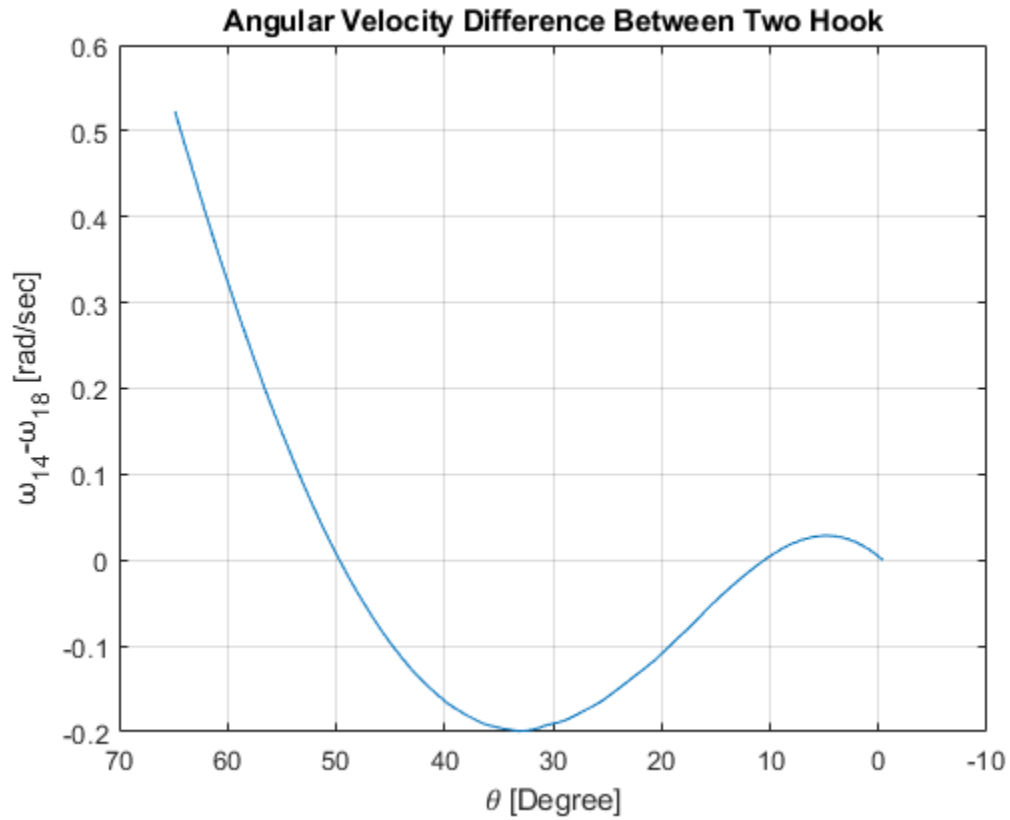


Figure 52 - Angular Velocity Difference Between Two Hook

4.1.1.3. Angular Acceleration Analysis

- Numerical equations, which is explain under Chapter 2.2, are used to obtain “ α_{12} ” and “ α_{16} ” depending on related link lengths, angles and angular velocities.

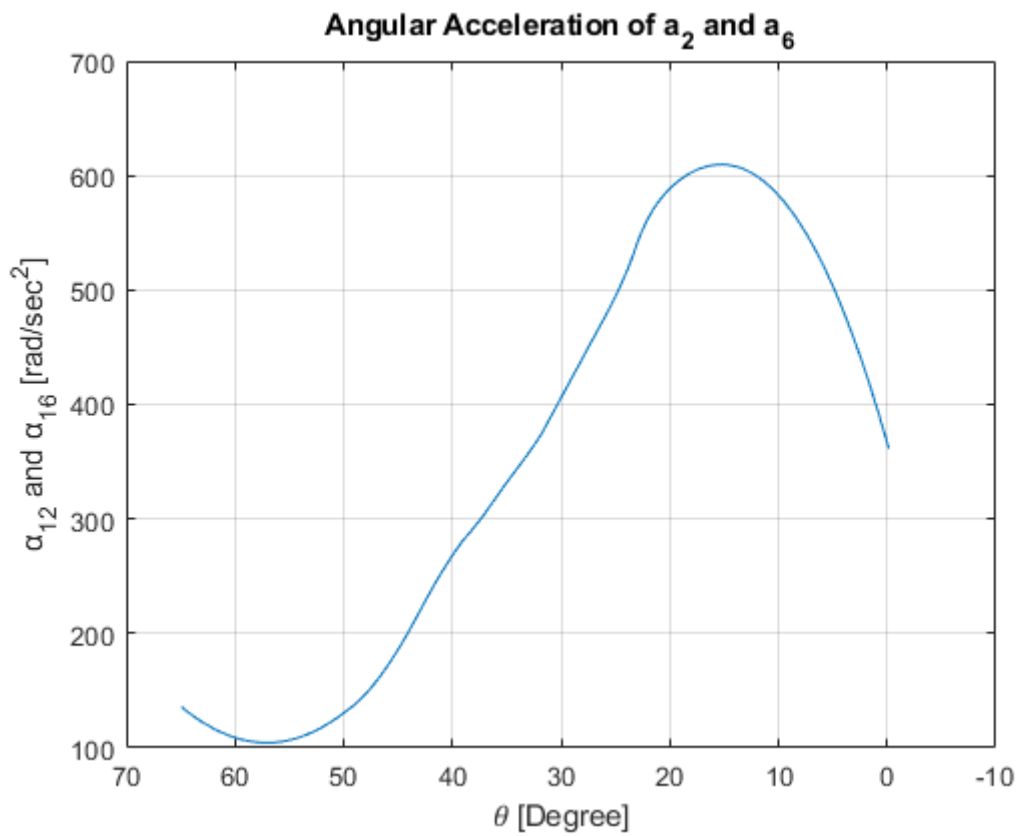


Figure 53 - Angular Acceleration of “a₂” and “a₆”

- Numerical equations, which is explain under Chapter 2.2, are used to obtain “α₁₃” depending on related link lengths, angles and angular velocities.

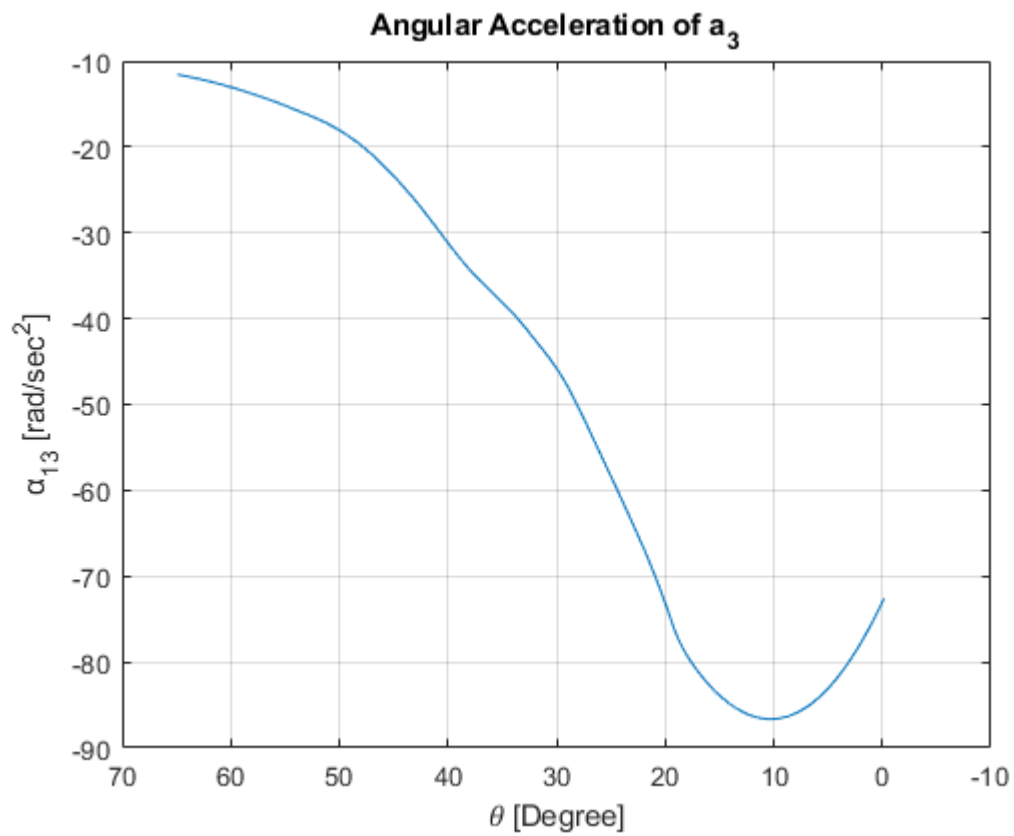


Figure 54 - Angular Acceleration of “a₃”

- Numerical equations, which is explain under Chapter 2.2, are used to obtain “α₁₇” depending on related link lengths, angles and angular velocities.

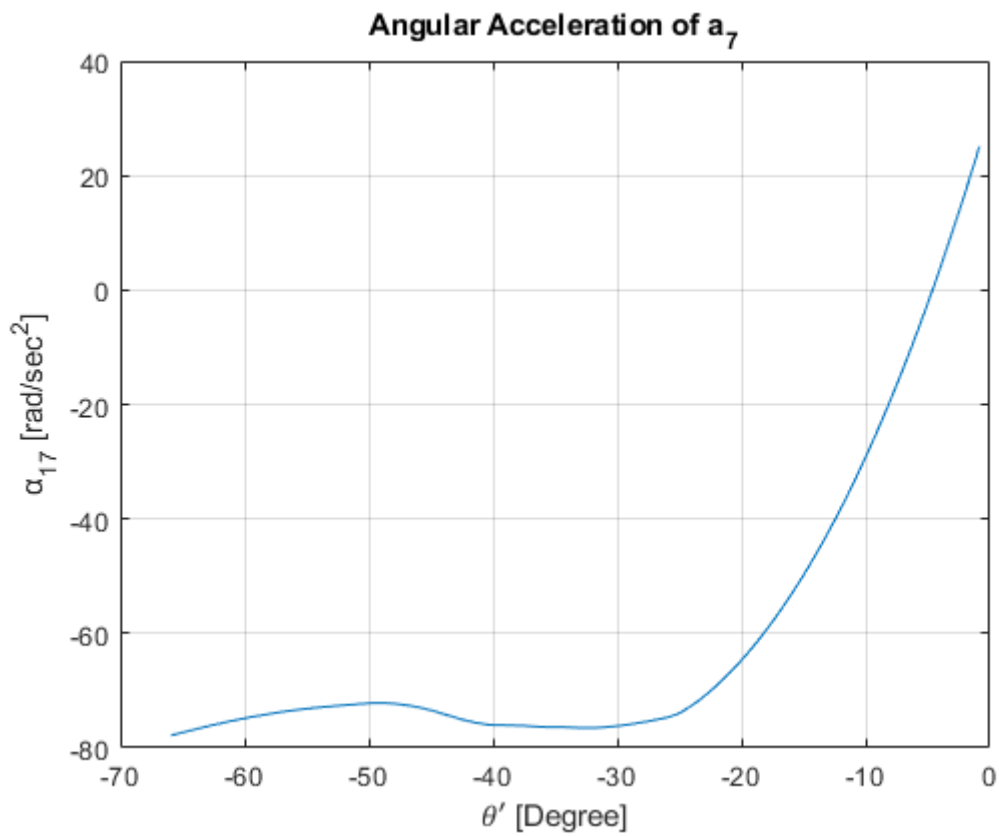


Figure 55 - Angular Acceleration of “a₇”

- Numerical equations, which is explain under Chapter 2.2, are used to obtain “ α_{14} ” depending on related link lengths, angles and angular velocities.

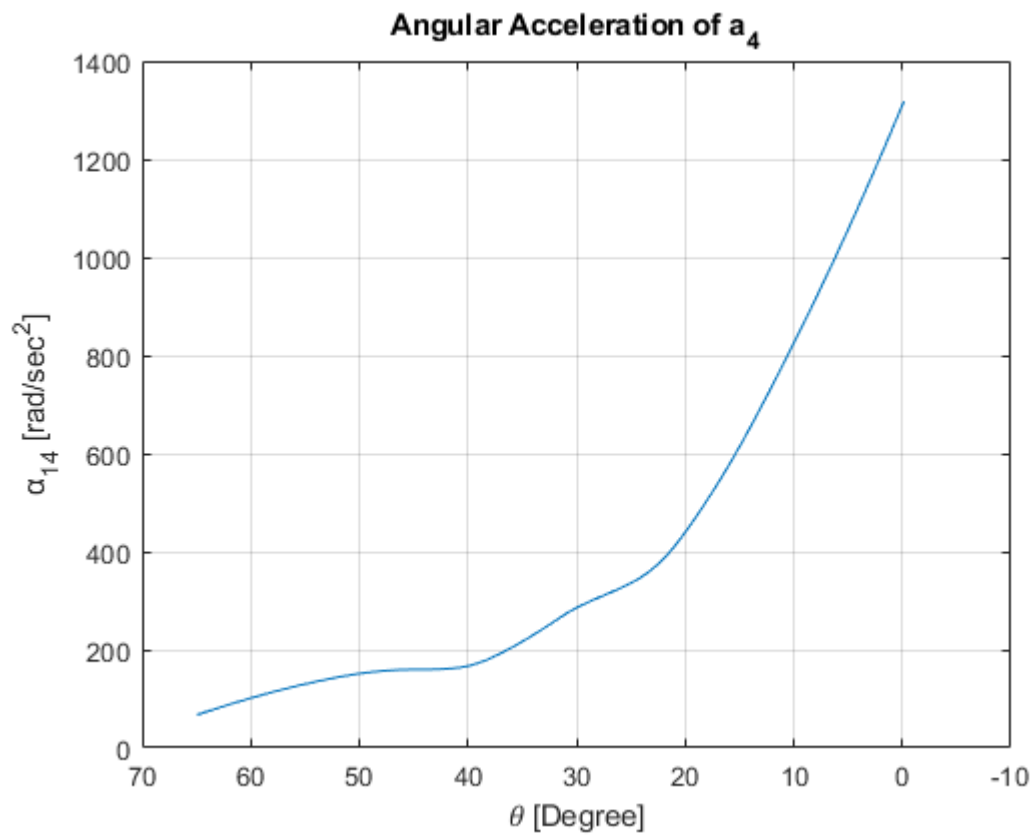


Figure 56 - Angular Acceleration of “a4”

- Numerical equations, which is explain under Chapter 2.2, are used to obtain “ α_{18} ” depending on related link lengths, angles and angular velocities.

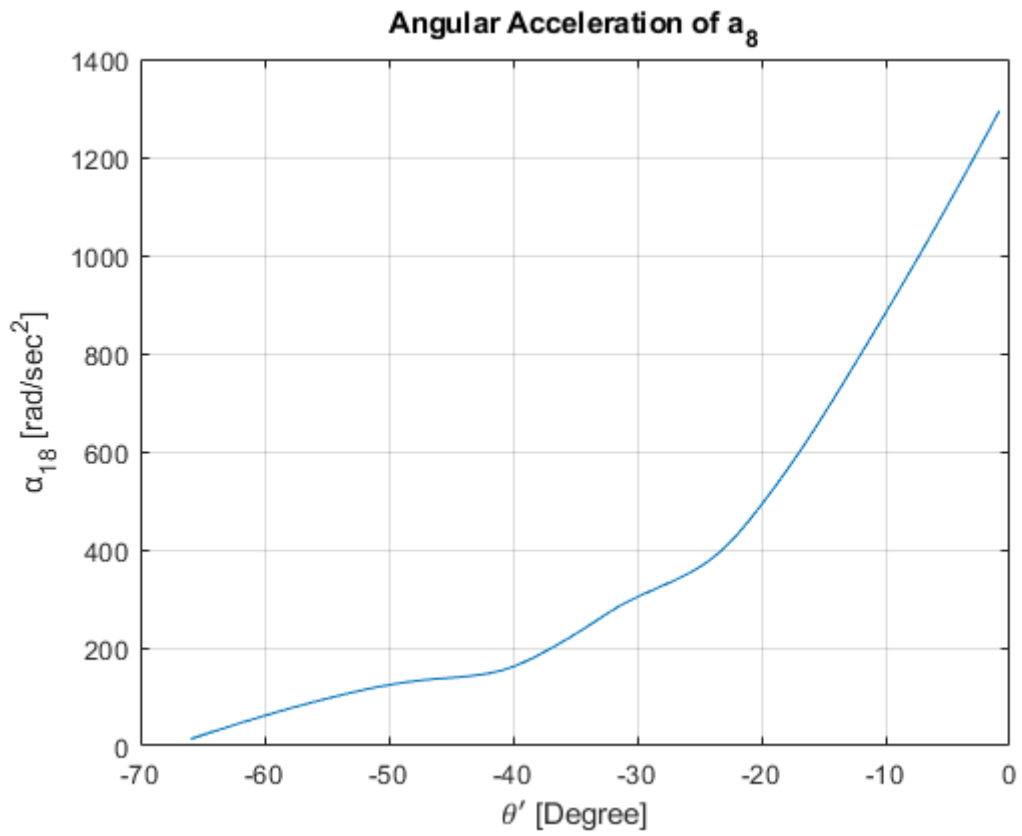


Figure 57 - Angular Acceleration of “a₈”

- Angular acceleration difference between two hooks are shown in Figure 62.

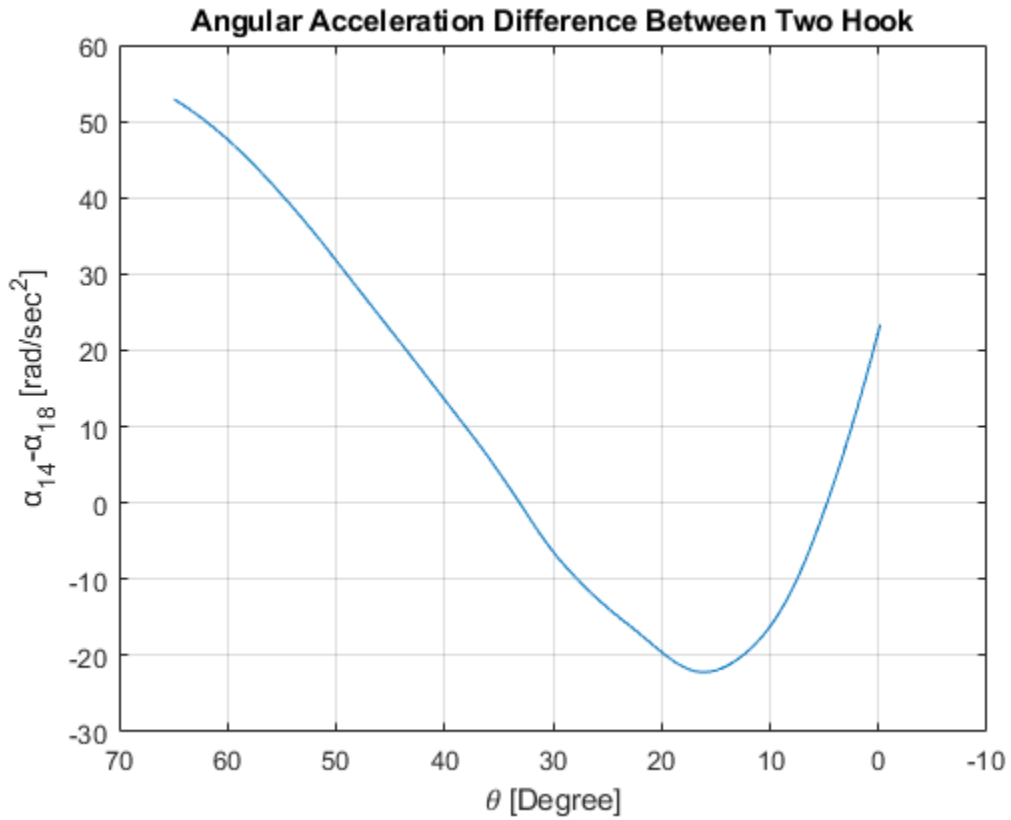


Figure 58 - Angular Acceleration Difference between Two Hook

4.1.1.4. Linear Acceleration Analysis

Under this title linear accelerations obtain with equation which explained in Chapter 2.2. In Figure 63, linear acceleration directions are shown as representative. Linear accelerations of links are center of gravity points of parts as shown below.

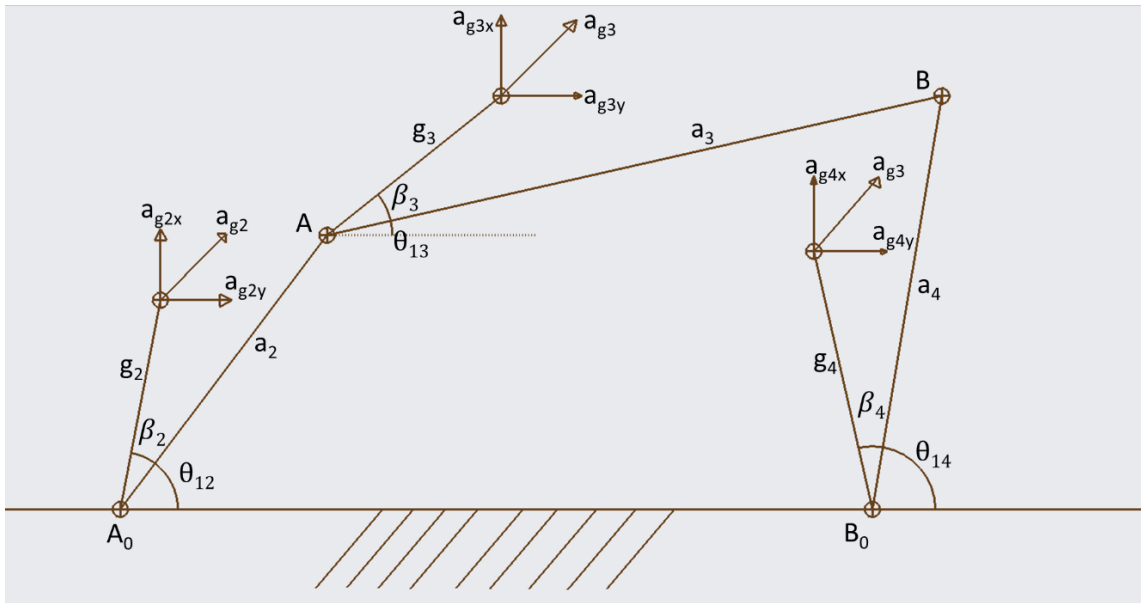


Figure 59 – Linear Acceleration Representative Points

The real positions of the linear accelerations acting on the centers of gravity of the mechanism on the left below are shown.

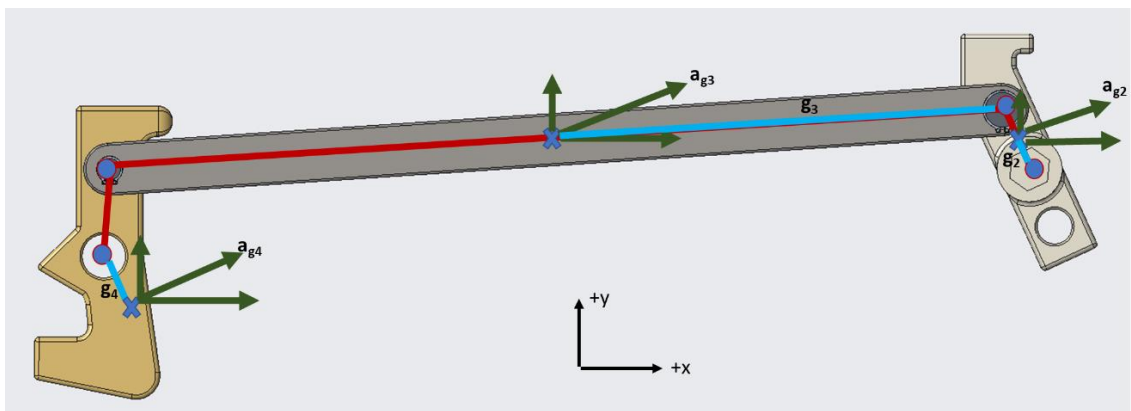


Figure 60 – Linear Acceleration Point on Left Mechanism

Here are the values seen in Figure 63 and Figure 64;

$$g_2 = 23.21[\text{mm}]$$

$$\beta_2 \approx 0 [\text{degree}]$$

$$g_3 = 208[\text{mm}]$$

$$\beta_3 = 0 [\text{degree}]$$

$$g_4 = 2.86[\text{mm}]$$

$$\beta_4 \approx 140.4 [\text{degree}]$$

These values are measured from the CAD program by assigning the material after the 3D design. The fact that the “ a_2 ” and “ a_3 ” links are almost symmetrical and homogeneous in design has ensured that the Beta values are “0”.

In addition, the real positions of the linear accelerations acting on the centers of gravity of the mechanism on the right are shown.

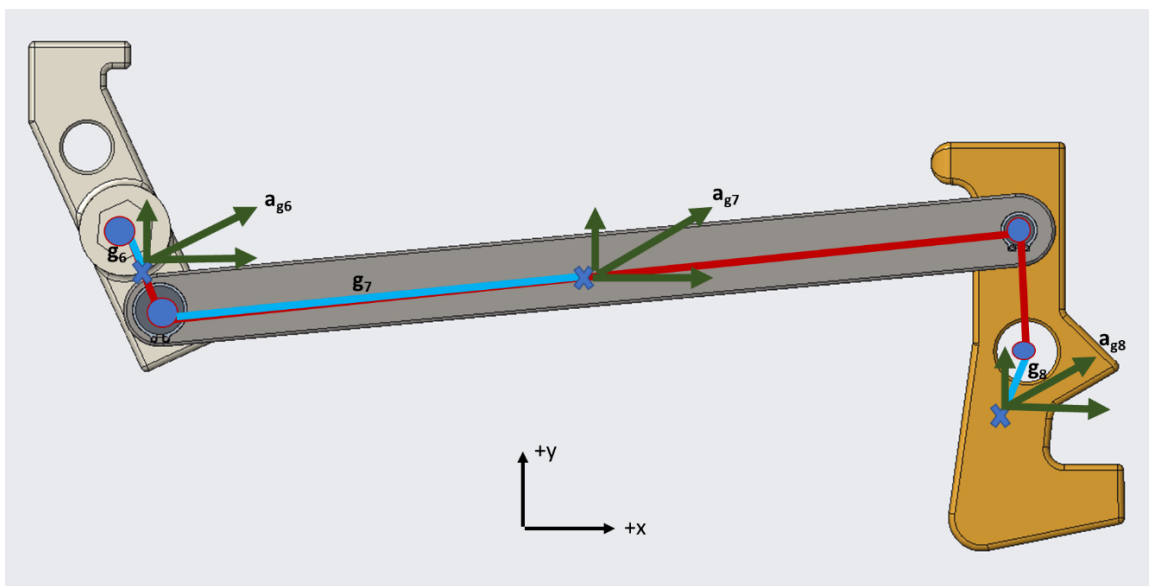


Figure 61 - Linear Acceleration Point on Right Mechanism

Here are the values seen in Figure 63 and Figure 65;

$$g_6 = 14.2[\text{mm}]$$

$$\beta_6 = 0 [\text{degree}]$$

$$g_7 = 144.3[\text{mm}]$$

$$\beta_7 = 0 [\text{degree}]$$

$$g_8 = 2.86[\text{mm}]$$

$$\beta_8 = 140.4 [\text{degree}]$$

These values are measured from the CAD program by assigning the material after the 3D design. The fact that the “ a_6 ” and “ a_7 ” links are almost symmetrical and homogeneous in design has ensured that the Beta values are “0”.

- Numerical equations, which is explain under Chapter 2.2, are used to obtain “ a_{G2} ” and “ a_{G6} ” depending on related link CoG lengths, angles, angular velocities and angular accelerations.

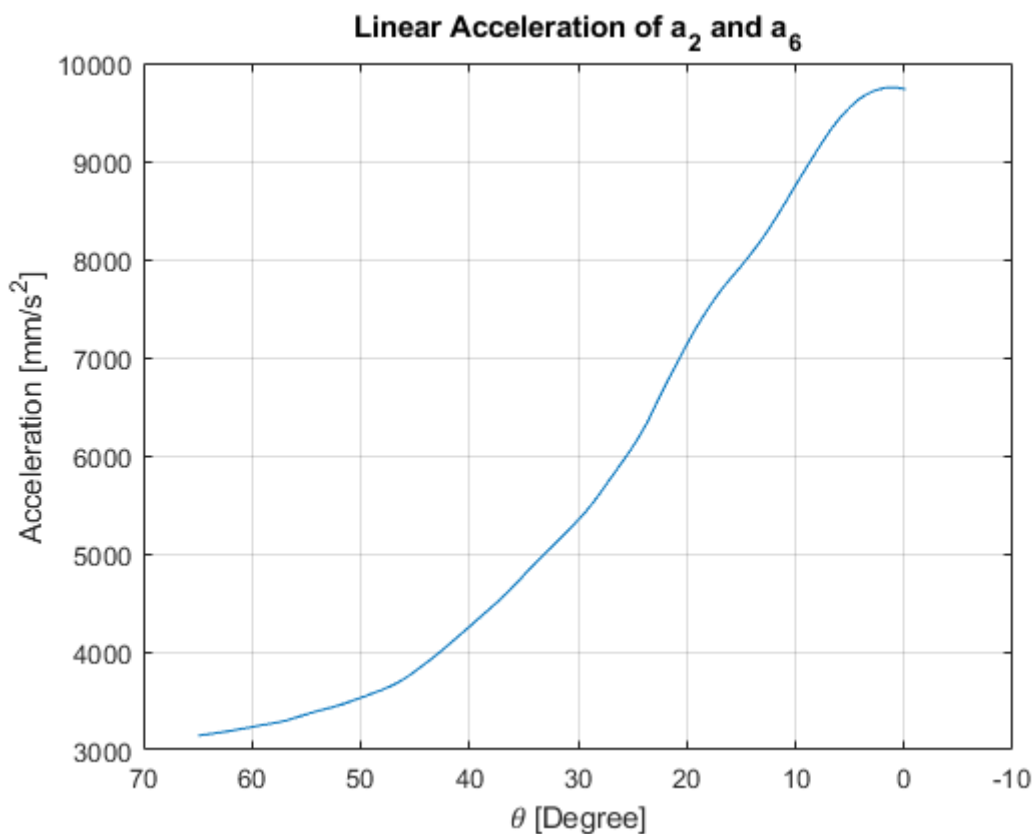


Figure 62 - Linear Acceleration of “ a_2 ” and “ a_6 ”

- Numerical equations, which is explain under Chapter 2.2, are used to obtain “ a_{G3} ” depending on related link CoG lengths, angles, angular velocities and angular accelerations.

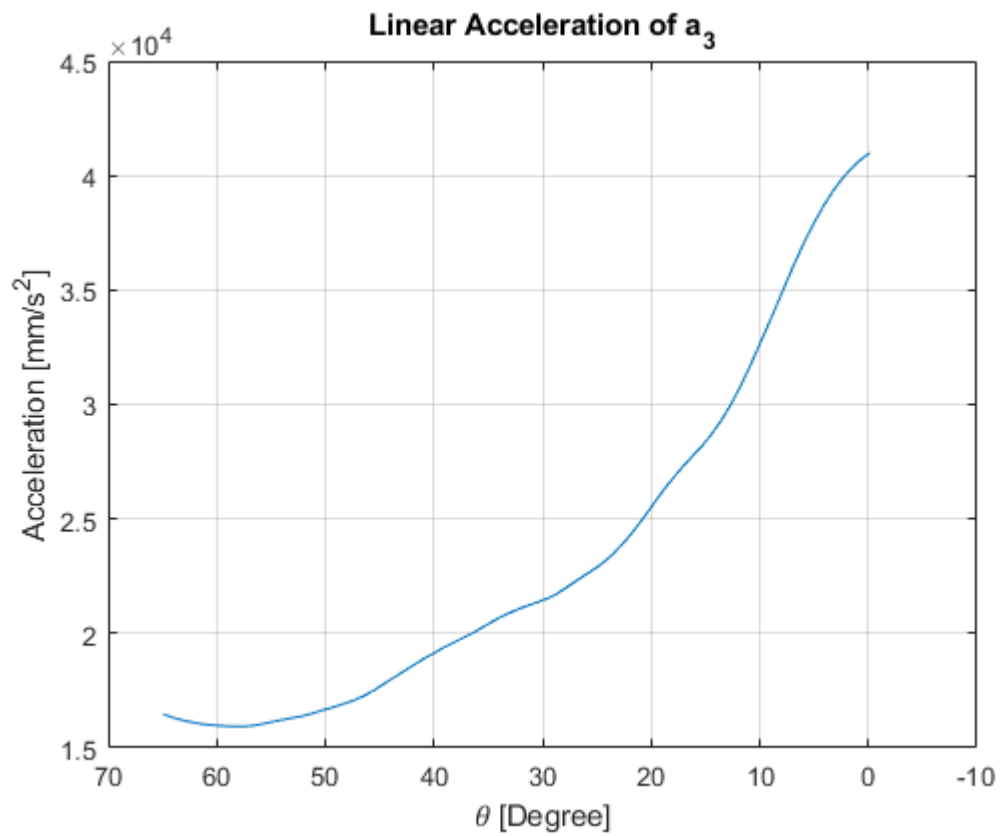


Figure 63 – Linear Acceleration of “ a_3 ”

- Numerical equations, which is explain under Chapter 2.2, are used to obtain “ a_{G7} ” depending on related link CoG lengths, angles, angular velocities and angular accelerations.

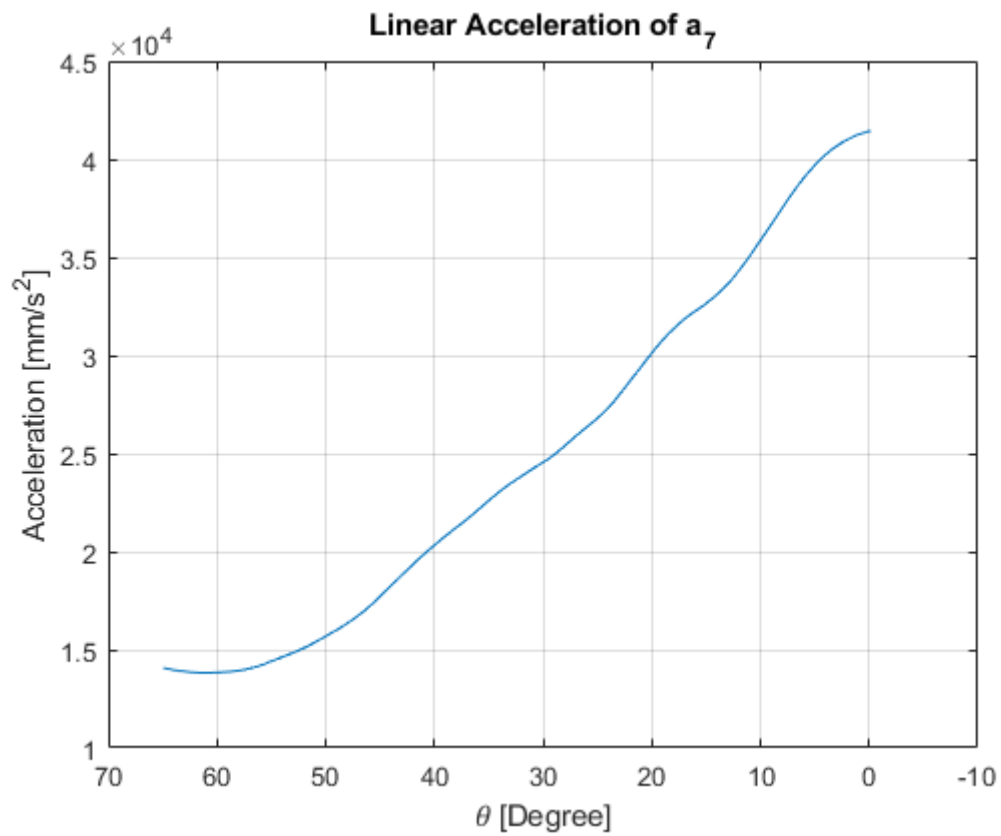


Figure 64 – Linear Acceleration of “ a_7 ”

- Numerical equations, which is explain under Chapter 2.2, are used to obtain “ a_{G4} ” depending on related link CoG lengths, angles, angular velocities and angular accelerations.

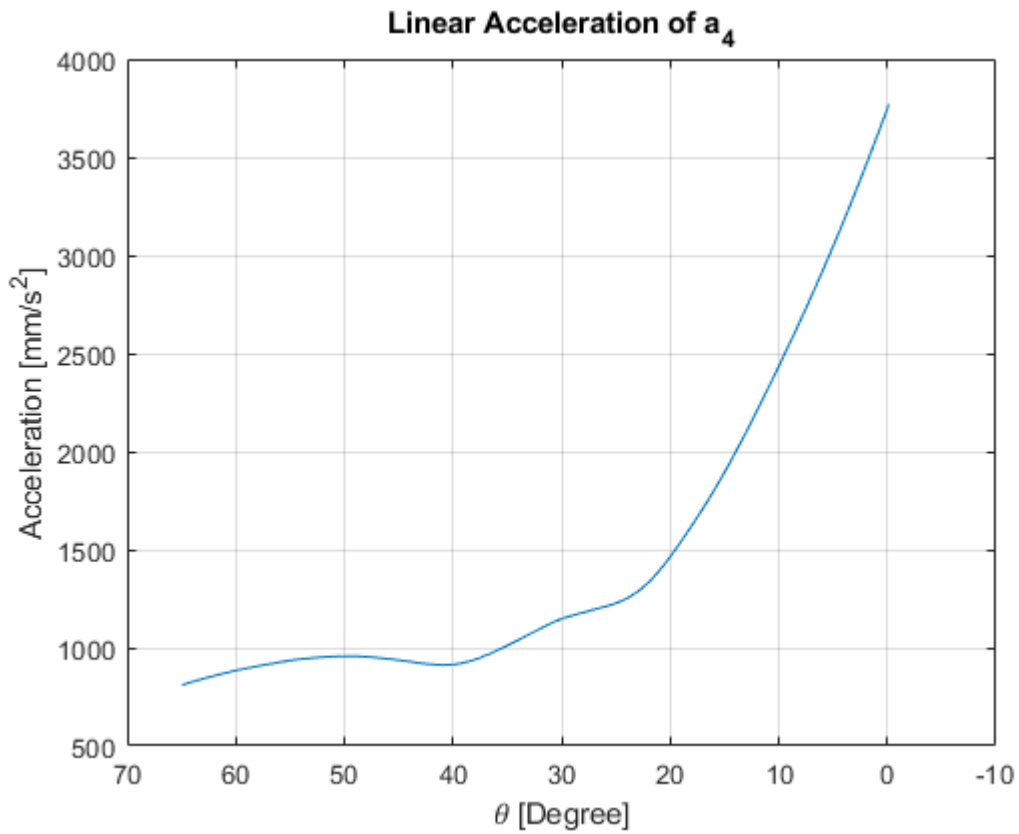


Figure 65 - Linear Acceleration of “a₄”

- Numerical equations, which is explain under Chapter 2.2, are used to obtain “ a_{G8} ” depending on related link CoG lengths, angles, angular velocities and angular accelerations.

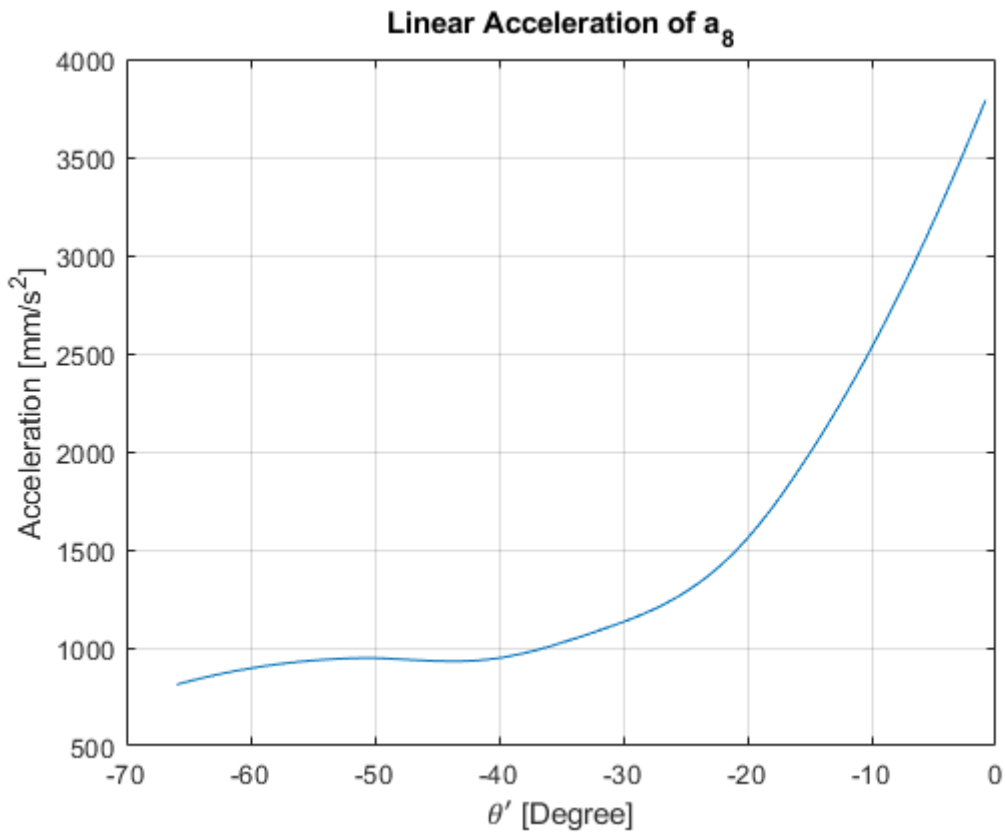


Figure 66 – Linear Acceleration of “ a_g ”

4.1.2. Analytical Analysis in ANSYS

Under this title analytical analyzes outputs are shown and explained. Analytical analyzes performed in ANSYS software. Outputs should be examined within working range of the mechanism. Therefore only related period of outputs are cropped and plotted in MATLAB software to clear illustration.

Under this analysis section: angular velocity, angular acceleration, linear acceleration are output for kinematic analysis in ANSYS.

4.1.2.1. ANSYS Settings

The geometry is drawn as CAD file in Creo design program and directly paired with Geometry tab in Rigid Dynamic module. Finite element method is used by this module.

Following steps are used for proceeding of the ANSYS as given below;

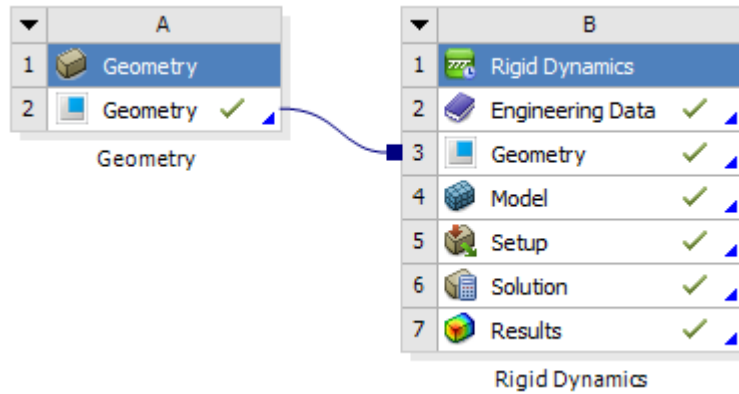


Figure 67 – ANSYS Workbench Window

Since all geometry is synchronized with 3D model in ANSYS, model can be seen in Figure 72. Only “Front Plate” and “Screws/Bolts” are suppressed due to simplified model, which are not necessary and ineffective for the analysis of mechanism.

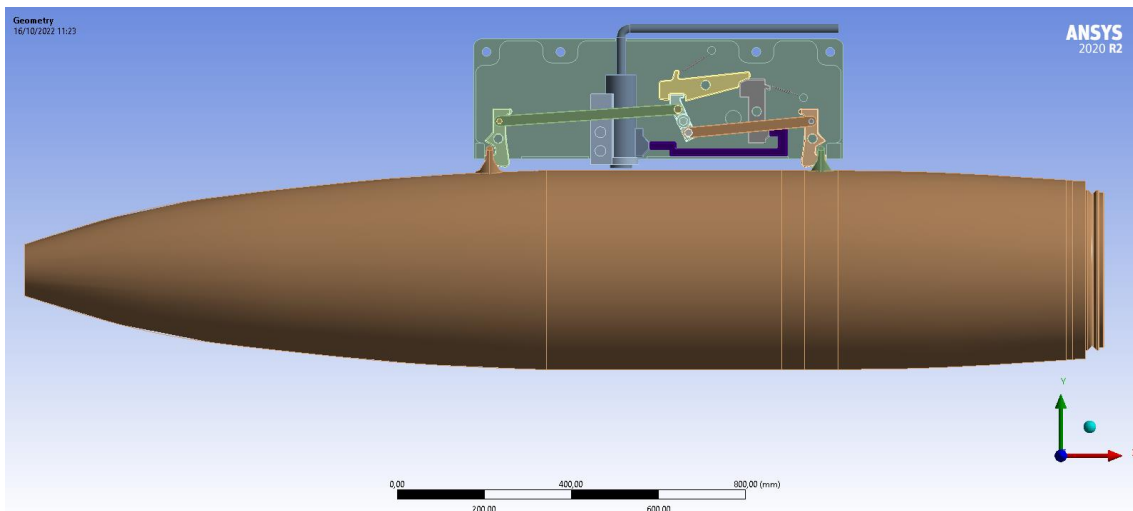


Figure 68 – 3D Model in ANSYS Mechanical

In Figure 73, due to prevent interference between rods, pins, and fixed parts, “Forced Frictional Sliding” contacts are assigned. As it is known, it should be assigned a kinetic friction to this sliding parts. So “0.6” is assigned as friction coefficient.

Joints are determined under three options. These options are;

- 1) Revolute
- 2) Fixed
- 3) General

Revolute joints are assigned for rotation movements parts which are “Hinge” , “Lock Part 1” , “Lock Part 2” , “Hook” , “Pins” and joint of parts with pins.

Fixed joints are assigned to fixed parts which are “Pneumatic” , “Pneumatic Tube” , “Pneumatic Holder” , “Clips” on the pins slot and “Lug” to warhead.

General joints are assigned to munition since it has 6 DOF after release are happened.

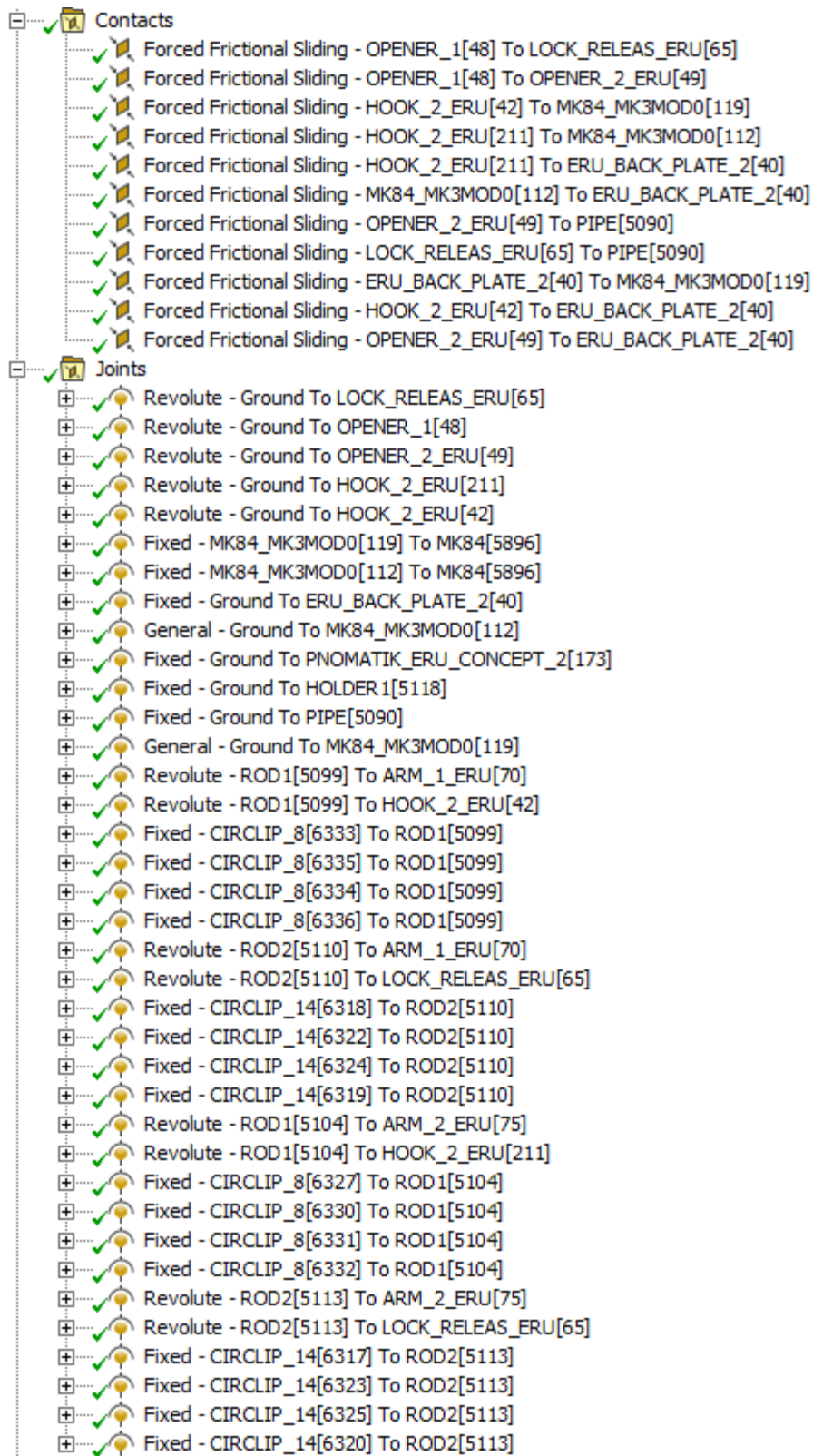


Figure 69 – Contacts and Joint in ANSYS

As it is determined in Chapter 3.5, exact preload, length, and stiffness are assigned.

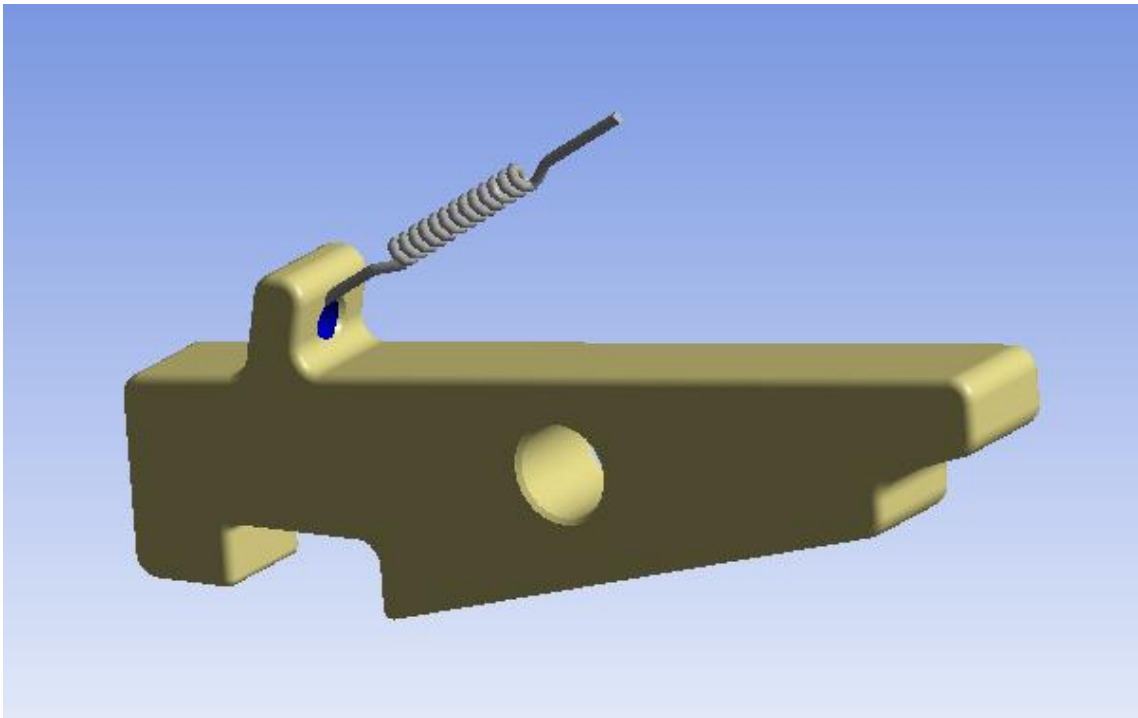


Figure 70 – Tension Spring Model in ANSYS

Details of "Spring"	
+ Graphics Properties	
[-] Definition	
Type	Longitudinal
Spring Behavior	Tension Only
<input type="checkbox"/> Longitudinal Stiffness	20, N/mm
<input type="checkbox"/> Longitudinal Damping	0, N·s/mm
Preload	Free Length
<input type="checkbox"/> Free Length	80, mm
Suppressed	No
Spring Length	95,971 mm
[-] Scope	
Scope	Body-Ground
[-] Reference	
Coordinate System	Global Coordinate System
Reference X Coordinate	-902, mm
Reference Y Coordinate	498, mm
Reference Z Coordinate	2,0003 mm

Figure 71 – Tension Spring Properties in ANSYS

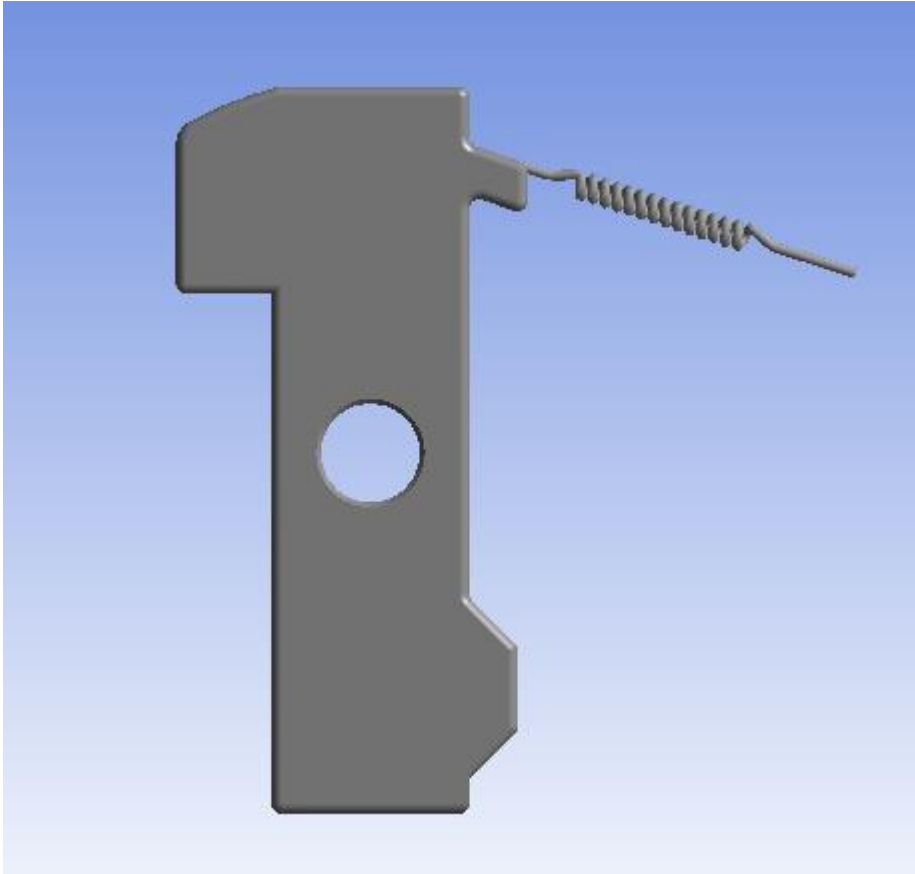


Figure 72 – Compression Spring Model in ANSYS



Details of "Longitudinal - Ground To OPENER_2"  	
+ Graphics Properties	
[-] Definition	
Type	Longitudinal
Spring Behavior	Compression Only
<input type="checkbox"/> Longitudinal Stiffness	20, N/mm
<input type="checkbox"/> Longitudinal Damping	0, N-s/mm
Preload	Free Length
<input type="checkbox"/> Free Length	82,055 mm
Suppressed	No
Spring Length	82,055 mm
[-] Scope	
Scope	Body-Ground
[-] Reference	
Coordinate System	Global Coordinate System
Reference X Coordinate	-700, mm
Reference Y Coordinate	400, mm
Reference Z Coordinate	2, mm

Figure 73 – Compression Spring Properties in ANSYS

As explained in Chapter 3.4, pneumatic actuation is initiation of start. Therefore, gas pressure is needed to push the “Lock Part 2” to move against “Spring2” (Compression Spring). It is calculated that ten bar is implementing as 338[N] depending on the surface area of the implementation face. This force is assigned as Remote Force in ANSYS to actuate mechanism as shown in Figure 78.

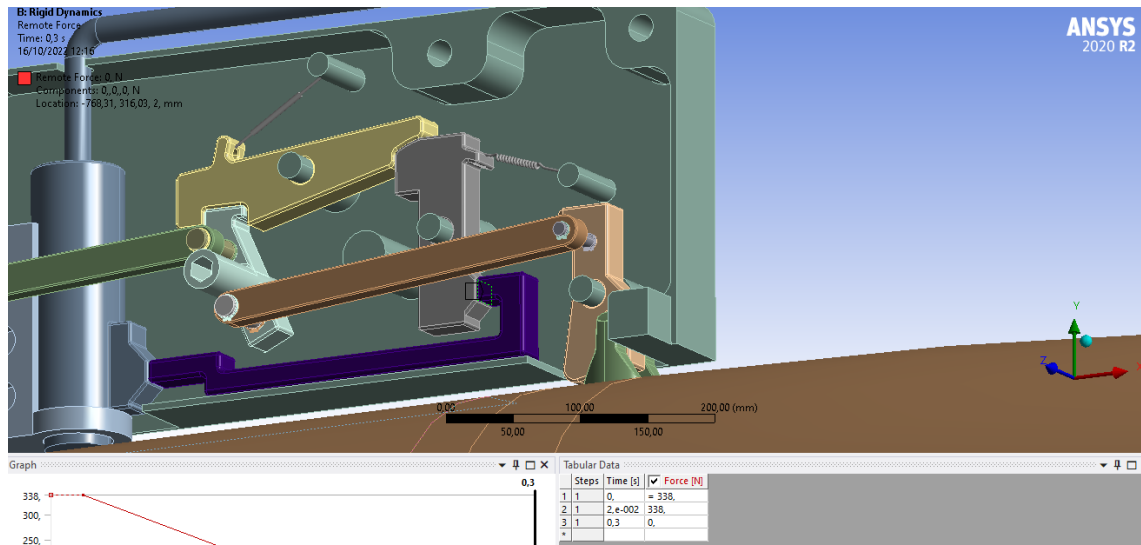


Figure 74 – Pneumatic Actuation Assignment

In “Rigid Body Dynamic” module, meshes are created for only related parts which are defined with contacts and joints parts. Under “Mesh” tab “Body Sizing” are assigned as “5” [mm] for element size. Mesh web structure can be seen in Figure 79.

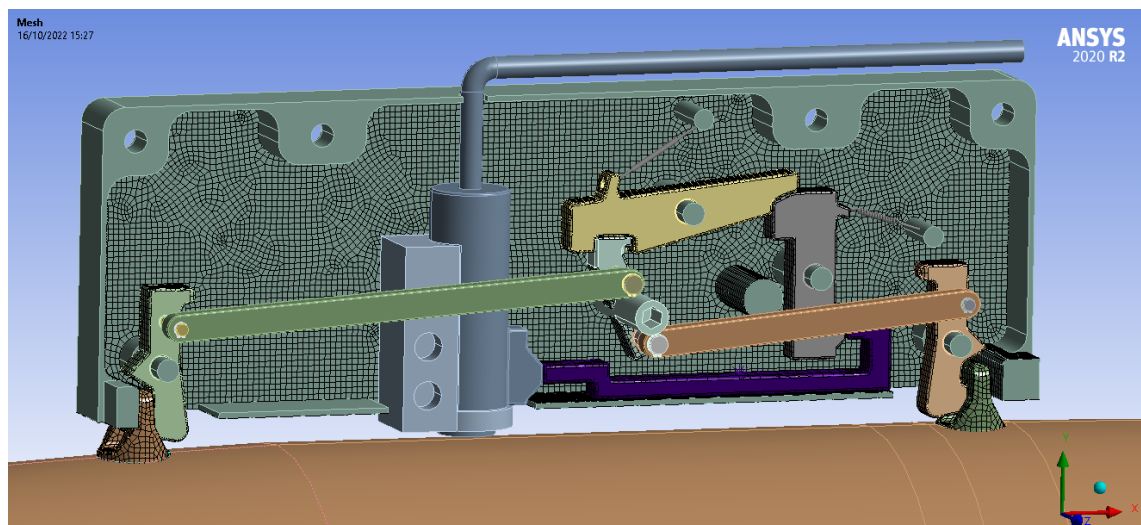


Figure 75 – Mesh Analysis of Mechanism

At the end for post-processes “Solutions” are defined one-by-one. Our aim for this thesis is obtaining kinematic results. For kinematic point view; angular velocity, angular acceleration and linear acceleration are acquired to compare with MATLAB results. And, for dynamic point of view; springs and links force reactions are obtained as shown in Figure 80.

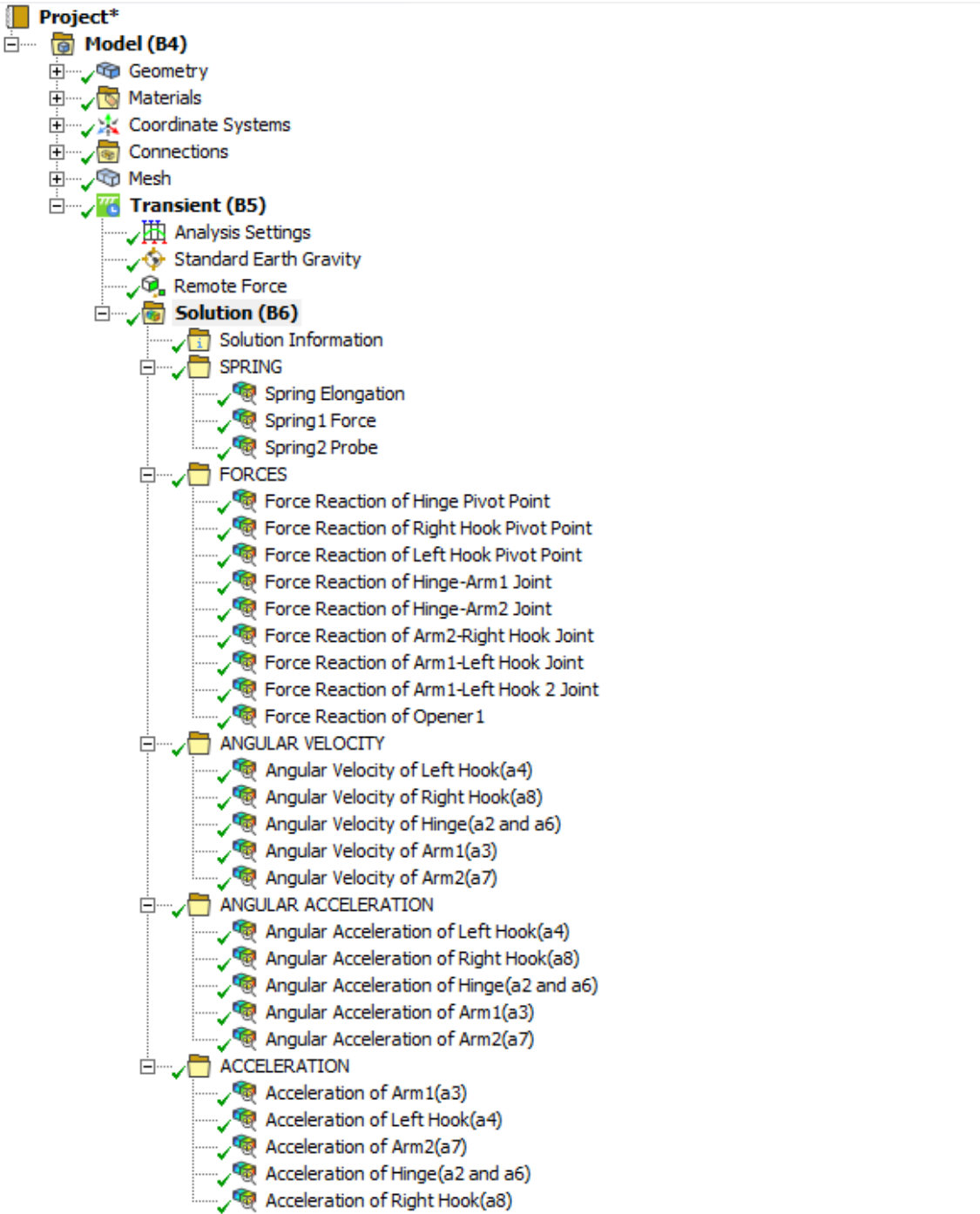


Figure 76 – Solutions Tab in ANSYS

4.1.2.2. Angular Velocity Outputs

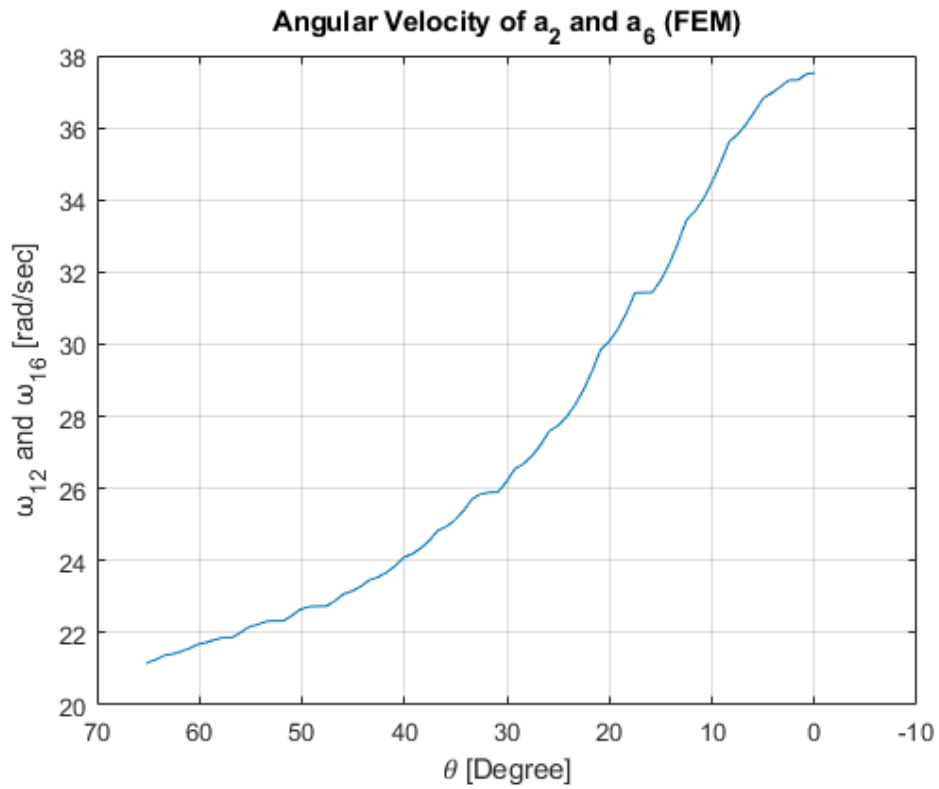


Figure 77 - Angular Velocity of “ a_2 ” and “ a_6 ”

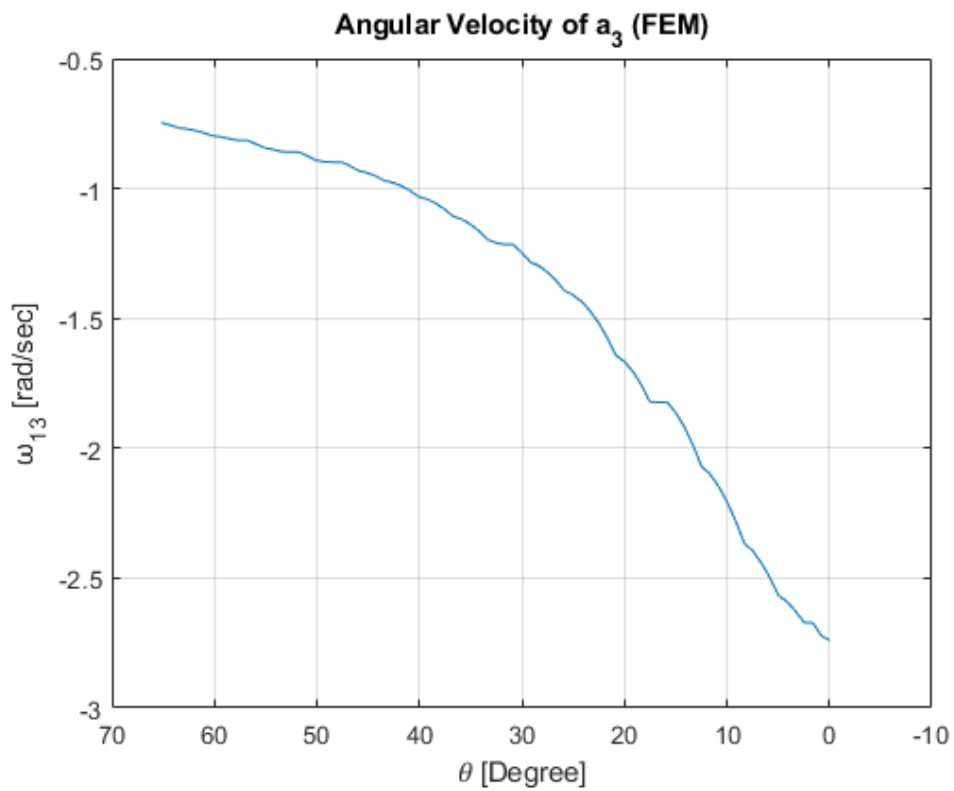


Figure 78 - Angular Velocity of “ a_3 ”

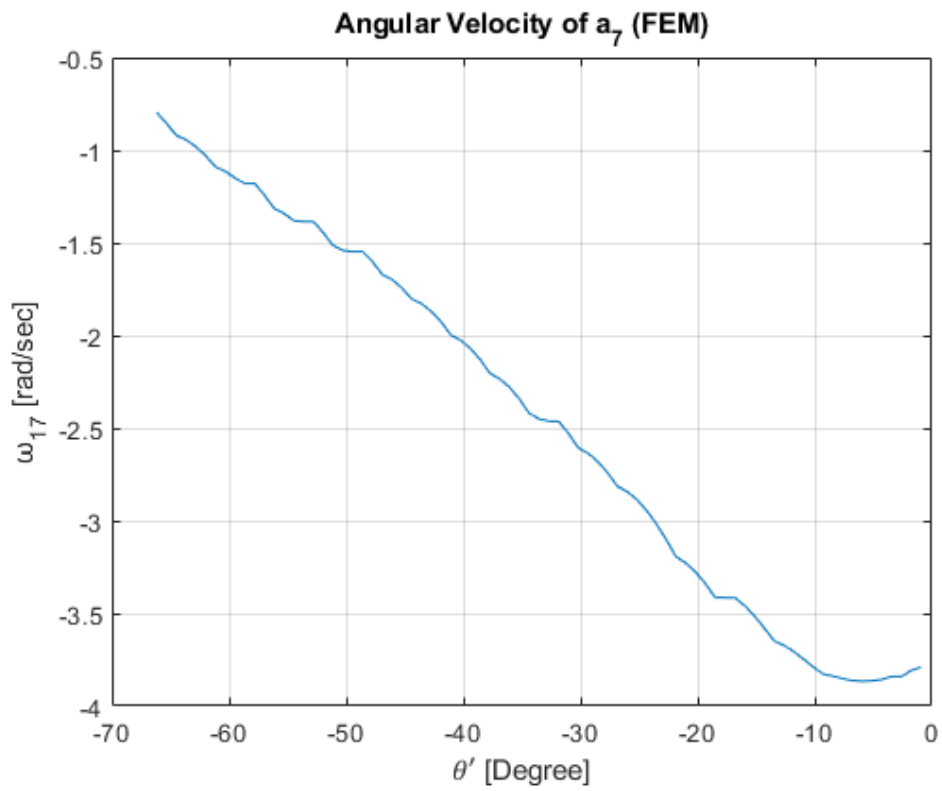


Figure 79 - Angular Velocity of “a₇”

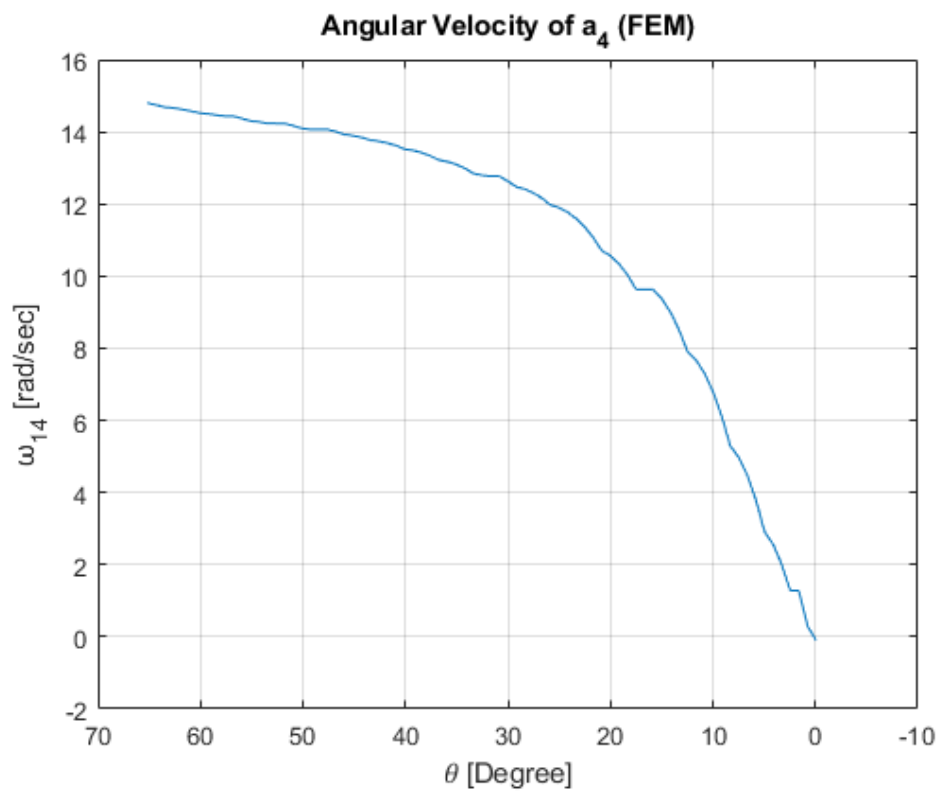


Figure 80 - Angular Velocity of “a₄”

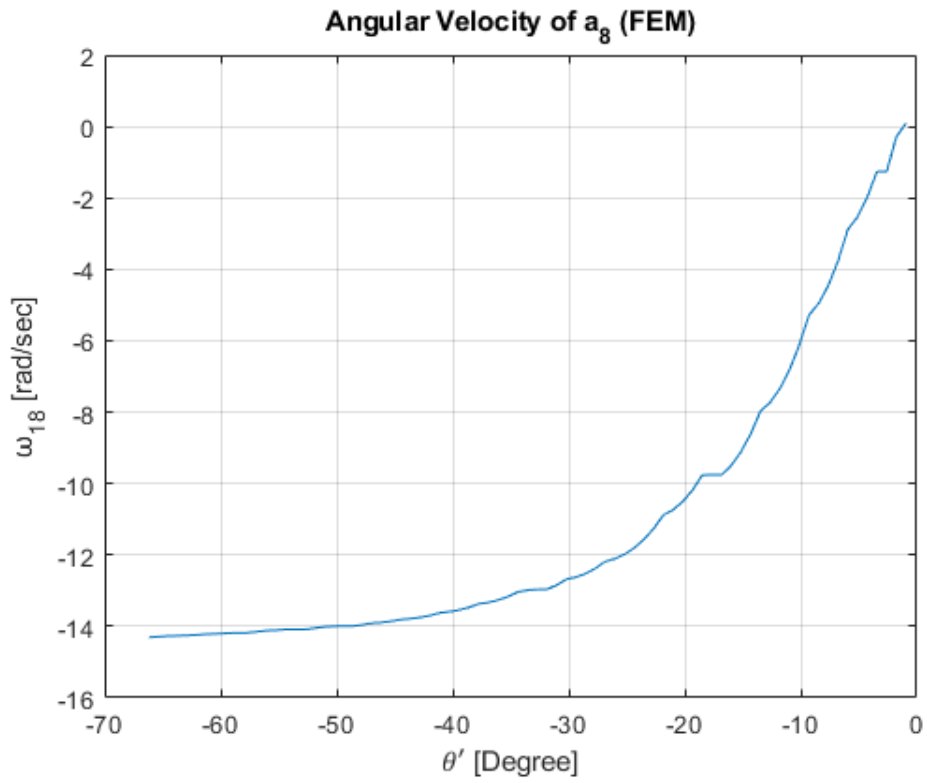


Figure 81 - Angular Velocity of “a₈”

4.1.2.3. Angular Acceleration Outputs

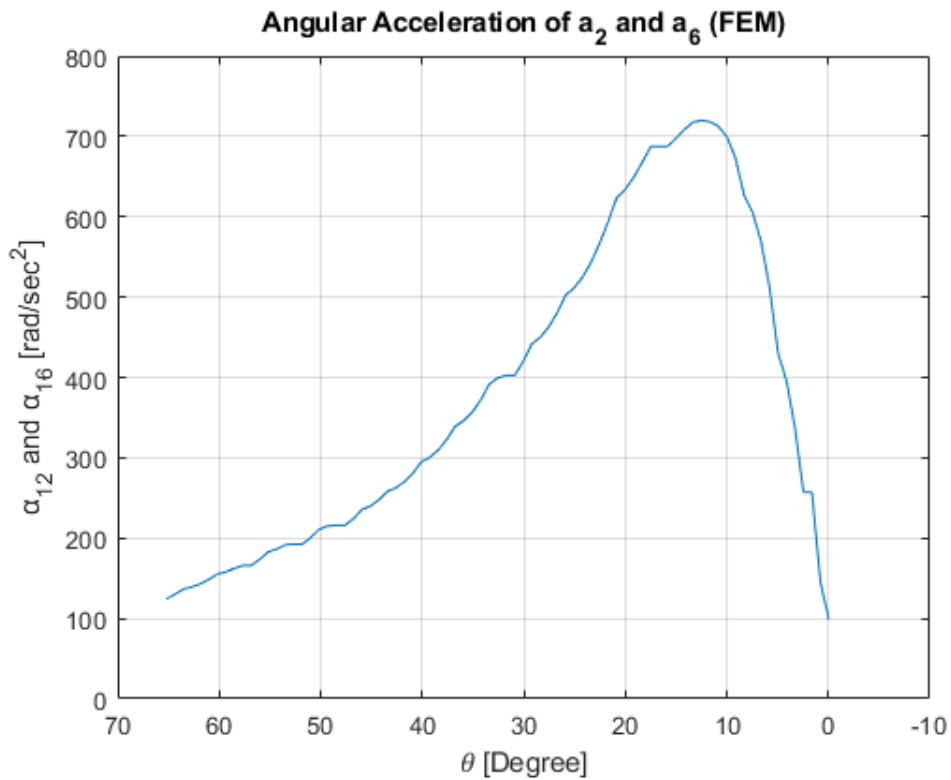


Figure 82 - Angular Acceleration of “a₂” and “a₆”

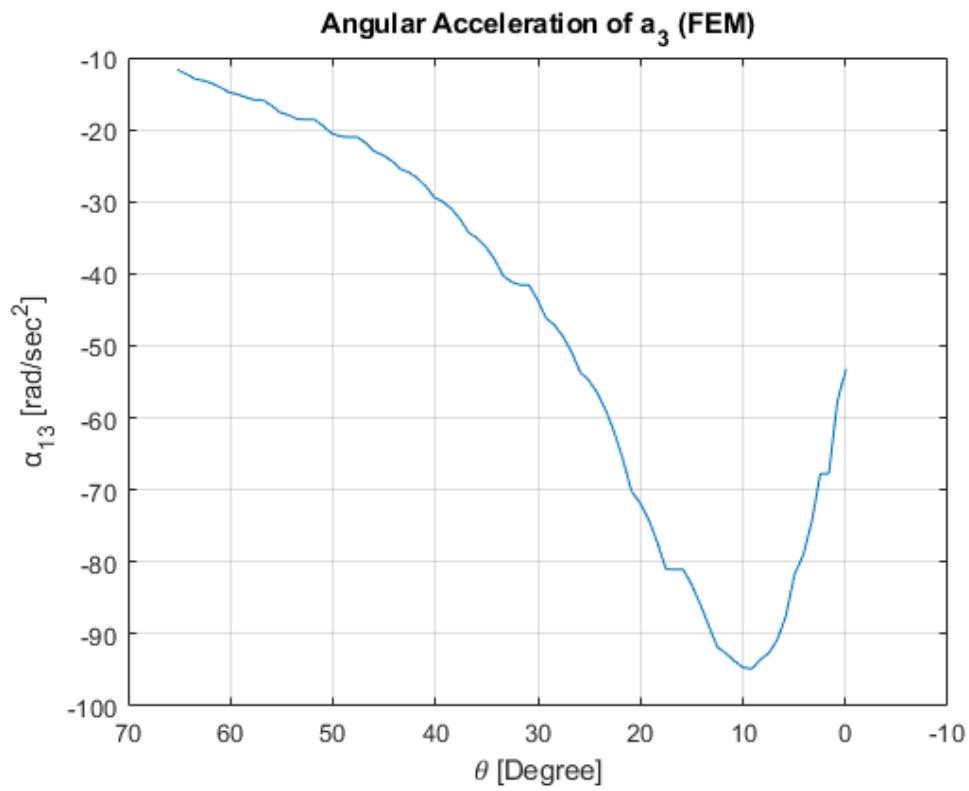


Figure 83 - Angular Acceleration of “ a_3 ”

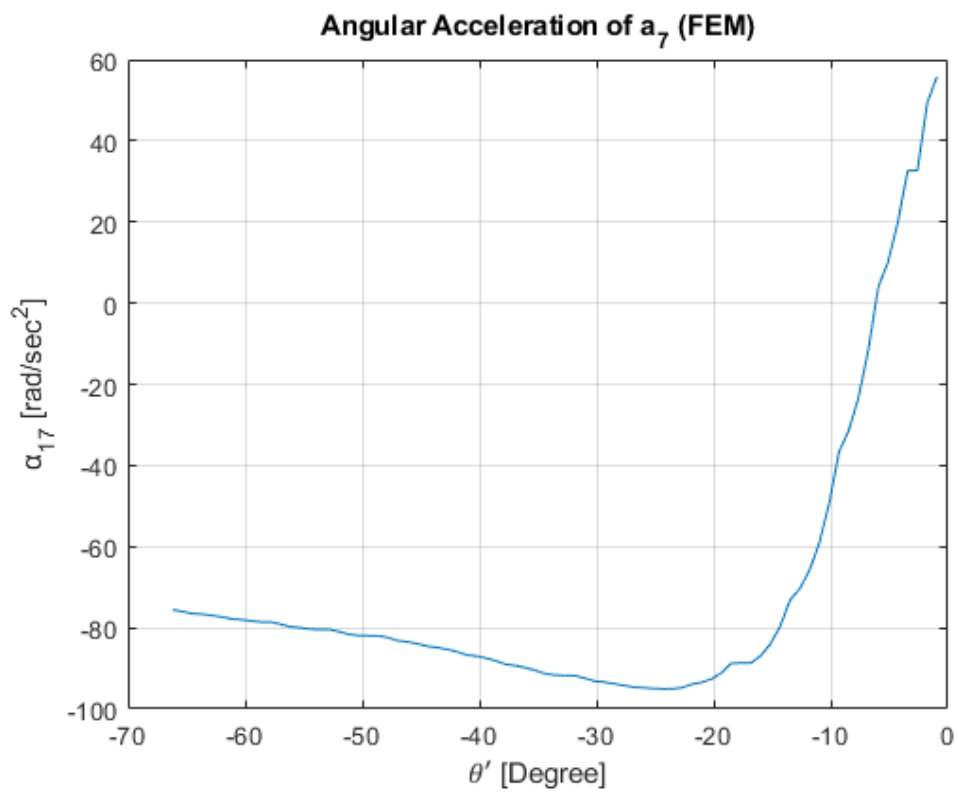


Figure 84 - Angular Acceleration of “ a_7 ”

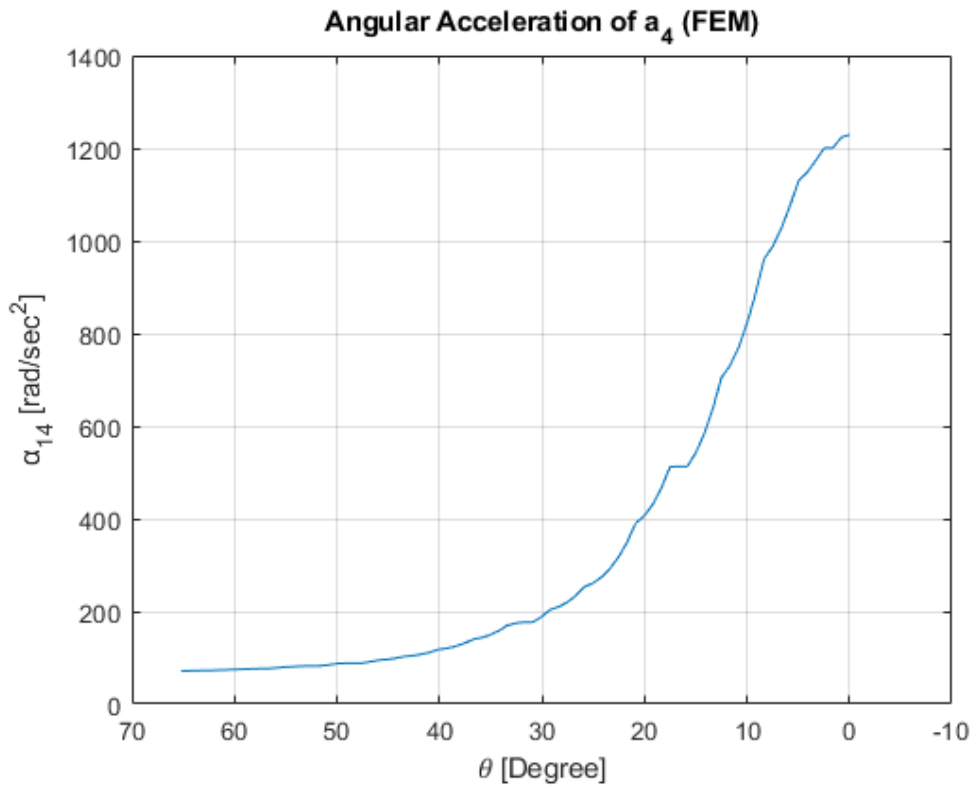


Figure 85 - Angular Acceleration of “ a_4 ”

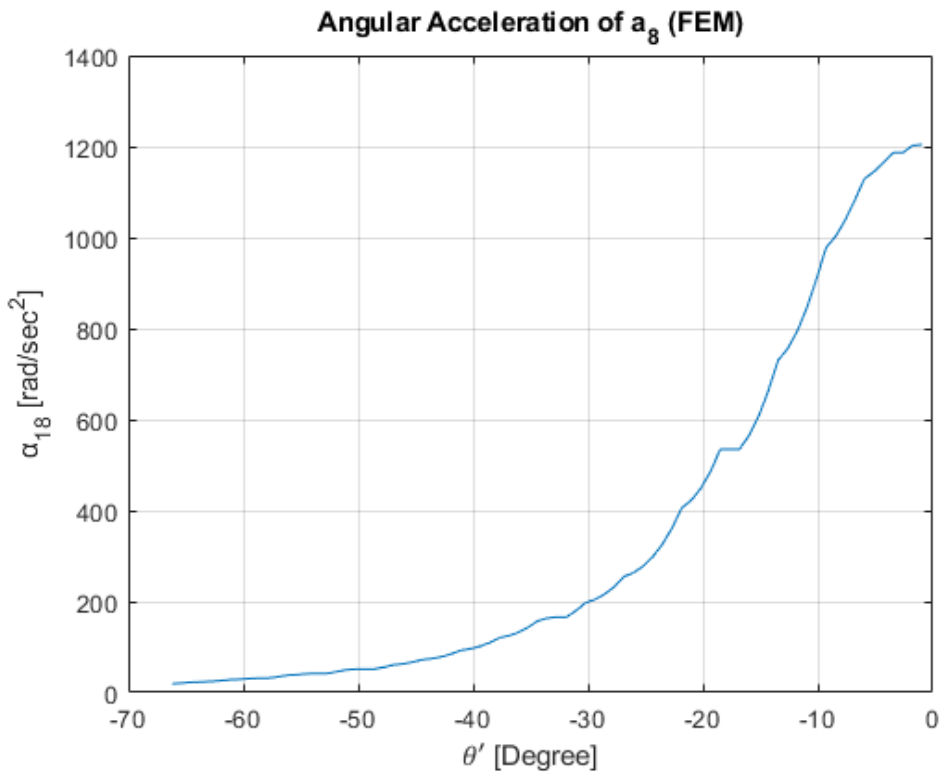


Figure 86 - Angular Acceleration of “ a_8 ”

4.1.2.4. Linear Acceleration Outputs

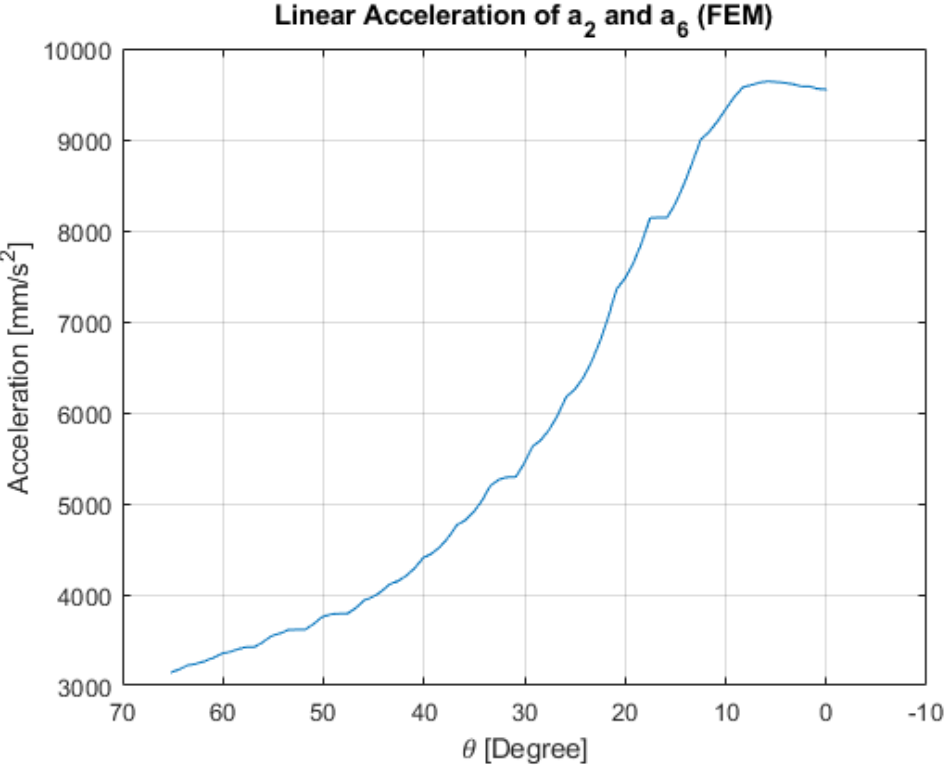


Figure 87 - Linear Acceleration of “a₂” and “a₆”

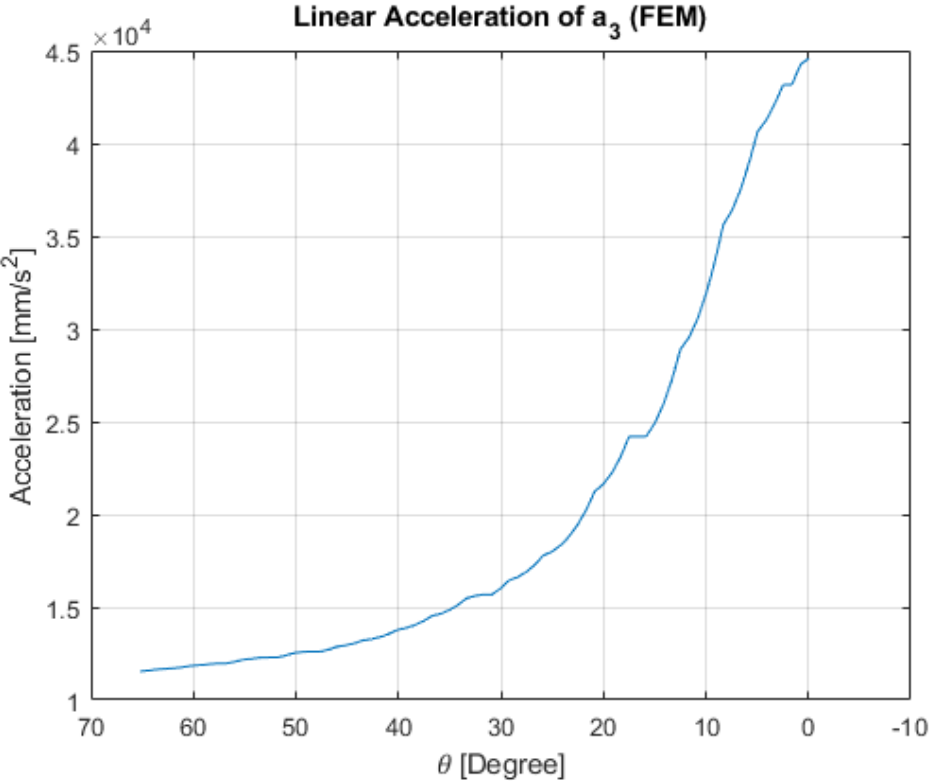


Figure 88 - Linear Acceleration of “a₃”

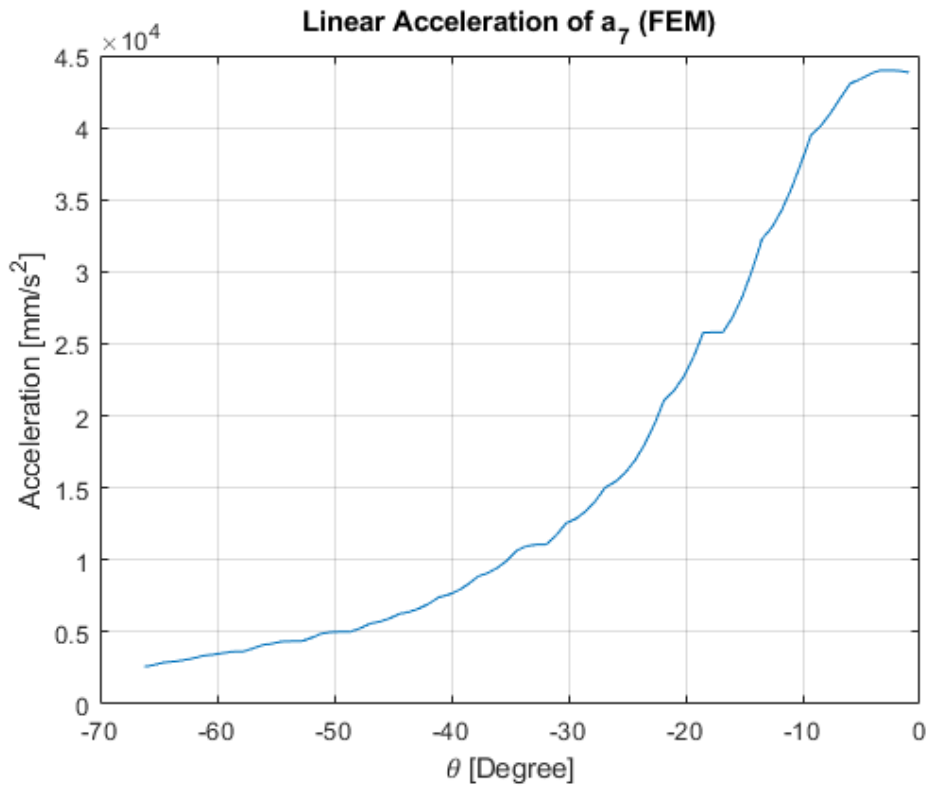


Figure 89 - Linear Acceleration of “ a_7 ”

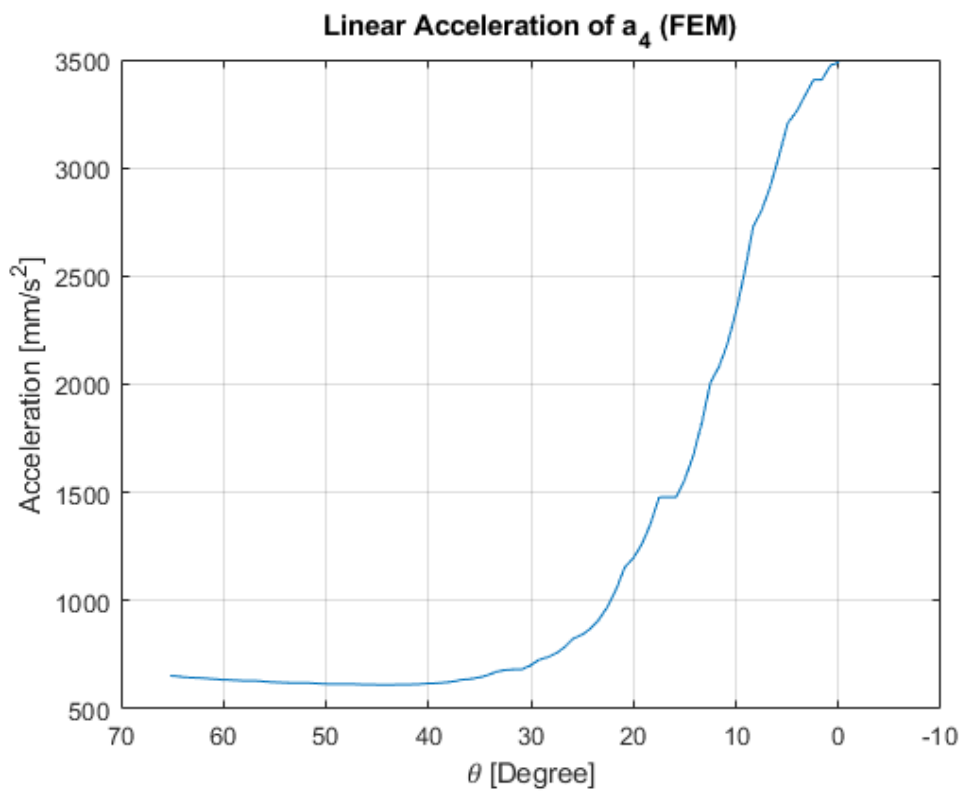


Figure 90 - Linear Acceleration of “ a_4 ”

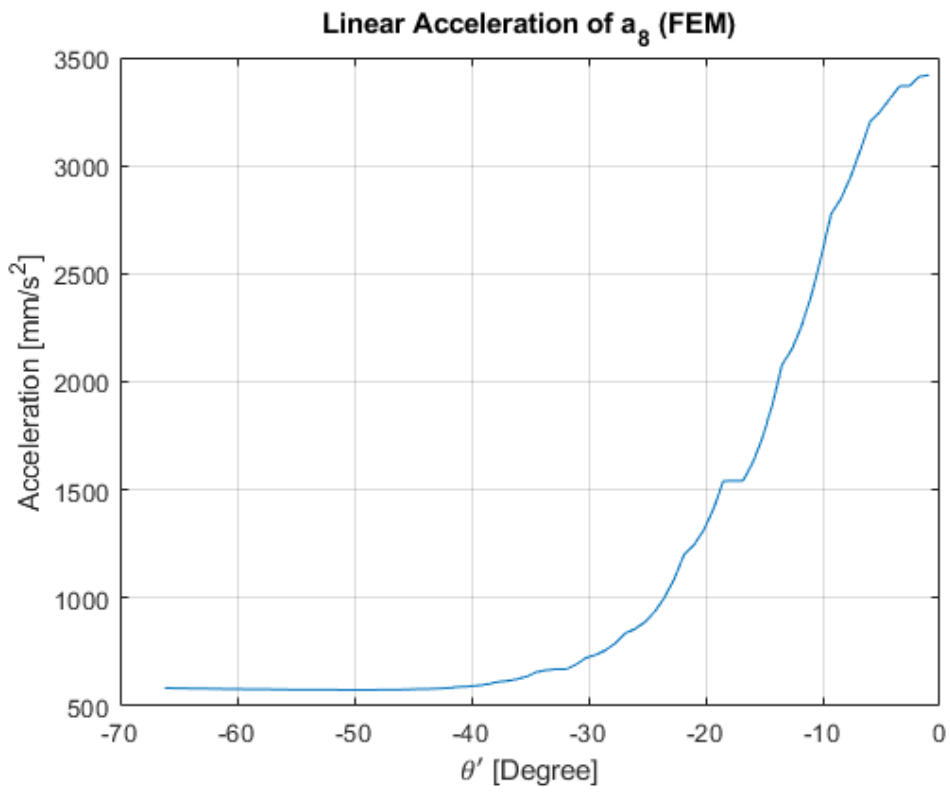


Figure 91 - Linear Acceleration of “ a_8 ”

4.2. ANSYS Rigid Body Dynamic Interface Output

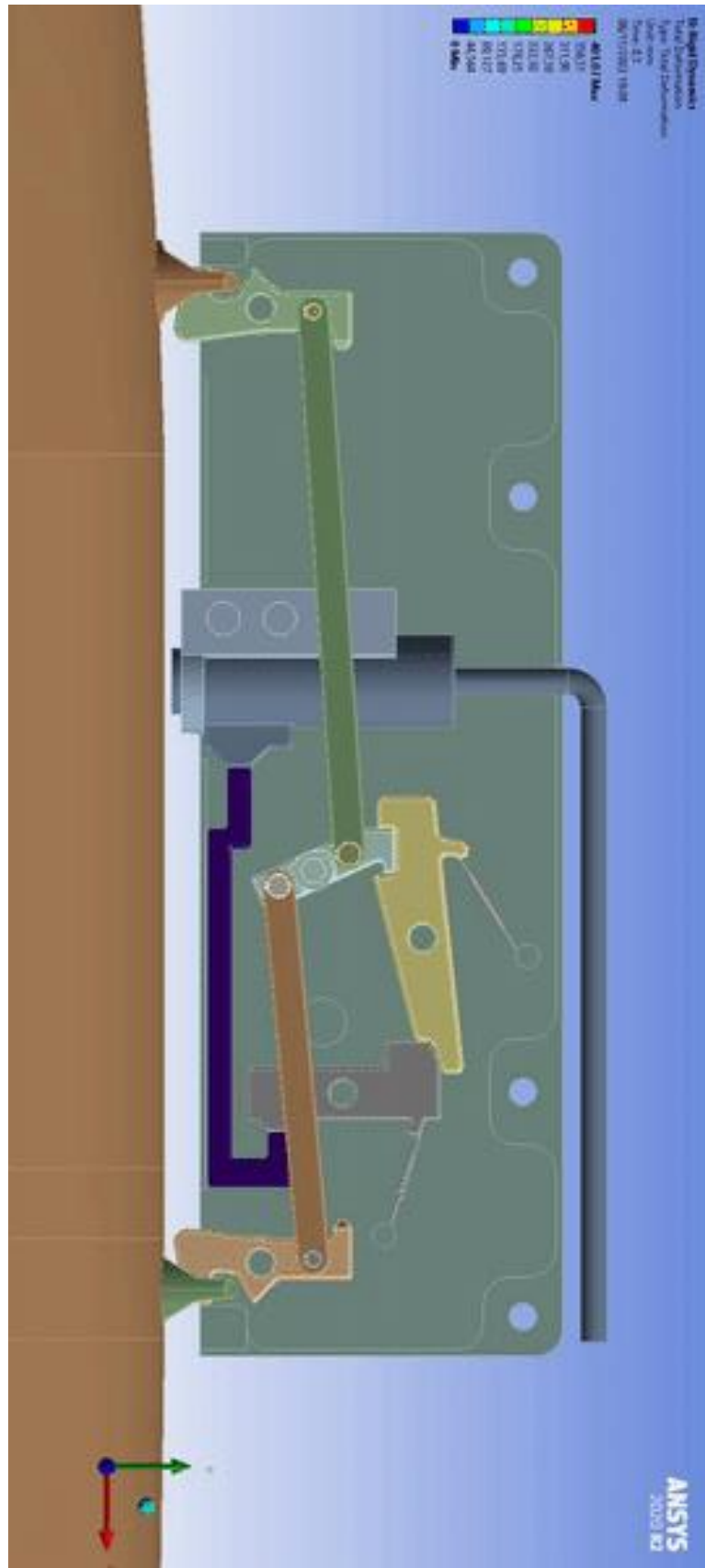


Figure 92 - Representation of the Mechanism Running

5. CONCLUSION

Ammunition throwing mechanisms based on the old days are still used today in different types. Design, kinematic analyzes have an important place in these mechanisms, which generally use different four-bar mechanisms.

In ammunition release mechanisms with such a degree of freedom, opening the two hooks holding the ammunition handles at equal angles to each other is a crucial and design optimization task.

In this thesis work, the code that gives the rod dimensions of mechanisms that will open at equal angles according to the input values that will satisfy the boundary conditions. While finding these sizes, Freudenstein and circuit closure equations were used. Additional advantage: With this code, it is possible to obtain any mechanism that opens at equal angles in an optimized manner that gives the required rod dimensions according to the inputs of the mechanism at desired step intervals. Then, the design was detailed in the 3D design program, and besides the mechanism design, the necessary details such as spring, lock mechanism, actuator and outer box were also designed.

After this step, " θ_{14} " and " θ_{18} " angles, which are all output angles, were found with certain step intervals corresponding to the given input angles " θ_{12} " and " θ_{16} ". These angles help us to find kinematic analysis outputs such as velocity and acceleration in every range. In addition, the kinematic analysis was also performed in the FEM program, and the values seem to be very close.

The design of an ejector release mechanism, the kinematic analyzes findings are achieved using the four-bar mechanism of this design are provided in this thesis. The final design was used to achieve the outcomes, and the design cycle which are ANSYS, MATLAB, GeoGebra and Creo 3D were employed extensively during the design phase.

REFERENCES

- [1] G. N. Sandor and A. G. Erdman, *Advanced Mechanism Design V. 2: Analysis and Synthesis*. Prentice-Hall, **1984**.
- [2] Donald H. Herbert, "Aircraft Supported Launchable Weapon Release Assembly", p. 4,008,645, **1977**.
- [3] Carl Thumim, Yeadon, Pa., "*Bomb Release Rack*", I. T. E. Circuit Breaker Corporation, p. S2,491,400, **1949**.
- [4] Emmett T. La Roe, "*Store Rack Hook Assembly*", McDonnell Douglas Corporation, p. 3,677,506 **1972**.
- [5] Paul F. Peterson, Rancho Palos Verdes, "*Ejector Rack*", The United States of America as represented by the Secretary of the Air Force, p. 4,050,656 **1977**.
- [6] Ervin Edelstein, Mordechai Berenson, Haim Maslovitz, David Elnekave "*Extendible Sway Brace for an Airborne Payload Rack and a Rack Containing Same*", Israel Aerospace Industries Limited, p. US 8,196,866 B2, **2012**.
- [7] Samuel W. Craigie, "*Ejector Release Unit for Use in Aircraft*", M. L. Aviation Company Limited., p. 3,898,909, **1975**.
- [8] Thaddeus Jakubowski, JR., John K. Foster, "*Store Ejector Rack*", Yee & Associates, p. 2010/0024632 A1, **2010**.
- [9] Harvey Stewart Dand, "*Store Release Mechanisms*", McDonnell Douglas Corporation, p. US3,722,944, **1973**.
- [10] Paul F. Peterson, Rancho Palos Verdes, "*Ejector Rack*", The United States of America as represented by the Secretary of the Air Force, p. US4,050,656, **1977**.
- [11] Dennis Griffen, Rancho Palos Verdes "*Ejector Rack*", The United States of America as represented by the Secretary of the Air Force, p. 4,669,356 **1987**.
- [12] Cyril Newell, "*Ejector Release Units*", The Secretary of State for Defense in Her Britannic Majesty's Government of the United Kingdom of Great Britain and Northern Ireland, p. US3,784,132, **1974**.
- [13] Paul Anthony Gerald Middleton, "*Cartridge for Store Ejection from Aircraft*", Flight Refuelling Limited, p. US8,353,237, **2013**.
- [14] Ronaldo A. Bajuyo, Benjamin J. Galanti, Armando Guerrero, "*Assembly for Carrying and Ejecting Stores*", Raytheon Company, p. US7,083,148 B2, **2006**.

- [15] Samuel W. Craigie, "*Ejector Release Units for Use in Aircraft*", Maidenhead, M. L. Aviation Company Limited, Slough, England, p. US3,610,094, **1971**.
- [16] Steven D. Kay, "*Low Force Bomb Rack Release Mechanism*", Exelis, Inc., p. US8,127,655 B1, **2012**.
- [17] Ashitava Ghosal, *The Freudenstein Equation and Design of Four-link Mechanisms*, IISC Bangalore Department of Mechanical Engineering, **2010**.
- [18] Prof. Eres Söylemez, Position Analysis of Mechanism by Meant of Complex Numbers, <https://ocw.metu.edu.tr/mod/resource/view.php?id=2098> (Date of Access: 17 July 2022)
- [19] Prof. Eres Söylemez. "*Makine Teorisi-2, Makine Dinamiği*", Birsen Yayınevi, İstanbul, Chapter 1.3, **2017**.
- [20] David H. Myszka, *Machines and Mechanisms: Applied Kinematic Analysis —4th Edition.*” **2012**.
- [21] Dana G. RIZESCU and Ciprian Ion G. RIZESCU, *Kinematic and Dynamic Analysis of Planar Linkages*, „Politehnica” University of Timisoara, **2008**.
- [22] Military Specification, MIL-A-8591, *Airborne Stores, Suspension Equipment and Aircraft-Store Interface (Carriage Phase)*, Design Criteria Standard, MIL-A-8591H, **1990**.
- [23] Kimsey, Kent D., George H. Jonas, and Jonas A. Zukas. "*Computer Simulation of Scaled MARK 84 Bomb Impact into Concrete.*”, **1983**.
- [24] Philippe Guitaut, "*Use of Cold Gas Energy for Tactical Missile In-Flight Release*", ALKAN Corporation, RTO AVT Symposium on “Functional and Mechanical Integration of Weapons and Land and Air Vehicles”, Williamsburg, VA, USA, 7-9 June **2004**.
- [25] Danielle Collins, What Are Hexapod Robots Stewart Platforms, <https://www.linearmotiontips.com/what-are-hexapod-robots-stewart-platforms/> (Date of Access: 05 November 2022)

APPENDICES

APPENDIX A

```
clear all; close all hidden; clc;

%Left Hook Fixed Point Position
B0y= -39.9309;
B0x= -425.542;
Thb= atan(B0y/B0x);

Th=0.41; %Last Position of a2 with respect to Ground[rad]
Th=Th*pi/180;
Th1=Thb-Th; %Theta1-Last Angle of a2

DTh=65.83; %Operating Angle Delta Theta
DTh=DTh*pi/180;
Th2=Th1+DTh; %From Theta1 to Theta2

Fi=113.205*pi/180; %Last Position of a4 with respect to Ground
Fi1=pi-Fi+Thb; %Fi1-Last Angle of a4
DFi=27*pi/180; %Operating Angle Delta Fi
Fi2=Fi1+DFi; %From Fi1 to Fi2

%Freudenstein's Equations and Its Derivation Matrix;
KL=[cos(Fi1) -cos(Th1) 1;0 -sin(Th1) 0; cos(Fi2) -cos(Th2) 1];
%Right Hand Side of Equation's of Freudenstein's Equations and Its
Derivation Matrix;
KR=[cos(Fi1-Th1);-sin(Fi1-Th1);cos(Fi2-Th2)];

K2= KR(2,1)/KL(2,2);

%Freudenstein's Equations and Its Derivation Matrix After Finding K2;
KL2=[cos(Fi1) 1; cos(Fi2) 1];
%Right Hand Side of Equation's of Freudenstein's Equations and Its
Derivation Matrix After Finding K2;
KR2=[cos(Fi1-Th1)-(-K2*cos(Th1)); cos(Fi2-Th2)-(-K2*cos(Th2))];

%Calculating K1 and K3;
K13=KL2\KR2; % K13=inv(KL2)*KR2;
K1=K13(1,1);
K3=K13(2,1);

%Rod Dimensions(Left)
a1=sqrt((B0y^2)+(B0x^2));
a2=a1/K1;
a4=a1/K2;
a3=sqrt((a1^2)+(a2^2)+(a4^2)-(2*K3*a4*a2));

%%

% Right Hand Side
Gama=(180-0.99)*pi/180; %0.987835999999999 Angle between Two Arm(a2-a6)
[rad]
```

```

B0yR=-B0y; %On the Coincident Horizontal Plane
B0xR=296.548;
ThRb= atan(B0yR/B0xR);

ThR=pi-Gama-Th;
ThR1=ThRb-ThR;
DThR=DTh;
ThR2=ThR1-DThR;

FiR=(180-113.205)*pi/180;
FiR1=ThRb+FiR;
DFiR=27*pi/180;
FiR2=FiR1+DFiR;

%Freudenstein's Equations and Its Derivation Matrix;
KLR=[cos(FiR1) -cos(ThR1) 1;0 -sin(ThR1) 0; cos(FiR2) -cos(ThR2) 1];
%Right Hand Side of Equation's of Freudenstein's Equations and Its
Derivation Matrix;
KRR=[cos(FiR1-ThR1);-sin(FiR1-ThR1);cos(FiR2-ThR2)];

K2R= KRR(2,1)/KLR(2,2);

%Freudenstein's Equations and Its Derivation Matrix After Finding K'2;
KL2R=[cos(FiR1) 1; cos(FiR2) 1];
%Right Hand Side of Equation's of Freudenstein's Equations and Its
Derivation Matrix After Finding K'2;
KR2R=[cos(FiR1-ThR1)-(-K2R*cos(ThR1)); cos(FiR2-ThR2)-(-
K2R*cos(ThR2))];

%Calculating K'1 and K'3;
K13R=KL2R\KR2R; % K13R=inv(KL2R)*KR2R;
K1R=K13R(1,1);
K3R=K13R(2,1);

%Rod Dimensions(Right)
a5=sqrt((B0yR^2)+(B0xR^2));
a6=a5/K1R;
a8=a5/K2R;
a7=sqrt((a5^2)+(a6^2)+(a8^2)-(2*K3R*a8*a6));

%%

%Angles Figures(Left)

Th1=Th1:0.00442:Th2;
% Th1=Th1:0.0146:Th2;
for i=1:1:length(Th1)
syms Fi1

x_hook1=a1;
y_hook1=0;

Cal_Fi1= ((-(x_hook1)-(a4*cos(Fi1)))+(a2*cos(Th1(1,i))))^2)+((-(
y_hook1)-(a4*sin(Fi1)))+(a2*sin(Th1(1,i))))^2)-(a3^2)==0 ;
Fi1=(double(solve(Cal_Fi1,Fi1)));
Fi1(1,i)=Fi1(2,1);

```

```

i=i+1;
end

Fill=flip(Fi11);
Th1=flip(Th1);

figure(1);
plot((Th1-Thb)*180/pi, (Fi11-Thb)*180/pi);
grid on;
set(gca, 'XDir', 'reverse');
xlabel('? [Degree]');
ylabel('? (?_1_4) [Degree]');
title('Angle of a_4');

%Angles Figures(Right)

ThR1=ThR1:-0.00442:ThR2;
for i=1:1:length(ThR1)
syms FiR1
x_hook2=a5;
y_hook2=0;

Cal_FiR1= ((-x_hook2)-(a8*cos(FiR1))+(a6*cos(ThR1(1,i))))^2+((-
(y_hook2)-(a8*sin(FiR1))+(a6*sin(ThR1(1,i))))^2)-(a7^2)==0 ;
FiR1=(double(solve(Cal_FiR1,FiR1)));
if FiR1(1,1)<=0
    FiR1(1,1)=FiR1(2,1);
else
    FiR1(1,1)=FiR1(1,1);
end
end
FiR11(1,i)=FiR1(1,1);

i=i+1;
end

FiR11=flip(FiR11);
ThR1=flip(ThR1);

figure(2)
plot((ThR1-ThRb)*180/pi, (FiR11-ThRb)*(180/pi));
grid on;
xlabel('?? [Degree]');
ylabel('?? (?_1_8) [Degree]');
title('Angle of a_8');

%Delta Angle Between Two Lug
CompletionPi=(Fi11-Thb)-(FiR11-ThRb);
CompletionAng=CompletionPi*180/pi;
figure(3);
plot((Th1-Thb)*180/pi,CompletionAng);
set(gca, 'XDir', 'reverse');
xlabel('? [Degree]'); %Theta Left(Degree)
ylabel('? - ?? [Degree]'); %Gap Between Two Hook(Degree)
title('Angle Difference Between Two Hook');
grid on;

%%

```

```

%Velocity Analysis(Left)

xs1=-a1+a2*cos(Th1);
ys1=+a2*sin(Th1);
s1=sqrt(xs1.^2+ys1.^2);
% Alfa=atan(xs1/ys1);
% Si=Alfa-Fill1;
Mu1=double(acos((a3^2+a4^2-s1.^2)/(2*a3*a4)));%Transmission
Angle(Left)
Th13=Fill1-Mu1;

% b=2:1:length(Th1);
% W12A= Th1(1,b)-Th1(1,b-1); %rad/sec
figure(4);
plot((Th1-Thb))*180/pi,Th13*180/pi);
grid on;
set(gca, 'XDir','reverse');
xlabel('? [Degree]');
ylabel('?_1_3 [Degree]');
title('Angle of a_3');

filename = 'ANGULAR_VELOCITY_OF_HINGE.xlsx';
sheet = 1;
xlRange = 'C89:C167'; % 'F163:F230'
W12= xlsread(filename,sheet,xlRange); %Output Values from ANSYS
Analysis
W12= W12'; %Middle Hinge Angular Velocity[rad/sec]
figure(5);

TH1I=1.23118557768578:-0.0146:0.0864055776857790;
TH1IR=-1.02105557552758:0.0146:0.123724424472422;

W12=smooth((TH1I-Thb)*180/pi,W12,0.15,'rloess');

xq = (TH1I-Thb)*180/pi:-1/4:0.25;
vq1=interp1((TH1I-Thb)*180/pi,W12,xq);
W12=vq1;
plot((Th1-Thb)*180/pi,W12);
set(gca, 'XDir','reverse');
xlabel('? [Degree]');
ylabel('?_1_2 and ?_1_6 [rad/sec]');
title('Angular Velocity of a_2 and a_6');
grid on;

filename = 'AW2.xlsx';
sheet = 1;
xlRange = 'C89:C167'; % 'F163:F230'
W2FEM= xlsread(filename,sheet,xlRange); %Output Values from ANSYS
Analysis
figure(39);
plot((TH1I-Thb)*180/pi,W2FEM);
set(gca, 'XDir','reverse');
xlabel('? [Degree]');
ylabel('?_1_2 and ?_1_6 [rad/sec]');
title('Angular Velocity of a_2 and a_6 (FEM)');
grid on;

```

```

W13= ((a2*sin(Th1-Fi11))./(a3*sin(Fi11-Th13))).*W12;
W14= ((a2*sin(Th1-Th13))./(a4*sin(Fi11-Th13))).*W12;
W14R=real(W14');

figure(6);

plot((Th1-Thb)*180/pi,W13);
set(gca, 'XDir','reverse');
xlabel('? [Degree]');
ylabel('?_1_3 [rad/sec]');
title('Angular Velocity of a_3');
grid on;

filename = 'AW3.xlsx';
sheet = 1;
xlRange = 'C89:C167'; % 'F163:F230'
W3FEM= xlsread(filename,sheet,xlRange); %Output Values from ANSYS
Analysis
figure(40);
plot((TH1I-Thb)*180/pi,W3FEM);
set(gca, 'XDir','reverse');
xlabel('? [Degree]');
ylabel('?_1_3 [rad/sec]');
title('Angular Velocity of a_3 (FEM)');
grid on;

figure(7);
plot((Th1-Thb)*180/pi,W14);
set(gca, 'XDir','reverse');
xlabel('? [Degree]');
ylabel('?_1_4 [rad/sec]');
title('Angular Velocity of a_4');
grid on;

filename = 'AW4.xlsx';
sheet = 1;
xlRange = 'C89:C167'; % 'F163:F230'
W4FEM= xlsread(filename,sheet,xlRange); %Output Values from ANSYS
Analysis
figure(41);
plot((TH1I-Thb)*180/pi,W4FEM);
set(gca, 'XDir','reverse');
xlabel('? [Degree]');
ylabel('?_1_4 [rad/sec]');
title('Angular Velocity of a_4 (FEM)');
grid on;

%Velocity Analysis(Right)

xs2=+a5-a6*cos(ThR1);
ys2=a6*sin(ThR1);
s2=sqrt(xs2.^2+ys2.^2);
% Alfa=atan(xs2/ys2);
% Si=Alfa-Fi11;
Mu2=double(acos((a7^2+a8^2-s2.^2)/(2*a7*a8))); %Transmission
Angle(Right)
Th17=FiR11-Mu2;
W16= W12; %rad/sec
W17= ((a6*sin(ThR1-FiR11))./(a7*sin(FiR11-Th17))).*W12;
W18= ((a6*sin(ThR1-Th17))./(a8*sin(FiR11-Th17))).*W12;

```

```

W18R=real(W18');

figure(8);
plot((ThR1-ThRb)*180/pi,Th17*180/pi);
grid on;
xlabel('?? [Degree]');
ylabel('?_1_7 [Degree]');
title('Angle of a_7');

figure(9);
plot((ThR1-ThRb)*180/pi,W17);
xlabel('?? [Degree]');
ylabel('?_1_7 [rad/sec]');
title('Angular Velocity of a_7');
grid on;

filename = 'AW7.xlsx';
sheet = 1;
xlRange = 'C89:C167'; % 'F163:F230'
W7FEM= xlsread(filename,sheet,xlRange); %Output Values from ANSYS
Analysis
figure(42);
plot((TH1IR-ThRb)*180/pi,W7FEM);
xlabel('?? [Degree]');
ylabel('?_1_7 [rad/sec]');
title('Angular Velocity of a_7 (FEM)');
grid on;

figure(10);
plot((ThR1-ThRb)*180/pi,W18);
xlabel('?? [Degree]');
ylabel('?_1_8 [rad/sec]');
title('Angular Velocity of a_8');
grid on;

filename = 'AW8.xlsx';
sheet = 1;
xlRange = 'C89:C167'; % 'F163:F230'
W8FEM= xlsread(filename,sheet,xlRange); %Output Values from ANSYS
Analysis
figure(43);
plot((TH1IR-ThRb)*180/pi,W8FEM);
xlabel('?? [Degree]');
ylabel('?_1_8 [rad/sec]');
title('Angular Velocity of a_8 (FEM)');
grid on;

figure(11);
subplot(2,1,1);
plot((Th1-Thb)*180/pi,Mu1*180/pi);
set(gca, 'XDir','reverse');
xlabel('? [Degree]');
ylabel('?_1 [Degree]');
title('Transmission Angle(Left)');
grid on;
subplot(2,1,2);
plot((ThR1-ThRb)*180/pi,Mu2*180/pi);
xlabel('?? [Degree]');
ylabel('?_2 [Degree]');

```

```

title('Transmission Angle(Right)');
grid on;

%Angular Velocity Gap Between Two Lug;
AngularVelGap=W18+W14;
figure(12);
plot((Th1-Thb)*180/pi,AngularVelGap);
set(gca, 'XDir','reverse');
xlabel('? [Degree]');
ylabel('?_1_4-?_1_8 [rad/sec]');
title('Angular Velocity Difference Between Two Hook');
grid on;

%%

%Acceleration Analysis

u=2:1:259;

W13R=real(W13');
W17R=real(W17');

Alfa2=((+W12(1,u+1)-W12(1,u-1))./(2*0.00442)).*W12(u);

Alfa4=(-W14R(u+1,1)+W14R(u-1,1))./(2*0.00442)).*W12(u)'; %Angular
Acceleration(Left Hook)0.00442 0.0170 0.000884
% Alfa2=(Alfa4'.*a4.*sin((Fi11(u)-Th13(u)))-
a2.*(W12(u).^2).*cos((Th1(u)-Th13(u)))-a4.*(W14(u).^2).*cos((Fi11(u)-
Th13(u)))+a3.*(W13(u).^2))./(a2.*sin((Th1(u)-Fi11(u)))); %Angular
Acceleration(a2)
% Alfa3=(-a2.*(W12(u).^2).*cos((Th1(u)-
Fi11(u)))+a2.*Alfa2.*sin((Th1(u)-Fi11(u)))-
a3.*(W13(u).^2).*cos((Fi11(u)-
Th13(u)))+a4.*(W14(u).^2))./(a3.*sin((Fi11(u)-Th13(u)))); %Angular
Acceleration(a3)
% Alfa3=(+a2.*(W12(u).^2).*cos((Th1(u)-
Fi11(u)))+a2.*Alfa2.*sin((Th1(u)-Fi11(u)))-
a3.*(W13(u).^2).*cos((Fi11(u)-Th13(u)))-
a4.*(W14(u).^2))./(a3.*sin((Fi11(u)-Th13(u)))); %Angular
Acceleration(a3)
Alfa3=((+W13R(u+1,1)-W13R(u-1,1))./(2*0.00442)).*W12(u)';

Alfa8=((W18R(u+1,1)-W18R(u-1,1))./(2*0.00442)).*W12(u)'; %Angular
Acceleration(Right Hook)
% Alfa6=(Alfa8'.*a8.*sin((FiR11(u)-Th17(u)))-
a6.*(W16(u).^2).*cos((ThR1(u)-
Th17(u)))+a8.*(W18(u).^2).*cos((FiR11(u)-Th17(u)))-
a7.*(W17(u).^2))./(a6.*sin((ThR1(u)-FiR11(u)))); %Angular
Acceleration(a6)
% Alfa7=(+a6.*(W16(u).^2).*cos((ThR1(u)-
FiR11(u)))+a6.*Alfa6.*sin((ThR1(u)-FiR11(u)))-
a7.*(W17(u).^2).*cos((FiR11(u)-Th17(u)))-
a8.*(W18(u).^2))./(a7.*sin((FiR11(u)-Th17(u)))); %Angular
Acceleration(a7)
Alfa7=((+W17R(u+1,1)-W17R(u-1,1))./(2*0.00442)).*W12(u)';

Alfa2=smooth((Th1(1,u)-Thb)*180/pi,Alfa2,0.4,'rloess');
figure(13);
plot((Th1(1,u)-Thb)*180/pi,Alfa2);

```



```

set(gca, 'XDir','reverse');
xlabel('? [Degree]');
ylabel('?_1_2 and ?_1_6 [rad/sec^2]');
title('Angular Acceleration of a_2 and a_6');
grid on;

filename = 'AAHINGE.xlsx';
sheet = 1;
xlRange = 'C89:C167'; % 'F163:F230'
Alfa2FEM= xlsread(filename,sheet,xlRange); %Output Values from ANSYS
Analysis
figure(34);
plot((TH1I-Thb)*180/pi,Alfa2FEM);
set(gca, 'XDir','reverse');
xlabel('? [Degree]');
ylabel('?_1_2 and ?_1_6 [rad/sec^2]');
title('Angular Acceleration of a_2 and a_6 (FEM)');
grid on;

Alfa3=smooth((Th1(1,u)-Thb)*180/pi,Alfa3,0.3,'rloess');
figure(14);
plot((Th1(1,u)-Thb)*180/pi,Alfa3);
set(gca, 'XDir','reverse');
xlabel('? [Degree]');
ylabel('?_1_3 [rad/sec^2]');
title('Angular Acceleration of a_3');
grid on;

filename = 'ALFA3.xlsx';
sheet = 1;
xlRange = 'C89:C167'; % 'F163:F230'
Alfa3FEM= xlsread(filename,sheet,xlRange); %Output Values from ANSYS
Analysis
figure(35);
plot((TH1I-Thb)*180/pi,Alfa3FEM);
set(gca, 'XDir','reverse');
xlabel('? [Degree]');
ylabel('?_1_3 [rad/sec^2]');
title('Angular Acceleration of a_3 (FEM)');
grid on;

Alfa7=smooth((ThR1(1,u)-ThRb)*180/pi,Alfa7,0.3,'rloess');
figure(15);
plot((ThR1(1,u)-ThRb)*180/pi,Alfa7);
xlabel('?? [Degree]');
ylabel('?_1_7 [rad/sec^2]');
title('Angular Acceleration of a_7');
grid on;

filename = 'ALFA7.xlsx';
sheet = 1;
xlRange = 'C89:C167'; % 'F163:F230'
Alfa7FEM= xlsread(filename,sheet,xlRange); %Output Values from ANSYS
Analysis
figure(36);
plot((TH1IR-ThRb)*180/pi,Alfa7FEM);
xlabel('?? [Degree]');
ylabel('?_1_7 [rad/sec^2]');
title('Angular Acceleration of a_7 (FEM)');
grid on;

```

```

Alfa4=smooth((Th1(1,u)-Thb)*180/pi,Alfa4,0.2,'rloess');
figure(16);
plot((Th1(1,u)-Thb)*180/pi,Alfa4);
set(gca, 'XDir','reverse');
xlabel('? [Degree]');
ylabel('?_1_4 [rad/sec^2]');
title('Angular Acceleration of a_4');
grid on;

filename = 'ALFA4.xlsx';
sheet = 1;
xlRange = 'C89:C167'; % 'F163:F230'
Alfa4FEM= xlsread(filename,sheet,xlRange); %Output Values from ANSYS
Analysis
figure(37);
plot((TH1I-Thb)*180/pi,Alfa4FEM);
set(gca, 'XDir','reverse');
xlabel('? [Degree]');
ylabel('?_1_4 [rad/sec^2]');
title('Angular Acceleration of a_4 (FEM)');
grid on;

Alfa8=smooth((ThR1(1,u)-ThRb)*180/pi,Alfa8,0.2,'rloess');
figure(17);
plot((ThR1(1,u)-ThRb)*180/pi,Alfa8);
xlabel('?? [Degree]');
ylabel('?_1_8 [rad/sec^2]');
title('Angular Acceleration of a_8');
grid on;

filename = 'ALFA8.xlsx';
sheet = 1;
xlRange = 'C89:C167'; % 'F163:F230'
Alfa8FEM= xlsread(filename,sheet,xlRange); %Output Values from ANSYS
Analysis
figure(38);
plot((TH1IR-ThRb)*180/pi,Alfa8FEM);
xlabel('?? [Degree]');
ylabel('?_1_8 [rad/sec^2]');
title('Angular Acceleration of a_8 (FEM)');
grid on;

%Angular Acceleration Gap Between Two Lug;
AngularAccGap=-Alfa8+Alfa4;
figure(18);
plot((Th1(1,u)-Thb)*180/pi,AngularAccGap);
set(gca, 'XDir','reverse');
xlabel('? [Degree]');
ylabel('?_1_4-?_1_8 [rad/sec^2]');
title('Angular Acceleration Difference Between Two Hook');
grid on;

%%

%Force Analysis From ANSYS

filename = 'SPRING1 FORCE.xlsx';
sheet = 1;

```

```

xlRange = 'C67:C145';
Fs1= xlsread(filename,sheet,xlRange); %Output Values from ANSYS
Analysis
Fs1= Fs1'; %Spring Force Reaction[N]

filename = 'SPRING2 FORCE.xlsx';
sheet = 1;
xlRange = 'C67:C145';
Fs2= xlsread(filename,sheet,xlRange); %Output Values from ANSYS
Analysis
Fs2= Fs2'; %Spring Force Reaction[N]

figure(19);
plot((TH1I-Thb)*180/pi,Fs1);
set(gca, 'XDir','reverse');
xlabel('? [Degree]');
ylabel('F_S_T [N]');
title('Tension Spring Reaction Forces(FEM)');
grid on;

figure(20);
plot((TH1I-Thb)*180/pi,Fs2);
set(gca, 'XDir','reverse');
xlabel('? [Degree]');
ylabel('F_S_C [N]');
title('Compression Spring Reaction Forces(FEM)');
grid on;

filename = 'LEFT HOOK FORCE.xlsx';
sheet = 1;
xlRange = 'F89:F167';
Flh= xlsread(filename,sheet,xlRange); %Output Values from ANSYS
Analysis
Flh= Flh'; %Left Hook Force Reaction[N]

filename = 'RIGHT HOOK FORCE.xlsx';
sheet = 1;
xlRange = 'F89:F167';
Frh= xlsread(filename,sheet,xlRange); %Output Values from ANSYS
Analysis
Frh= Frh'; %Right Hook Force Reaction[N]

figure(21);
plot((TH1I-Thb)*180/pi,Flh);
set(gca, 'XDir','reverse');
xlabel('? [Degree]');
ylabel('F_L_H [N]');
title('Pivot Joint of Left Hook(a_4) Force Reaction(FEM)');
grid on;

figure(22);
plot((TH1IR-ThRb)*180/pi,Frh);
xlabel('?? [Degree]');
ylabel('F_R_H [N]');
title('Pivot Joint of Right Hook(a_8) Force Reaction(FEM)');
grid on;

```

```

filename = 'HINGE-ARM1 FORCE.xlsx';
sheet = 1;
xlRange = 'F89:F167';
Fallh= xlsread(filename,sheet,xlRange); %Output Values from ANSYS
Analysis
Fallh= Fallh'; %Joint Arm1-Hinge Force Reaction[N]

filename = 'HINGE-ARM2 FORCE.xlsx';
sheet = 1;
xlRange = 'F89:F167';
Fha1= xlsread(filename,sheet,xlRange); %Output Values from ANSYS
Analysis
Fha1= Fha1'; %Joint Hinge-Arm2 Force Reaction[N]

figure(23);
plot((TH1I-Thb)*180/pi,Fallh);
set(gca, 'XDir','reverse');
xlabel('? [Degree]');
ylabel('F_a_2_,_a_3 [N]');
title('Arm1-Hinge Force Reaction(FEM)');
grid on;

figure(24);
plot((TH1IR-ThRb)*180/pi,Fha1);
xlabel('?? [Degree]');
ylabel('F_a_6_,_a_7 [N]');
title('Arm2-Hinge Force Reaction(FEM)');
grid on;

filename = 'LEFT HOOK-ARM1 FORCE.xlsx';
sheet = 1;
xlRange = 'F89:F167';
Fa2rh= xlsread(filename,sheet,xlRange); %Output Values from ANSYS
Analysis
Fa2rh= Fa2rh'; %Joint Arm2-Right Hook Force Reaction[N]

filename = 'RIGHT HOOK-ARM2 FORCE.xlsx';
sheet = 1;
xlRange = 'F89:F167';
Fha2= xlsread(filename,sheet,xlRange); %Output Values from ANSYS
Analysis
Fha2= Fha2'; %Joint Hinge-Right Hook Force Reaction[N]

figure(25);
% subplot(2,1,1);
plot((TH1I-Thb)*180/pi,Fa2rh);
set(gca, 'XDir','reverse');
xlabel('? [Degree]');
ylabel('F_a_3_,_a_4 [N]');
title('Joint of Arm1-Left Hook(FEM)');
grid on;

figure(26);
plot((TH1IR-ThRb)*180/pi,Fha2);
xlabel('?? [Degree]');
ylabel('F_a_7_,_a_8 [N]');
title('Joint of Arm2-Right Hook(FEM)');
grid on;

```

```

filename = 'HINGE FORCE.xlsx';
sheet = 1;
xlRange = 'F89:F167';
Fh= xlsread(filename,sheet,xlRange); %Output Values from ANSYS
Analysis
Fh= Fh'; %Joint Hinge Force Reaction[N]

figure(27);
plot((TH1I-Thb)*180/pi,Fh);
set(gca, 'XDir','reverse');
xlabel('? [Degree]');
ylabel('F_H [N]');
title('Pivot Joint of Hinge Force Reaction(FEM)');
grid on;

%% FORCE ANALYSIS ANALYTICAL

ThS=32.37*pi/180:-0.00176:24.67*pi/180; %Working Range of Tension
Spring
k=20; %Stiffness Coefficient of Spring [N/mm]
l_load1=95.971; %Preloaded Length [mm]
l_load2=81.3; %Last Position of Preloaded Length [mm]
l_free=80; %Free Length of Spring [mm]
l_range=l_load1:-0.191:l_load2; %Length Change in Working Range
Fspring=k*(l_range*10^-3-l_free*10^-3); %Due to Stretch of Spring
Fspring_x=Fspring(1:1:32).*cos(ThS(1:1:32)) ;
Fspring_x = [Fspring_x,zeros(1,258-32)];
Fspring_y=Fspring(1:1:32).*sin(ThS(1:1:32)) ;
hs1=58*10^-3;
hs2=98*10^-3;

g2=6.71; %Center of Gravity Distance of a2 Relative to Fixed Point
[mm] 23.1
g3=208 ; %Center of Gravity Distance of a3 Relative to a2-a3 Pivot
Point [mm]
g4=2.86; %Center of Gravity Distance of a4 Relative to Fixed Point
[mm]

Beta2=0 ; %Angle Difference between a2 and g2
Beta3=0 ; %Angle Difference between a3 and g3
Beta4=140.440*pi/180 ; %Angle Difference between a4 and g4

g6=14.2; %Center of Gravity Distance of a2 Relative to Fixed Point
[mm]
g7=144.3 ; %Center of Gravity Distance of a3 Relative to a2-a3 Pivot
Point [mm]
g8=2.86; %Center of Gravity Distance of a4 Relative to Fixed Point
[mm]

Beta6=0 ; %Angle Difference between a2 and g2
Beta7=0 ; %Angle Difference between a3 and g3
Beta8=140.440*pi/180 ; %Angle Difference between a4 and g4

acc_a2_x=-g2.*(W12(u).^2).*cos((Th1(u)))-
real(g2.*Alfa2'.*sin((Th1(u))))); %Linear Acceleration of CoG of a2(x-
Direction) [mm/s^2]
acc_a2_y=-
g2.*(W12(u).^2).*sin((Th1(u)))+real(g2.*Alfa2'.*cos((Th1(u)))));
%Linear Acceleration of CoG of a2(y-Direction) [mm/s^2]

```

```

acc_a3_x=+a2.*(W12(u).^2).*cos((Th1(u)))-a2.*Alfa2'.*sin((Th1(u)))-
g3.*(W13(u).^2).*cos(Th13(u))-g3.*Alfa3'.*sin(Th13(u)); %Linear
Acceleration of CoG of a3(x-Direction)
acc_a3_y=-a2.*(W12(u).^2).*sin((Th1(u)))-
a2.*Alfa2'.*sin((Th1(u)))+g3.*(W13(u).^2).*cos(Th13(u))+g3.*Alfa3'.*si
n(Th13(u)); %Linear Acceleration of CoG of a3(y-Direction)
acc_a4_x=+g4.*(W14R(u).^2)'.*cos((Fill(u)+Beta4))+g4.*Alfa4'.*sin((Fil
l(u)+Beta4)); %Linear Acceleration of CoG of a4(x-Direction)
acc_a4_y=+g4.*(W14R(u).^2)'.*sin((Fill(u)+Beta4))+g4.*Alfa4'.*cos((Fil
l(u)+Beta4)); %Linear Acceleration of CoG of a4(y-Direction)

acc_a6_x=-g6.*(W16(u).^2).*cos((ThR1(u)))-g6.*Alfa2'.*sin((ThR1(u)));
%Linear Acceleration of CoG of a6(x-Direction)
acc_a6_y=-g6.*(W16(u).^2).*sin((ThR1(u)))+g6.*Alfa2'.*cos((ThR1(u)));
%Linear Acceleration of CoG of a6(y-Direction)
acc_a7_x=-a6.*(W16(u).^2).*cos((ThR1(u)))+a6.*Alfa2'.*sin((ThR1(u)))-
g7.*(W17(u).^2).*cos((Th17(u)))-g7.*Alfa7'.*sin((Th17(u))); %Linear
Acceleration of CoG of a7(x-Direction)
acc_a7_y=-a6.*(W16(u).^2).*sin((ThR1(u)))-
a6.*Alfa2'.*sin((ThR1(u)))+g7.*(W17(u).^2).*cos((Th17(u)))+g7.*Alfa7'
.*sin((Th17(u))); %Linear Acceleration of CoG of a7(y-Direction)
acc_a8_x=+g8.*(W18R(u).^2)'.*cos((Fill(u)+Beta8))-
g8.*Alfa8'.*sin((FiR11(u)+Beta8)); %Linear Acceleration of CoG of
a8(x-Direction)
acc_a8_y=-
g8.*(W18R(u).^2)'.*sin((Fill(u)+Beta8))+g8.*Alfa8'.*cos((FiR11(u)+Beta
8)); %Linear Acceleration of CoG of a8(y-Direction)

acc_a2=sqrt((acc_a2_x.^2)+(acc_a2_y.^2))*10^-3; %Total Linear
Acceleration of a2 [m/s^2]
acc_a3=sqrt((acc_a3_x.^2)+(acc_a3_y.^2))*10^-3; %Total Linear
Acceleration of a3 [m/s^2]
acc_a4=sqrt((acc_a4_x.^2)+(acc_a4_y.^2))*10^-3; %Total Linear
Acceleration of a4 [m/s^2]
acc_a6=sqrt((acc_a6_x.^2)+(acc_a6_y.^2))*10^-3; %Total Linear
Acceleration of a6 [m/s^2]
acc_a7=sqrt((acc_a7_x.^2)+(acc_a7_y.^2))*10^-3; %Total Linear
Acceleration of a7 [m/s^2]
acc_a8=sqrt((acc_a8_x.^2)+(acc_a8_y.^2))*10^-3; %Total Linear
Acceleration of a8 [m/s^2]

acc_h_x=acc_a2_x-acc_a6_x;
acc_h_y=acc_a2_y+acc_a2_y;

figure(28);
plot((Th1(u)-Thb)*180/pi,acc_a2*10^3);
set(gca, 'XDir','reverse');
xlabel('? [Degree]');
ylabel('Acceleration [mm/s^2]');
title('Linear Acceleration of a_2 and a_6');
grid on;

filename = 'A2.xlsx';
sheet = 1;
xlRange = 'F89:F167';
A2FEM= xlsread(filename,sheet,xlRange); %Output Values from ANSYS
Analysis

figure(44);
plot((TH1I-Thb)*180/pi,A2FEM);

```

```

set(gca, 'XDir','reverse');
xlabel('? [Degree]');
ylabel('Acceleration [mm/s^2]');
title('Linear Acceleration of a_2 and a_6 (FEM)');
grid on;

figure(29);
plot((Th1(u)-Thb)*180/pi,acc_a3*10^3);
set(gca, 'XDir','reverse');
xlabel('? [Degree]');
ylabel('Acceleration [mm/s^2]');
title('Linear Acceleration of a_3');
grid on;

filename = 'A3.xlsx';
sheet = 1;
xlRange = 'F89:F167';
A3FEM= xlsread(filename,sheet,xlRange); %Output Values from ANSYS
Analysis

figure(45);
plot((TH1I-Thb)*180/pi,A3FEM);
set(gca, 'XDir','reverse');
xlabel('? [Degree]');
ylabel('Acceleration [mm/s^2]');
title('Linear Acceleration of a_3 (FEM)');
grid on;

figure(30);
plot((Th1(u)-Thb)*180/pi,acc_a4*10^3);
set(gca, 'XDir','reverse');
xlabel('? [Degree]');
ylabel('Acceleration [mm/s^2]');
title('Linear Acceleration of a_4');
grid on;

filename = 'A4.xlsx';
sheet = 1;
xlRange = 'F89:F167';
A4FEM= xlsread(filename,sheet,xlRange); %Output Values from ANSYS
Analysis

figure(46);
plot((TH1I-Thb)*180/pi,A4FEM);
set(gca, 'XDir','reverse');
xlabel('? [Degree]');
ylabel('Acceleration [mm/s^2]');
title('Linear Acceleration of a_4 (FEM)');
grid on;

figure(31);
plot((Th1(u)-Thb)*180/pi,acc_a7*10^3);
set(gca, 'XDir','reverse');
xlabel('? [Degree]');
ylabel('Acceleration [mm/s^2]');
title('Linear Acceleration of a_7');
grid on;

filename = 'A7.xlsx';

```

```

sheet = 1;
xlRange = 'F89:F167';
A7FEM= xlsread(filename, sheet, xlRange); %Output Values from ANSYS
Analysis

figure(47);
plot((Th1IR-ThRb)*180/pi,A7FEM);
xlabel('? [Degree]');
ylabel('Acceleration [mm/s^2]');
title('Linear Acceleration of a_7 (FEM)');
grid on;

figure(32);
plot((Th1(u)-Thb)*180/pi,acc_a8*10^3);
set(gca, 'XDir','reverse');
xlabel('?? [Degree]');
ylabel('Acceleration [mm/s^2]');
title('Linear Acceleration of a_8');
grid on;

filename = 'A8.xlsx';
sheet = 1;
xlRange = 'F89:F167';
A8FEM= xlsread(filename, sheet, xlRange); %Output Values from ANSYS
Analysis

figure(48);
plot((Th1IR-ThRb)*180/pi,A8FEM);
xlabel('?? [Degree]');
ylabel('Acceleration [mm/s^2]');
title('Linear Acceleration of a_8 (FEM)');
grid on;

m2=0.972-0.450; %Mass of a2[kg]
m3=1.36; %Mass of a3[kg]
m4=0.94; %Mass of a4[kg]
m6=0.450; %Mass of a5[kg]
m7=0.943; %Mass of a6[kg]
m8=0.94; %Mass of a7[kg]

I2= 2.668*10^-4; % Inertia of a2 with respect to Center of Gravity
[m^2*kg]
I3= 1.996*10^-2; % Inertia of a3 with respect to Center of Gravity
[m^2*kg]
I4= 1.737*10^-3; % Inertia of a4 with respect to Center of Gravity
[m^2*kg]
I6= 9.67*10^-5; % Inertia of a6 with respect to Center of Gravity
[m^2*kg]
I7= 6.754*10^-3; % Inertia of a7 with respect to Center of Gravity
[m^2*kg]
I8= 1.737*10^-3; % Inertia of a8 with respect to Center of Gravity
[m^2*kg]

F2=-m2.*acc_a2;
F3=-m3.*acc_a3;
F4=-m4.*acc_a4;
F6=-m6.*acc_a6;

```



```

F7=-m7.*acc_a7;
F8=-m8.*acc_a8;

T2=-I2*Alfa2;
T3=-I3*Alfa3;
T4=-I4*Alfa4;
T6=-I6*Alfa2;
T7=-I7*Alfa7;
T8=-I8*Alfa8;

m=[10, 60, 100, 150, 210, 240, 255];
n=[10, 30, 60, 100, 170, 240, 258];
l=[10, 30, 60, 100, 150, 210, 240];

counter = 1;
total_angles = 258;
rank = 1;
% solx =zeros(rank,count);
% soly =zeros(rank,count);

solF23x =zeros(rank,total_angles);
solF23y =zeros(rank,total_angles);
solG2x =zeros(rank,total_angles);
solG2y =zeros(rank,total_angles);
solF34x =zeros(rank,total_angles);
solF34y =zeros(rank,total_angles);
solG4x =zeros(rank,total_angles);
solG4y =zeros(rank,total_angles);

syms F23x F23y F34x F34y FG2x FG2y FG4x FG4y

f2=57.62*10^-3; %Opener Actuation Point to Hinge Head[m]
f2Angle=26.42*pi/180;

for counter = 1:total_angles
%For Linkage a2;
EQ1=-F23x-Fspring_x(counter)+FG2x-m2*real(acc_a2_x(counter))*10^-3==0
;
EQ2=-F23y+FG2y-m2*real(acc_a2_y(counter))*10^-3==0 ;
EQ3=(-Fspring_x(counter)*hs1)-F23x*a2*(10^-3).*sin(Th1(counter+1))-
F23y*a2*(10^-3).*sin((pi/2)-Th1(counter+1))-I2*Alfa2(counter)-
m2.*real(acc_a2_x(counter))*(10^-3)*g2*(10^-3).*sin(-Th1(counter+1)-
Thb-Beta2)-m2.*real(acc_a2_y(counter))*(10^-3)*g2*(10^-3).*sin((pi/2)-
Th1(counter+1)-Thb-Beta2)==0;

%For Linkage a3;
EQ4=+F23x-F34x-m3*real(acc_a3_x(counter))*10^-3==0 ;
EQ5=+F23y-F34y-m3*real(acc_a3_y(counter))*10^-3==0 ;
EQ6=-F34x*a3*(10^-3).*sin(Th13(counter+1)-Thb)-F34y*a3*(10^-
3).*sin((pi/2)-Th13(counter+1)-Thb)...
-I3*Alfa3(counter)-m3.*real(acc_a3_x(counter))*(10^-3)*g3*(10^-
3).*sin(-Th13(counter+1)-Thb-Beta3)-m3.*real(acc_a3_y(counter))*(10^-
3)*g3*(10^-3).*sin((pi/2)-Th13(counter+1)-Thb-Beta3)==0;

%For Linkage a4;
EQ7=FG4x-F34x-m4*real(acc_a4_x(counter))*10^-3==0 ;
EQ8=FG4y-F34y-m4*real(acc_a4_y(counter))*10^-3==0 ;

```

```

EQ9=-F34x*a4*(10^-3).*sin(Fi11(counter+1)-Thb)-F34y*a4*(10^-
3).*cos(Fi11(counter+1)-Thb)...
-I4*Alfa4(counter) '-m4.*real(acc_a4_x(counter))*(10^-3)*g4*(10^-
3).*sin(Fi11(counter+1)-Thb+Beta4)-m4.*real(acc_a4_y(counter))*(10^-
3)*g4*(10^-3).*cos(Fi11(counter+1)-Thb+Beta4)==0;

```

```

[res1,res2,res3,res4,res5,res6,res7,res8] =
solve(EQ1,EQ2,EQ3,EQ4,EQ5,EQ6,EQ7,EQ8);

```

```

solF23x(:,counter) =res1;
solF23y(:,counter) =res2;
solF34x(:,counter) =res3;
solF34y(:,counter) =res4;
solG2x(:,counter) =res5;
solG2y(:,counter) =res6;
solG4x(:,counter) =res7;
solG4y(:,counter) =res8;

```

```
end
```

```

F23=real(sqrt(solF23x.^2+solF23y.^2));
F34=real(sqrt(solF34x.^2+solF34y.^2));
FG2=real(sqrt(solG2x.^2+solG2y.^2));
FG4=real(sqrt(solG4x.^2+solG4y.^2));

```

```

figure(99);
plot((Th1(1)-Thb)*180/pi,FG2(1),'-o');
set(gca, 'XDir','reverse');
xlabel('? [Degree]');
ylabel('F_H [N]');
title('Pivot Joint of Hinge Force Reaction');
grid on;

```

```

figure(100);
plot((Th1(n)-Thb)*180/pi,F23(n),'-o');
set(gca, 'XDir','reverse');
xlabel('? [Degree]');
ylabel('F_a_2_a_3 [N]');
title('Arm1-Hinge Joint Force Reaction');
grid on;

```

```

figure(101);
plot((Th1(1)-Thb)*180/pi,F34(1),'-o');
set(gca, 'XDir','reverse');
xlabel('? [Degree]');
ylabel('F_a_3_a_4 [N]');
title('Arm1-Left Hook Joint Force Reaction');
grid on;

```

```

figure(102);
plot((Th1(1)-Thb)*180/pi,FG4(1),'-o');
set(gca, 'XDir','reverse');
xlabel('? [Degree]');
ylabel('F_L_H [N]');
title('Pivot Joint of Left Hook(a_4) Force Reaction');
grid on;

```

```
%% Right Force
```

```

solF67x =zeros(rank,total_angles);
solF67y =zeros(rank,total_angles);
solG6x =zeros(rank,total_angles);
solG6y =zeros(rank,total_angles);
solF78x =zeros(rank,total_angles);
solF78y =zeros(rank,total_angles);
solG8x =zeros(rank,total_angles);
solG8y =zeros(rank,total_angles);

syms F67x F67y F78x F78y FG6x FG6y FG8x FG8y

f2=57.62*10^-3; %Opener Actuation Point to Hinge Head[m]
f2Angle=26.42*pi/180;

for counter = 1:total_angles
%For Linkage a2;
EQ10=-F67x-Fspring_x(counter)-FG6x-m6*real(acc_a2_x(counter))*10^-3==0
;
EQ11=-F67y-FG6y-m6*real(acc_a2_y(counter))*10^-3==0 ;
EQ12=(-Fspring_x(counter)*hs2)+F67x*a6*(10^-
3).*sin(ThR1(counter+1))+F67y*a6*(10^-3).*sin((-pi/2)-ThR1(counter+1)-
ThRb)-I6*Alfa2(counter)-m6.*real(acc_a2_x(counter))*(10^-3)*g6*(10^-
3).*sin(-ThR1(counter+1)-Beta6-ThRb)-m6.*real(acc_a2_y(counter))*(10^-
3)*g6*(10^-3).*sin((pi/2)-ThR1(counter+1)-Beta6)==0;

%For Linkage a3;
EQ13=+F67x+F78x-m7*real(acc_a7_x(counter))*10^-3==0 ;
EQ14=+F67y+F78y-m7*real(acc_a7_y(counter))*10^-3==0 ;
EQ15=+F78x*a7*(10^-3).*sin(pi-Th17(counter+1)-ThRb)+F78y*a7*(10^-
3).*sin((-pi/2)-Th17(counter+1))...
-I7*Alfa7(counter)-m7.*real(acc_a7_x(counter))*(10^-3)*g7*(10^-
3).*sin(-Th17(counter+1)-Beta7)-m7.*real(acc_a7_y(counter))*(10^-
3)*g7*(10^-3).*sin((3*pi/2)+Th17(counter+1)-Beta7-ThRb)==0;

%For Linkage a4;
EQ16=-FG8x+F78x-m8*real(acc_a8_x(counter))*10^-3==0 ;
% EQ8=FG4y-F34y+m4*real(acc_a4_y(counter))*10^-3==0 ;
EQ17=+FG8y+F78y-m8*real(acc_a8_y(counter))*10^-3==0 ;
EQ18=-F78x*a4*(10^-3).*sin(FiR11(counter+1)-ThRb)+F78y*a8*(10^-
3).*cos(FiR11(counter+1)-ThRb)...
-I8*Alfa8(counter)-m8.*real(acc_a8_x(counter))*(10^-3)*g8*(10^-
3).*sin(FiR11(counter+1)-ThRb+Beta8)-m8.*real(acc_a8_y(counter))*(10^-
3)*g8*(10^-3).*cos(FiR11(counter+1)-ThRb+Beta8)==0;

[res10,res11,res12,res13,res14,res15,res16,res17] =
solve(EQ10,EQ11,EQ12,EQ13,EQ14,EQ15,EQ16,EQ17);

solF67x(:,counter) =res10;
solF67y(:,counter) =res11;
solF78x(:,counter) =res12;
solF78y(:,counter) =res13;
solG6x(:,counter) =res14;
solG6y(:,counter) =res15;
solG8x(:,counter) =res16;
solG8y(:,counter) =res17;

```

```

end

F67=real(sqrt(solF67x.^2+solF67y.^2));
F78=real(sqrt(solF78x.^2+solF78y.^2));
FG6=real(sqrt(solG6x.^2+solG6y.^2));
FG8=real(sqrt(solG8x.^2+solG8y.^2));

figure(104);
plot((ThR1(m)-ThRb)*180/pi,F67(m),'-o');
xlabel('?? [Degree]');
ylabel('F_a_6,_a_7 [N]');
title('Arm2-Hinge Joint Force Reaction');
grid on;

figure(105);
plot((ThR1(n)-ThRb)*180/pi,F78(n),'-o');
xlabel('?? [Degree]');
ylabel('F_a_7,_a_8 [N]');
title('Joint of Arm2-Right Hook');
grid on;

figure(106);
plot((ThR1(n)-ThRb)*180/pi,FG8(n),'-o');
xlabel('?? [Degree]');
ylabel('F_R_H [N]');
title('Pivot Joint of Right Hook(a_8) Force Reaction');
grid on;

%% COMPARISON BETWEEN ANSYS AND MATLAB

figure(49);
plot((Th1-Thb)*180/pi,W12);
set(gca, 'XDir','reverse');
grid on;
hold on;
plot((TH1I-Thb)*180/pi,W2FEM);
set(gca, 'XDir','reverse');
xlabel('? [Degree]');
ylabel('?_1_2 and ?_1_6 [rad/sec]');
title('Comparison Angular Velocity of a_2 and a_6');
grid on;
legend('MATLAB','ANSYS','Location','southeast');
hold off;

figure(50);
plot((Th1-Thb)*180/pi,W13);
set(gca, 'XDir','reverse');
grid on;
hold on;
plot((TH1I-Thb)*180/pi,W3FEM);
set(gca, 'XDir','reverse');
xlabel('? [Degree]');
ylabel('?_1_3 [rad/sec]');
title('Comparison Angular Velocity of a_3');
grid on;
legend('MATLAB','ANSYS');
hold off;

```

```

figure(51);
plot((Th1-Thb)*180/pi,W14);
set(gca, 'XDir','reverse');
grid on;
hold on;
plot((TH1I-Thb)*180/pi,W4FEM);
set(gca, 'XDir','reverse');
xlabel('? [Degree]');
ylabel('?_1_4 [rad/sec]');
title('Comparison Angular Velocity of a_4');
grid on;
legend('MATLAB','ANSYS');
hold off;

figure(52);
plot((ThR1-ThRb)*180/pi,W17);
grid on;
hold on;
plot((TH1IR-ThRb)*180/pi,W7FEM);
xlabel('?? [Degree]');
ylabel('?_1_7 [rad/sec]');
title('Comparison Angular Velocity of a_7');
grid on;
legend('MATLAB','ANSYS');
hold off;

figure(53);
plot((ThR1-ThRb)*180/pi,W18);
grid on;
hold on;
plot((TH1IR-ThRb)*180/pi,W8FEM);
xlabel('?? [Degree]');
ylabel('?_1_8 [rad/sec]');
title('Comparison Angular Velocity of a_8');
grid on;
legend('MATLAB','ANSYS','Location','southeast');
hold off;

figure(54);
plot((Th1(1,u)-Thb)*180/pi,Alfa2);
set(gca, 'XDir','reverse');
xlabel('? [Degree]');
ylabel('?_1_2 and ?_1_6 [rad/sec^2]');
grid on;
hold on;
plot((TH1I-Thb)*180/pi,Alfa2FEM);
set(gca, 'XDir','reverse');
xlabel('? [Degree]');
ylabel('?_1_2 and ?_1_6 [rad/sec^2]');
title('Comparison Angular Acceleration of a_2 and a_6');
grid on;
legend('MATLAB','ANSYS');
hold off;

figure(55);
plot((Th1(1,u)-Thb)*180/pi,Alfa3);
grid on;

```

```

hold on;
plot((Th1I-Thb)*180/pi,Alfa3FEM);
set(gca, 'XDir','reverse');
xlabel('? [Degree]');
ylabel('?_1_3 [rad/sec^2]');
title('Comparison Angular Acceleration of a_3');
grid on;
legend('MATLAB','ANSYS');
hold off;

figure(56);
plot((Th1(1,u)-Thb)*180/pi,Alfa4);
grid on;
hold on;
plot((Th1I-Thb)*180/pi,Alfa4FEM);
set(gca, 'XDir','reverse');
xlabel('? [Degree]');
ylabel('?_1_4 [rad/sec^2]');
title('Comparison Angular Acceleration of a_4');
grid on;
legend('MATLAB','ANSYS','Location','southeast');
hold off;

figure(57);
plot((ThR1(1,u)-ThRb)*180/pi,Alfa7);
grid on;
hold on;
plot((Th1IR-ThRb)*180/pi,Alfa7FEM);
% set(gca, 'XDir','reverse');
xlabel('?? [Degree]');
ylabel('?_1_7 [rad/sec^2]');
title('Comparison Angular Acceleration of a_7');
grid on;
legend('MATLAB','ANSYS');
hold off;

figure(58);
plot((ThR1(1,u)-ThRb)*180/pi,Alfa8);
grid on;
hold on;
plot((Th1IR-ThRb)*180/pi,Alfa8FEM);
xlabel('?? [Degree]');
ylabel('?_1_8 [rad/sec^2]');
title('Comparison Angular Acceleration of a_8');
grid on;
legend('MATLAB','ANSYS');
hold off;

figure(59);
plot((Th1(1,u)-Thb)*180/pi,acc_a2*10^3);
grid on;
hold on;
plot((Th1I-Thb)*180/pi,A2FEM);
set(gca, 'XDir','reverse');
xlabel('? [Degree]');
ylabel('Acceleration [mm/s^2]');
title('Comparison Linear Acceleration of a_2 and a_6');
grid on;
legend('MATLAB','ANSYS','Location','southeast');
hold off;

```

```

figure(60);
plot((Th1(1,u)-Thb)*180/pi,acc_a3*10^3);
grid on;
hold on;
plot((TH1I-Thb)*180/pi,A3FEM);
set(gca, 'XDir','reverse');
xlabel('? [Degree]');
ylabel('Acceleration [mm/s^2]');
title('Comparison Linear Acceleration of a_3');
grid on;
legend('MATLAB','ANSYS','Location','southeast');
hold off;

```

```

figure(61);
plot((Th1(1,u)-Thb)*180/pi,acc_a4*10^3);
grid on;
hold on;
plot((TH1I-Thb)*180/pi,A4FEM);
set(gca, 'XDir','reverse');
xlabel('? [Degree]');
ylabel('Acceleration [mm/s^2]');
title('Comparison Linear Acceleration of a_4');
grid on;
legend('MATLAB','ANSYS','Location','southeast');
hold off;

```

```

figure(62);
plot((ThR1(1,u)-ThRb)*180/pi,acc_a7*10^3);
grid on;
hold on;
plot((TH1IR-ThRb)*180/pi,A7FEM);
xlabel('?? [Degree]');
ylabel('Acceleration [mm/s^2]');
title('Comparison Linear Acceleration of a_7');
grid on;
legend('MATLAB','ANSYS','Location','southeast');
hold off;

```

```

figure(63);
plot((ThR1(1,u)-ThRb)*180/pi,acc_a8*10^3);
grid on;
hold on;
plot((TH1IR-ThRb)*180/pi,A8FEM);
xlabel('?? [Degree]');
ylabel('Acceleration [mm/s^2]');
title('Comparison Linear Acceleration of a_8');
grid on;
legend('MATLAB','ANSYS','Location','southeast');
hold off;

```

```

figure(200);
plot((TH1I-Thb)*180/pi,Fh);
set(gca, 'XDir','reverse');
grid on;
hold on;
plot((Th1(1)-Thb)*180/pi,FG2(1),'-o');
set(gca, 'XDir','reverse');
xlabel('? [Degree]');
ylabel('F_H [N]');

```

```

title('Pivot Joint of Hinge Force Reaction');
grid on;
legend('ANSYS', 'MATLAB', 'Location', 'southeast');
hold off;

figure(201);
plot((TH1I-Thb)*180/pi, Fallh);
set(gca, 'XDir', 'reverse');
grid on;
hold on;
plot((Th1(n)-Thb)*180/pi, F23(n), '-o');
set(gca, 'XDir', 'reverse');
xlabel('? [Degree]');
ylabel('F_a_2_a_3 [N]');
title('Arm1-Hinge Joint Force Reaction');
grid on;
legend('ANSYS', 'MATLAB', 'Location', 'southeast');
hold off;

figure(202);
plot((TH1I-Thb)*180/pi, Flh);
set(gca, 'XDir', 'reverse');
grid on;
hold on;
plot((Th1(l)-Thb)*180/pi, FG4(l), '-o');
set(gca, 'XDir', 'reverse');
xlabel('? [Degree]');
ylabel('F_L_H [N]');
title('Pivot Joint of Left Hook(a_4) Force Reaction');
grid on;
legend('ANSYS', 'MATLAB', 'Location', 'southeast');
hold off;

figure(203);
plot((TH1I-Thb)*180/pi, Fa2rh);
set(gca, 'XDir', 'reverse');
grid on;
hold on;
plot((Th1(l)-Thb)*180/pi, F34(l), '-o');
set(gca, 'XDir', 'reverse');
xlabel('? [Degree]');
ylabel('F_a_3_a_4 [N]');
title('Joint of Arm1-Left Hook');
grid on;
legend('ANSYS', 'MATLAB', 'Location', 'southeast');
hold off;

figure(205);
plot((TH1IR-ThRb)*180/pi, Fha1);
grid on;
hold on;
plot((ThR1(m)-ThRb)*180/pi, F67(m), '-o');
xlabel('?? [Degree]');
ylabel('F_a_6_a_7 [N]');
title('Arm2-Hinge Joint Force Reaction');
grid on;
legend('ANSYS', 'MATLAB', 'Location', 'southeast');
hold off;

figure(206);

```



```

plot((TH1IR-ThRb)*180/pi,Fha2);
grid on;
hold on;
plot((ThR1(n)-ThRb)*180/pi,F78(n),'-o');
xlabel('?? [Degree]');
ylabel('F_a_7,_a_8 [N]');
title('Joint of Arm2-Right Hook');
grid on;
legend('ANSYS','MATLAB','Location','southeast');
hold off;

figure(207);
plot((TH1IR-ThRb)*180/pi,Frh);
grid on;
hold on;
plot((ThR1(n)-ThRb)*180/pi,FG8(n),'-o');
xlabel('?? [Degree]');
ylabel('F_R_H [N]');
title('Pivot Joint of Right Hook(a_8) Force Reaction');
grid on;
legend('ANSYS','MATLAB','Location','southeast');
hold off;

```